TECHNICAL UNIVERSITY of CATALONIA

Contribution to the validation of best estimate plus uncertainties coupled codes for the analysis of NK-TH nuclear transients

by

Raimon Pericas

A thesis submitted in partial fulfillment for the
degree of Doctor of Philosophy

in the
ETSEIB
Physics and Nuclear Engineering Deparment

March 2015

Declaration of Authorship

I, RAIMON PERICAS, declare that this thesis titled, 'Contribution to the validation of best estimate plus uncertainties coupled codes for the analysis of NK-TH nuclear transients' and the work presented in it are my own. I confirm that:

- This work was done wholly or mainly while in candidature for a research degree at this University.
- Where any part of this thesis has previously been submitted for a degree or any other qualification at this University or any other institution, this has been clearly stated.
- Where I have consulted the published work of others, this is always clearly attributed.
- Where I have quoted from the work of others, the source is always given. With the exception of such quotations, this thesis is entirely my own work.
- I have acknowledged all main sources of help.
- Where the thesis is based on work done by myself jointly with others, I have made clear exactly what was done by others and what I have contributed myself.

Signed: _____

Date: _____

"The block of granite which was an obstacle in the pathway of the weak, became a stepping-stone in the pathway of the strong."

Thomas Carlyle

TECHNICAL UNIVERSITY of CATALONIA

Abstract

ETSEIB
Physics and Nuclear Engineering Deparment

Doctor of Philosophy

by Raimon Pericas

The typical conservative nuclear safety margins limit the actual industrial needs to increase the Nuclear Power Plant (NPP) power production. Best Estimate Plus Uncertainty (BEPU) calculations are the most advanced tool in nuclear system codes analysis. This technique is superior when compared to the old conservative methodology, where the safety margins were established by experts, operation hypothesis and conservative assumptions. The BEPU methodology is capable of providing a solution in terms of increasing the nuclear power production without compromising the safety margins. This study presents a comparison between the BEPU methodology and the Conservative Bounding methodology. Within the framework of safety analysis with nuclear system codes, neutron kinetics and thermal hydraulics (NK-TH) calculations are also the most advanced tool, and they are specially indicated for those transients which involves asymmetrical core conditions and return to critically scenarios. Main Steam Line Break (MSLB) in Ascó (NPP) fits these pre-conditioners and thus is the selected transient for the present report. Some code improvements were needed when validating the used models, those improvements are presented in this study also. Finally, moreover the BEPU analysis with NK-TH coupled codes, the present study also shows a methodology of XS library creation valid for any point of the cycle life of the studied reactor.

Acknowledgements

I am using this opportunity to express my gratitude to everyone who supported me throughout the course of this Ph.D project. I am thankful for their aspiring guidance, invaluably constructive criticism and friendly advice during the project work. I am sincerely grateful to them for sharing their truthful and illuminating views on a number of issues related to the project.

Foremost, I would like to express my sincere gratitude to my advisors Prof. Francesc Reventós and Prof. Lluís Batet for the continuous support of my Ph.D study and research, for their patience, motivation, enthusiasm, and immense knowledge. Their guidance helped me in all the time of research and writing of this thesis report. I could not have imagined having better advisors and mentors for my Ph.D study.

Besides my advisors, I would like to thank the rest of my thesis committee: Prof. Kostadin N. Ivanov, Prof. Maria del Carmen Pretel Sánchez, Prof. Rafael Miró Herrero, Prof. Maria N. Avramova and Dra. Patricia Pla Freixa for their encouragement, insightful comments, and hard questions.

My sincere thanks also goes to Prof. Kostadin Ivanov for his hospitality, for offering me the summer internship opportunities in his group and leading me working on the neutron kinetics part of the project.

I thank my fellow lab mates in Technical University of Catalonia for the stimulating discussions, coffee talks and for all the fun we have had in the last years. Also I thank my friends in Universitat de Vic, Miquel Caballeria, Carme Vernís, Manel Vilar and Josep Ayats for encouraging me through all the project duration.

I thank Rafael Mendizabal from *Consejo de Seguridad Nuclear* for their funding support and *Asociación Nuclear Ascó - Vandellós II* for providing data necessary for this project. I also thank, Dr. Rafael Miró from *Universitat Politècnica de València* for his help in coding part of the project.

Special thanks to Dr. Chris Allison and all *Innovative Systems Software* community (Zheng, Brian, Judy, Jenny, Peggy, Larry and Dick) for trusting me, for their help, advice, hospitality and support.

Last but not the least, I would like to thank all my family for supporting me spiritually throughout this long journey.

To all thanks for helping and supporting me through all the project.

Raimon.

Contents

List of Figures

List of Tables

Abbreviations

ACR	**A**dvanced **C**ANDU **R**eactor
AFW	**A**uxiliary **F**eed **W**ater
ATHLET	**A**nalysis of **T**hermal-hydraulics of **Le**aks and **T**ransients
ATWS	**A**nticipated **T**ransient **W**ithout **S**CRAM
ANM	**A**nalytic **N**odal **M**ethod
BE	**B**est **E**stimated
BEBCC	**B**est **E**stimated **B**ase **C**ase **C**alculation
BEPU	**B**est **E**stimated **P**lus **U**ncertainty
BiCGSTAB	**Bi**-**C**onjugate **G**radient **STAB**ilized algorithm
BILU3D	**B**lockwise **I**ncomplete **LU** preconditioner
BOC	**B**egin **O**f **C**ycle
BWR	**B**oiling **W**ater **R**eactor
CCFL	**C**ounter **C**urrent **F**low **L**imitation
CHF	**C**ritical **H**eat **F**lux
CIAU	**C**ode with capability of **I**nternal **A**ssessment of **U**ncertainty
CMFD	**C**oarse **M**esh **F**inite **D**ifference
CNCC	**C**orrective **N**odal **C**oupling **C**oefficient
CRISSUE	**C**ritical **Issue**s in Nuclear Reactor Technology
CSN	**C**onsejo de **S**eguridad **N**uclear
DAKOTA	**D**esign **A**nalysis **K**it for **O**ptimization and **T**erascale **A**pplication
DBA	**D**esign from **B**asis **A**ccident
DNBR	**D**eparture from **N**ucleate **B**oiling **R**atio
DOE	**D**epartment **O**f **E**nergy
ECCS	**E**mergency **C**ore **C**ooling **S**ystem
EFPD	**E**quivalent **F**ull **P**ower **D**ays

EOC	**E**nd **O**f **C**ycle
ESBWR	**E**conomic **S**implified **B**oiling **W**ater **R**eactor
FMFD	**F**ine **M**esh **F**inite **D**ifference
FoM	**F**igure **o**f **M**erit
FW	**F**eed **W**ater
GenPMAXS	**G**eneration of the **P**urdue **M**acroscopic **XS** sets
GET	**G**rup d'**E**studis **T**ermohidràulics
GMRES	**G**eneralized **M**inimum **R**esidual method
HPIS	**H**igh **P**ressure **I**njection **S**ystem
HS	**H**eat **S**tructure
IDN	**I**nforme de **D**isñeo **N**uclear
ITF	**I**ntegral **T**est **F**acility
LBLOCA	**L**arge **B**reak **L**oss **O**f **C**oolant **A**ccident
LOCA	**L**oss **O**f **C**oolant **A**ccident
LPIS	**L**ow **P**ressure **I**njection **S**ystem
LWR	**L**ight **W**ater **R**eactor
MCP	**M**ain **C**oolant **P**umps
MFW	**M**ain **F**eed **W**ater
MOC	**M**id **O**f **C**ycle
MSIV	**M**ain **S**team **I**solation **V**alve
MSLB	**M**ain **S**team **L**ine **B**reak
NEA	**N**uclear **E**nergy **A**gency
NEM	**N**odal **E**xpansion **M**ethod
NESTLE	**N**odal **E**igenvalue, **S**teady-state, **T**ransient, **L**e core **E**valuator
NK-TH	**N**eutron **K**inetics and **T**hermal **H**ydraulics
NPP	**N**uclear **P**ower **P**lant
NRC	**N**uclear **R**egulatory **C**ommission
OECD	**O**rganization for **E**conomic **C**o-operation and **D**evelopment
PARCS	**P**urdue **A**dvanced **R**eactor **C**ore **S**imulator
PCT	**P**eak **C**ladding **T**emperature
PDF	**P**robability **D**ensity **F**unction
PIRT	**P**henomenon **I**dentification and **R**anking **T**ables
PSU	**P**ennsylvania **S**tate **U**niversity

PWR	**P**ressurizer **W**ater **R**eactor
RDFMG	**R**eactor **D**ynamics and **F**uel **M**anagement Research **G**roup
RELAP	**R**eactor **E**xcursion and **L**eak **A**nalysis **P**rogram
SETF	**S**eparate **E**ffects **T**est **F**acility
SBLOCA	**S**mall **B**reak **L**oss **O**f **C**oolant **A**ccident
SCRAM	**S**afety **C**ontrol **R**od **A**xe **M**an
SNAP	**S**ymbolic **N**uclear and **A**nalysis **P**rogram
SP	**S**pecial **P**rocesses
TH	**T**hermal **H**ydraulics
TMI	**T**hee **M**ile **I**sland
TPEN	**T**riangle-based **P**olynomial **E**xpansion **N**odal
TRAC	**T**ransient **R**eactor **A**nalysis **C**ode
TRACE	**T**RACE/RELAP **A**dvanced and **C**omputational **E**ngine
VVER	**V**odo-**V**odyanoi **E**nergetichesky **R**eaktor
UAM	**U**ncertainty **A**nalysis in **M**odelling
UPC	**U**niversitat **P**olitècnica de **C**atalunya
XS	Cross **S**ections

Symbols

symbol	name	unit
a	distance	(m)
a	subscript: absorption cross section	(-)
C_k^m	m node precursor density	(mol/m^3)
D_g	diffusion coefficient	(cm)
$D_i(\vec{r},t)$	concentration of the decay heat	
	precursors in decay heat group i	(J/cm^3)
d	subscript: delayed neutrons	(-)
E	energy	(J)
eff	superscript: effective	(-)
F	fission matrix	(-)
f	subscript: fission cross section	(-)
G	neutron energy group	
G_i	heavy metal loading in *ith* region	(kg)
G_c	heavy metal loading in the core	(kg)
g	subscript: fast/thermal neutron group	(-)
$g \rightarrow g'$	subscript: scattering group 1 to 2 cross section	(-)
H_j	energy of the decay heat precursor	
	concentration in group j	(J)
h	enthalpy	(J)
$\vec{J}$	neutron current	(neutron/m^{2}s)
$J_{gw}^{m^+_-}$	m node surface averaged net current	(neutron/m^{2}s)
J	number of decay heat groups	(-)
k_{eff}	effective neutron multiplication constant	(-)
K	subscript: delayed neutron group	(-)

L_g	groups leakage term	(neutron/m^{2}s)
l	subscript: liquid	(-)
M	non-fission matrix	(-)
m	superscript: m node	(-)
$N_i^l(t)$	nuclei number density of isotope i	(atom/m^3)
P	power	W (Js^{-1})
p	pressure	(Pa)
p	subscript: prompt neutrons	(-)
q'	heat transfer rate per unit volume	(W/m^2)
$\vec{q}$	heat flux	(W/m^2)
S_g	delayed neutron source term	(neutron/group)
s	subscript: scattering cross section	(-)
t	subscript: transport cross section	(-)
$\vec{v}$	velocity	(m/s)
$\overrightarrow{W}$	fluid velocity	(m/s)
w	subscript: wall	(-)

α	control rod fraction	(-)
β	confidence level	(%)
β^{eff}	effective fraction of the delayed neutrons	(-)
ΔB_i	core average burnup increment in one step	(MWd/kg)
Γ	volumetric mass exchange rate	(kg/m^{3}s)
γ	probability	(%)
γ_i^l	effective yield of isotope i	(atoms/fission)
λ_j^H	decay constant for decay-heat group j	(sec^{-1})
λ_i^l	decay constant of the isotope i	(sec^{-1})
ν	average number of neutrons produced per fission	(neutron/fission)
Σ	macroscopic cross section	(cm^{-1})
$\Sigma_{sgg'}$	groups-to-group scattering cross section	(cm^{-1})
σ	microscopic cross section	(cm^{-1})
ρ	density	(kg/m^3)

ω	angular frequency	(rads^{-1})
ϕ_g^m	m node averaged neutron flux	(cm^{-2}sec^{-1})
Ψ^m	m node fission source term	(neutron/fission)
χ_g	average fission spectrum	(cm^{-1})
Ω	unit vector in direction of motion	(solid angle)
$\zeta_k(t)$	decay constant of the decay heat group i	(sec^{-1})
$'$	superscript: incident neutron energy and direction	(-)
$\pm$	flux direction	(-)

A la meva família

Chapter 1

Introduction

The typical conservative nuclear safety margins limit the actual industrial needs of increasing the Nuclear Power Plant (NPP) power production. Best Estimate Plus Uncertainty (BEPU) calculations are the most advanced tool in nuclear system codes analysis. This technique is superior when compared to the old conservative methodology, where the safety margins were established by experts, operation hypothesis and conservative assumptions. The BEPU methodology is capable of providing a solution in terms of increasing the nuclear power production without compromising the safety margins. This study presents a comparison between the BEPU methodology and the Conservative Bounding methodology within the framework of the Neutron Kinetics and Thermal Hydraulics coupled systems. To perform such comparison the following tools have been selected: TRACE [1–3] for thermal-hydraulic system calculations, PARCS [4, 5] for reactor physics modeling and DAKOTA [6–9] for uncertainty and sensitivity analysis.

A Main Steam Line Break (MSLB) in a Pressurized Water Reactor (PWR) is the selected transient. The failure of a main steam line results in an initial increase in the steam flow, which decreases afterwards driven by the secondary pressure reduction. The break in the secondary causes a reduction in the coolant (moderator) temperature and pressure. In the presence of a large negative moderator temperature coefficient, the excess cooling results in a reduction of the core shutdown margin. Assuming that the most reactive control rod bundle remains stuck in its fully withdrawn position after the reactor SCRAM, it is possible that the reactor become critical and return to power in a local overcooled core region. A return to power after a MSLB is a potential problem, mainly due to the relatively high power density that can be achieved locally in the vicinity of the place where the most reactive control rod bundle should have been inserted. The core heating is finally stopped by the injection of boric acid discharged from the safety injection system.

For this scenario, results obtained using the BEPU and Conservative methodologies are compared. To perform such comparison, a Best Estimate Base Case Calculation (BE-BCC) is performed followed by BEPU calculations using a selection of perturbed parameters. The selection of the important parameters is based on the Priority Identification and Ranking Tables (PIRTs) [10–15], following the recommendations of OECD/NRC PWR MSLB benchmark project report [16–19] and CRISSUE [20–22] project guidelines. At the end, a comparison of predicted results is made between the predictions of the Conservative and BEPU methodologies.

The general objective of this study is resumed in its title, *contribution to the validation of best estimate plus uncertainties coupled codes for the analysis of 3D neutron kinetics-thermalhydraulics (NK-TH) nuclear transients.* The present study fits within the framework of the OECD UAM project [23]. The work presented is focused on one part of the entire OECD UAM project [23], since international benchmark has a wide range of uncertainties propagation from the Neutronic phase (computed by lattice physics codes) to the system phase (computed by system codes like the ones used in this thesis). Conclusions from the present research can be used by the participants of the UAM project [23] to enhance and optimize the results in that specific part, as the project is presently some steps before the uncertainties propagation range that is dealt with in the present thesis report. The general objective of the entire work can be subdivided in several parts which are explained below:

- To built a 3D NK-TH coupled model from the Ascó NPP using the TRACE/-PARCS [1–3] and [4, 5] system codes, and improving the code if required.A methodology on the use of information required to develop the models will be also established
- To establish a methodology of XS library generation, by using the Ascó NPP information [24–26]
  - By using the HELIOS-1.9 [27–29], and make it readable for GenPMXAS [30] to be input in PARCS [4, 5] code.
  - By using the HELIOS-1.9 [27–29], and make it readable for NEMTAB to be input in NESTLE [31–35] code. (See below and Appendix A)
- To contribute of the enhancement of the BEPU methodology with coupled 3D NK-TH calculation, in three steps:
  - First, selection of an adequate BE scenario to apply BEPU methodology with 3D NK-TH calculation.

  - Second, to establish some conservative assumptions for the selected transient for the Conservative Case calculation.
  - Finally, a list of perturbed coupled parameters for the BEPU methodology will be selected and to perform the BEPU calculation.

- To test previous results against the widely validated models hold by GET group in Technical University of Catalonia [36–40].
  - RELAP5 [41–49] point kinetics model
  - RELAP5-3D/NESTLE [31–35] neutron kinetics model
  - TRACE [1–3] point kinetics model
  - TRACE/PARCS [1–3], [4, 5] neutron kinetic model

With all of the above mentioned objectives, the present work will be used as reference in different activities of the GET group. After the development of this study, the GET group will hold full capability of 3D NK-TH coupled calculations that will be used in the future studies to validate models (either TH models or NK models) and to perform safety analyses, particularly for those scenarios where 3D NK representation becomes important (scenarios with important reactivity feedback effects and parametric asymmetries within the core). XS library creation methodology will be used in the future to improve the model of Ascó NPP of the GET group, and thus to increase its capacities of simulation. The library generated is a full-cycle library which makes the model able to reproduce any specific point of the 13th load cycle of Ascó II NPP. The library can be constructed for different cycles, using the information from the plant, so that any transient with any composition can be reproduced.

The BEPU analysis with 3D NK-TH coupled codes had not been applied before within the group experience. After this work, such capability will be available.

Chapter 2

Background

2.1 General overview

Several present and past international benchmarks projects, have being used as a reference studies for the development of the present thesis report. OECD PWR MSLB benchmark [16–19] was selected for its knowledge on the MSLB transient. Since one of the aims of the present study was to develop a full scope methodology for a coupled NK-TH transient, the MSLB transient was a very convenient transient since it has a very big (3D) effect which can test the accuracy of the developed model and the robustness of the methodology. OECD NEA PKL-2 [50, 51] project have being also used as a reference document when simulating and analyzing the MSLB scenario. Second selected reference Benchmark was the *CRISSUE-S Critical Issues in Nuclear Reactor Technology [20–22]: a State of the Art report*, which GET group was participating actively to the development of its phases. Present work is also closely related OECD UAM project [23]. Methodology developed in UAM project [23] has been a guideline to the development of the present thesis report. Finally since the present study intends to test the validity of th BEPU methodologies in front of the more classical BE and conservative approximations, uncertainty methodologies studies such [52–57] have being used in order to perform the BEPU calculations shown at the end of this report. PIRT's studies [10–15], were also used in order to determine the parameters of interest for the scenario and also for the coupled 3D NK-TH calculation.

2.2 OECD PWR MSLB benchmark

A brief description of the OECD PWR MSLB Benchmark [16–19] is given in this section, this benchmark is being widely used as an orientation of how to proceed when

modeling the study cases for the present report. OECD PWR MSLB Benchmark [16–19] was a international cooperation effort developed between 1999 and 2003. Multiple organizations worldwide where actively participating in this program. Since the new computational techniques and new power machines allow to perform higher computations compared to the old machines, this benchmark was born with the aim of testing the new capabilities on the field of 3D NK-TH coupling. The ultimate objectives of the OECD PWR MSLB benchmark [16–19] were to verify the capability of system codes to analyze complex transients with coupled core-plant interactions, to fully test the 3-D neutronics/thermal-hydraulic coupling and to evaluate discrepancies between predictions of coupled codes in best-estimate transient simulations. For that porpoise the PWR MSLB transient was chosen as a reference benchmark for the present study. As it is well known the MSLB transient initiation event is the double ended break in the main steam isolation valves line. There are some features of the transient which makes it to be very suitable for a coupled 3D NK-TH analysis. In that sense the transient is characterized by significant space-time effects in the core caused by asymmetric cooling due the ECCS injection in broken loop system. These asymmetries could be increased if a stuck rod during the reactor trip is assumed. Notice the stuck rod should be placed where the cold water is presupposed to flow through the core. With all the previous assumptions, a 3D NK-TH analysis will be required in order to obtain a clear evaluation of the core status during the transient rather the common one dimensional simulation carried out before coupled 3D NK-TH capability was available. OECD PWR MSLB benchmark [16–19] consists in different stages and it is divided in four volumes listed below:

- Volume 1: PWR MSLB Benchmark: Final Specifications (Phase I, II and III)
- Volume 2: Summary Results of Phase I (Point Kinetics)
- Volume 3: Summary Results of Phase II (3D Kinetics/Core T-H Boundary Model)
- Volume 4: Summary Results of Phase III (Best Estimate Coupled Simulation)

First report was setting the bases of the program it self. On the basis of the benchmark, three exercises were postulated in order to achieve the above mentioned objectives. First exercise called *Phase I* was a point kinetic benchmark exercise of the selected transient. *Phase II* exercise was a 3D Kinetics/Core T-H Boundary Model finally the *Phase III* exercise was a Best Estimate coupled calculation. In order to obtain some valuable conclusions over the benchmark, same data was distributed among the participants. Data distributed can be structured in the following parts:

- Core and Neutronic data

  - A general description of the fuel assemblies is given in this section, all the needed values are reported here. These values cover either geometry considerations and neutron modeling, which means the number of prompt and delayed groups, the decay heat constants and other classical considerations needed when modeling the neutron kinetics part of the reactor. Composition maps for the 2D and 3D assembly types is given here. Finally there is a cross section library is facilitated to the participants.

- Thermal-hydraulic data
  - Some geometrical specifications over the different thermal hydraulic components are given in this section. Reactor vessel, vent valves, steam generators, steam lines, feed water system, reactor coolant pumps...are some of the specified components in this section. Break modeling structure is also released here. Finally a set of boundary conditions in terms of Temperature, Pressure and Mass Flow is given in here.

- NK-TH coupling guidelines
  - Some guidelines over the mapping composition for the coupled calculation are given here. Some examples of mapping identification are also released to the participants.

- MSLB scenario
  - Finally a detailed description of the benchmark scenario is given at the end of this first volume. This scenario description includes: Initial steady state conditions; Point kinetics model input and Transient calculations

Since a benchmark consists in a comparison between different techniques, user and codes in this particular case, that is why at the end of this first volume the output requested values were listed. The basis of the future comparisons are being set up in this first stage of the benchmark

The second report consists in a point kinetics plant simulation. Such simulation models the primary and secondary systems. The aim of the second exercise of the OECD PWR MSLB benchmark [16–19] was to test the thermal-hydraulic system response. Each participant was provided with compatible point kinetics model inputs that preserve axial and radial power distribution, and scram reactivity obtained using a 3-D core neutronics model and a complete system description. First exercise was selected because traditionally the PWR MSLB transient was being modeled with the point kinetics approximation. By choosing the point kinetics approximation, several extremely conservative assumptions has to be taken. These assumptions are generally taken in order to account for

the asymmetry in the core region that takes place during the transient. By considering these conservative assumptions the analysis becomes very limited in terms of the total power upgrades and extension of fuel cycles analysis. Also by considering a point kinetics approach, the spatial changes of the power density could not be capt by the nature of the approximation itself. This point kinetics plant simulation exercise intends to provide a detailed description of the simulated main steam line break transient specified for OECD PWR MSLB benchmark problem [16–19]. To overcome some of the limitations of the point kinetics approach, the reactivity feedback components were spatially weighted in radial and axial directions. Nevertheless some parameters should be preserved when running a point kinetics approach is made, in order to make the obtained results comparable with the 3D NK.TH approach. These parameters include: Tripped rod worth; Radial power distribution; Axial power distribution; moderator temperature coefficient; Doppler coefficient and some Kinetics parameters. In the same way some initial boundary conditions need to be identical, these conditions are: Power level; Boron concentration; Axial power shape of the rods; *Xe* distribution and moderator temperature. A list of neutronic parameters and transient assumptions was distributed to the participants. Finally a standard techniques for comparison data was established in order to compare different calculations. This standard methodology for comparing date consists in 4 steps:

- Step 1: Isolate points of interest
- Step 2: Calculate mean values and standard deviations
- Step 3: Identify outliers and recalculate mean, if necessary
- Step 4: Determine and report the deviation and figure of merit for each participants value

At the end of the second report, a multiple comparison in between the different participants calculations was made. The key analyzed points where: Break mass flow rate, Reactor power; Pressure; temperatures; Reactivity and steam generator mass. First evaluation of the problem was achieved in this stage of the OECD PWR MSLB benchmark [16–19].

Third report consists in a coupled 3-D neutronics thermal-hydraulics evaluation of core response calculation. The aim of this third exercise of the OECD PWR MSLB benchmark [16–19] was to test the neutronics response to imposed thermal-hydraulic conditions. Each participant was provided with transient boundary conditions (radial distribution of mass flow rates and liquid temperatures at the core inlet, and radial averaged pressure versus time at both the core inlet and outlet), the initial axial liquid velocities,

the initial axial distribution of liquid temperatures and a complete core description. When using a 3D approach analysis, all the above mentioned extremely conservative assumptions taken into account when performing a point kinetics calculation, are not necessary. Thus the new 3D NK approach may provide a margin of return to critically status compared over the point kinetic approach. This margin may contribute to the improvement of the operational flexibility and nuclear power plant performance. In the same line as the previous exercise, there were some general specifications released to the participants of the OECD PWR MSLB benchmark [16–19] which need to be taken into account when performing the 3D NK-TH analysis in this case. These specifications cover now: Core neutronics model; Cross section library; NK-TH coupling; initial steady state conditions and transient calculations. Since the aim of this exercise is to test the neutron kinetics model over a fixed boundary conditions, the core TH boundary conditions model was made by defining an inlet condition at the vessel bottom and an outlet condition at the vessel top. The vessel in this case represents an isolated core with boundary conditions at its bottom and top. These boundary conditions are Inlet mass flow rates, Temperatures and inlet/outlet pressures. Those conditions where taken from a TRAC-P/NEM coupled calculation. After all these specifications another multiple comparison was made in the same way as the previous exercise plus a statistical analysis of normalized parameters. Some conclusions were taken at the end of this exercise. Detail of the core modeling and the coupling scheme turns out to be some significant parameters which may cause some deviation in the results. Also the spatial decay heat modeling plus the density and doppler temperatures correlations used by the thermal hydraulics code had a noticeable effect on the different calculation deviations.

Fourth part of the project is a best-estimate 3D NK-TH coupled core-plant transient model. Last exercise of the OECD PWR MSLB benchmark [16–19] was to simulate the entire transient and combine the first two exercises, fully testing the thermal-hydraulic/neutronic coupling. The different coupled codes predictions are compared and evaluated in regard to: time and value of the power peak before reactor trip; time and value of a power peak after reactor trip; Whether the system remains critical after the momentary return to power (if it occurs) for the transient duration. AS in the previous exercises several boundary conditions for the steady state and transient calculations where released, the difference in this exercise was the completely NK-TH feedback of the proposed exercise. As it was made in previous exercises, some multiple comparisons were made. The comparisons were basically made in two ways: Standard techniques for comparison of results and Statistical analysis of normalized parameters within these techniques, different key parameters were evaluated and compared. As general conclusions for the OECD PWR MSLB benchmark [16–19], a specific list of relevant parameters for comparison in each exercise has been finally determined. More

in detail it was determined that for the system behavior prediction in OECD PWR MSLB benchmark [16–19], key parameters were: The SG masses; The break flow rates; The coolant and fuel temperatures and the power. Also there is a big dependency on the TH core modeling. For the MSLB transients there is less dependency on the radial refinements of the neutronic model, this could be different for different scenarios.

As conclusions applicable to the present study, OECD PWR MSLB benchmark [16–19] was used as a guideline of how to model and behave over the different stages of the present study performed calculations. From the point kinetics input to the 3D coupled input going through the lattice physics code and cross section generation, all the knowledge learned from OECD PWR MSLB benchmark [16–19], was fully applicable to the present study.

2.2.1 PWR MSLB transient

The MSLB is the transient chosen for analysis in the present study. Within the GET group in Technical University of Catalonia there was some gained experience in MSLB scenarios on PWR's due the participation to the OECD PWR MSLB benchmark [16–19] and OECD NEA PKL-2 [50, 51] project but also due some published articles [58] which give some consistent background on the study of the MSLB scenario in Ascó NPP. Such knowledge was used in order to reproduce the MSLB scenario with the new developed models. A brief description and some results from the BEBCC (Best Estimate Base Case Calculation) selected is given in this section. This BEBCC is going to be used as a base case for the further comparison with the different methodologies and also as a base line for building the BE plus conservative assumptions case and BEPU case. Posterior analysis with conservative methodology and BEPU methodology are based in the transient presented a later sections of the present study. With all the related knowledge explained above the author consider that it is perfectly suitable to explain the selected transient and to show the BEBCC calculations in this chapter of the present study. A double ended MSLB in loop 2 is the initiating event. Immediately after the break, the high differential pressure between the steam lines causes activation of the high pressure injection systems. At the same time the turbine and the reactor are shut down. For this calculation we have postulated a control rod stuck in the withdrawn position during SCRAM. The high differential heat transfer ratio between the broken loop and the intact loop causes temperature and coolant density asymmetries in primary system, which is propagated into the core. There is some mixing effect between the three loops flows into the lower plenum, but, the cooler water mainly enters into the core region where the control rod is stuck in its fully withdrawn position. There is an increase of the total reactivity, mainly due to the density changes of the coolant (moderator). Table 2.1

shows the sequence of the main events for the calculated main steam line break scenario. Steady state values agreement can be found in table 4.4.

Table 2.1: Sequence of events in MSLB scenario.

Event	**Time (s)**
Double-ended loop 2 Main Steam Line Break opens	15.00
High differential pressure between steam lines signal. Safety Injection Signal. SCRAM signal	15.05
Steam isolation	15.50
Steam generator 2 empties	151.00
Manual AFW turbopump trip	195.00
Manual regulation of AFW valves (15%)	285.00
End of simulation	300.00

The power remains low and decreases quickly as is shown in figure 2.1. The boron injection from safety injection systems and the reactor scram reduce the power during the transient. Nevertheless, in the paper we are taking a closer look at the reactivity increase even if it remains at negative values. The reasons for the increase in reactivity are the local moderator density and the fuel temperature changes as well as the stuck control rod in its withdrawn position. The total reactivity evolution as function of time plus reactivity components are shown in figure 2.2. The three phenomena occur in the core region where a control rod is stuck in the withdrawn position and also where the main part of the coolant flow coming from the broken loops passes through. Figure 2.3 shows the 3D power distribution at steady state condition. The rest of the 3D graphics (figures 2.4, 2.5, 2.6, 2.7 and 2.8) show the evolution of the power during the SCRAM time when the total power decreases from 100% to almost 10% in 25.0 seconds window. These figures are divided in steps of 5.0 seconds wide each step. Notice the Z axis is a relative power. Also the influence of the control rod banks can bee seen in these plots, thus some local depression of the power is observed in the places where the control rod banks are inserted.

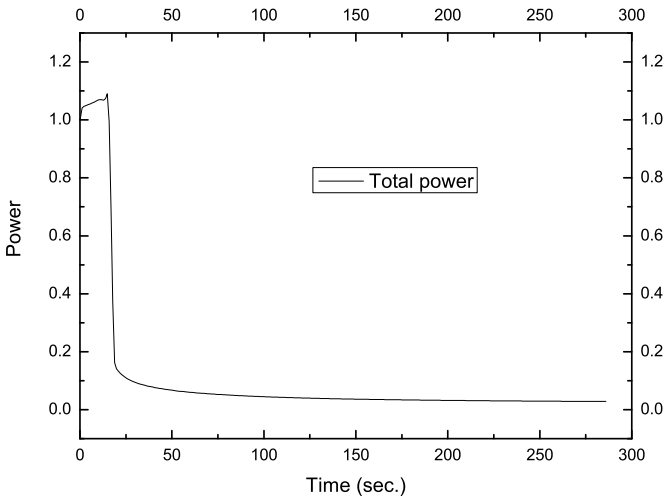

FIGURE 2.1: Total Power Best Estimate Base Case Calculation.

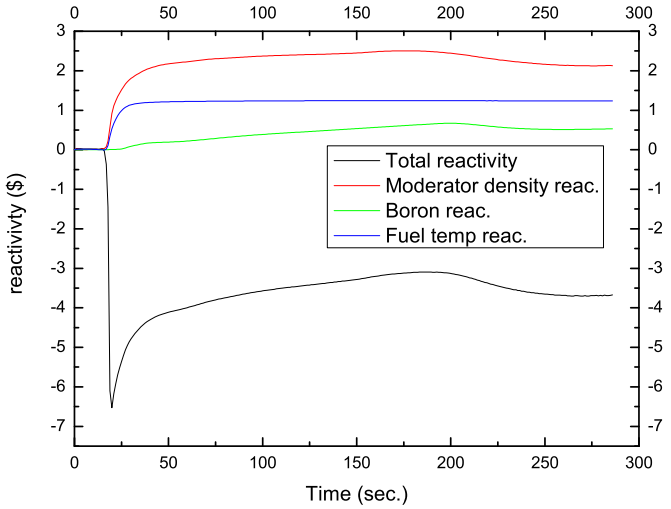

FIGURE 2.2: Total reactivity and its components in BEBCC.

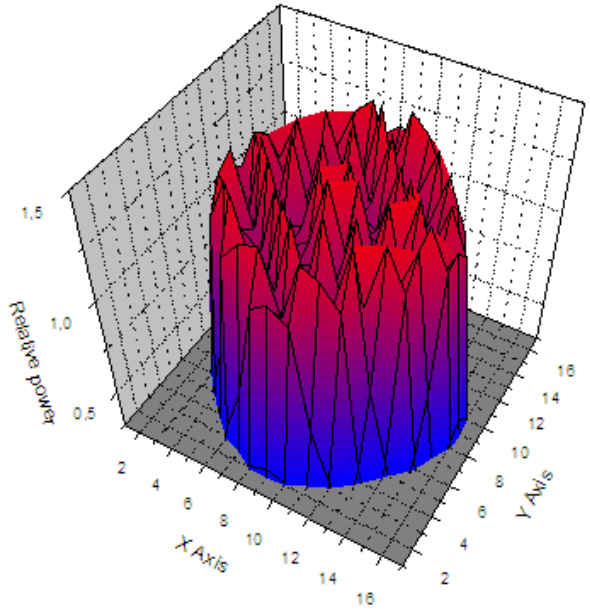

FIGURE 2.3: 3D power distribution at steady state.

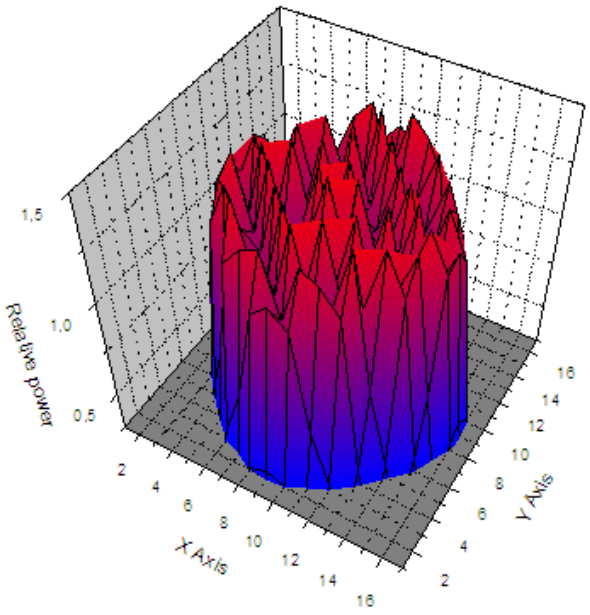

FIGURE 2.4: 3D power distribution during transient step 1.

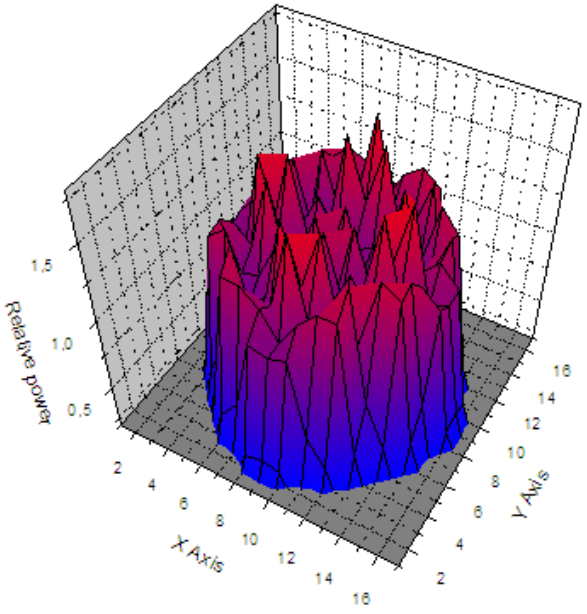

FIGURE 2.5: 3D power distribution during transient step 2.

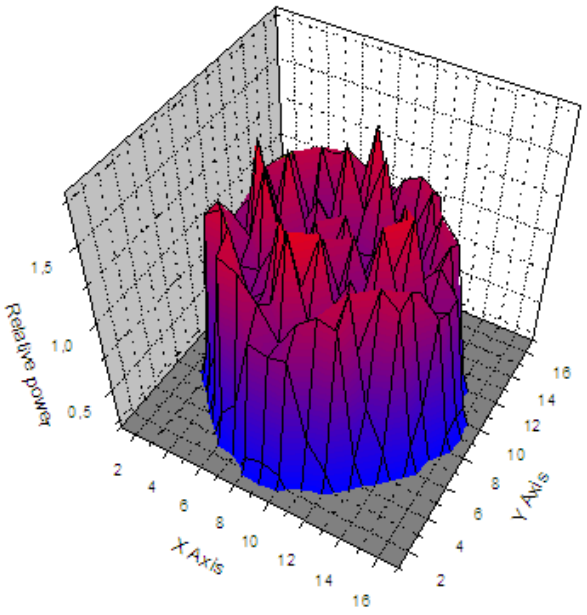

FIGURE 2.6: 3D power distribution during transient step 3.

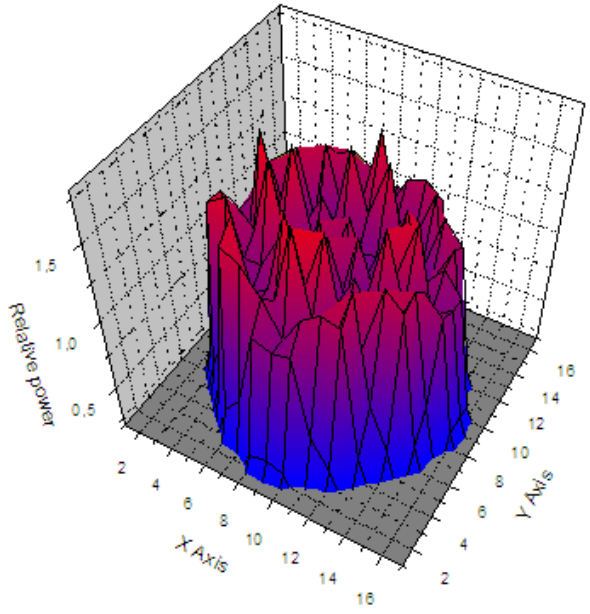

FIGURE 2.7: 3D power distribution during transient step 4.

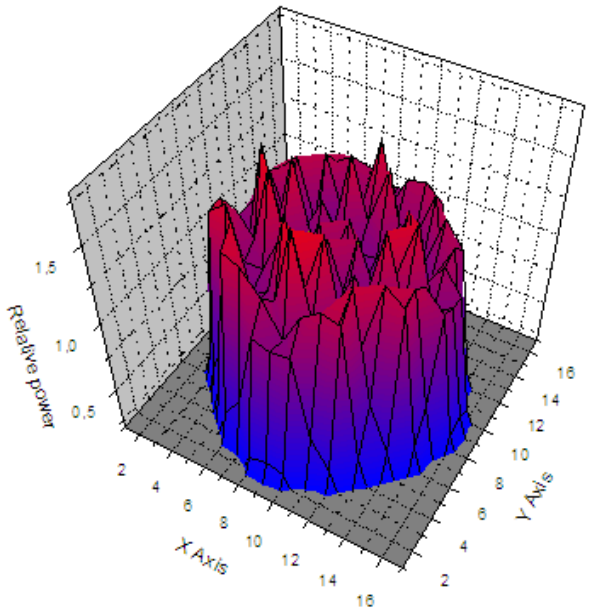

FIGURE 2.8: 3D power distribution during transient step 5.

2.3 PKL project

As it has been mentioned before the MSLB scenario is also been studied by the author of the present study by the participation in the OECD NEA PKL-2 [50, 51] project. OECD

NEA PKL-2 [50, 51] project is an extensive test programme which aims to investigate PWR's design concepts and PWR's safety issues. The OECD NEA PKL-2 [50, 51] project is mostly focused on boron precipitation processes and complex heat transfer mechanisms which may occur after some postulated scenarios. PKL facility consist in a AREVA's owned facility located in Germany which performs a serial of tests which are benchmark by several organizations world wide. OECD NEA PKL-2 [50, 51] project is been carried out for several years in different phases:

- G1: Systematic investigation of the heat transfer mechanisms in the SGs in presence of nitrogen, steam and water (2 tests, performed in July and August 2008)
- G2: Cool-down procedures with SGs isolated and emptied on the secondary side (1 test, 3 runs performed in December 2008)
- G3: Fast cool-down transients (main steam line break) (1 test, performed in July 2009)
- G4: Accident situation under reflux condenser conditions for new PWR design concept (1 test with two runs, performed in December 2009)
- G5: Boron precipitation following large break loss of coolant accidents.
- G6: RCS cool-down with void formation in RPV upper head (1 test performed in April 2011)
- G7: Counterpart Test with ROSA / LSTF on small break LOCA with Accident Management procedures (1 test performed in July 2011)

From the previous list it can be observed that several phenomenon will be studied in the framework of the OECD NEA PKL-2 [50, 51] project. From SG's heat transfer mechanisms to cool-down scenarios (procedures and fast cool-down transients) also Boron precipitation after LB-LOCA and studies over the RCS cool-down with the presence of void in the RPV upper head are covered in this project. Literature, simulations and analysis over this project are very extensive. Nevertheless in the framework of the present study, G3.1 test participation become relevant to the author of this thesis report because it has helped to achieve a better understanding of the phenomena carried out during the MSLB scenario specially with the heat transfer mechanisms.

Participation to the PKL-2 G3.1 [50, 51] test was made by using a RELAP5 3.3 [41–49] model held by the GET in Technical University of Catalonia. The important phenomena which can be observed in this scenario are for the primary side: Heat transfer to secondary side; Cool down rate and temperature distribution in U-tubes; Natural

circulation (single phase); PRZ thermal-hydraulics; Flow rate through the valve (PZR safety valve); Stratification in RCS legs (horizontal) during ECCS injection and Boron transport and mixing in (not applicable to PKL [50, 51]) during the ECCS injection. For the secondary side: Cool down rate; Flashing; Void fraction; Energy release from structures; Liquid entrainment/water separation; Main steam flow (flow rate through the break) and Heat transfer from the primary side.

Table 2.2: PKL-2 test G3.1, general information on the nodalization and the code option.

1	**ADOPTED CODE RESOURCES**	
1.1	Total number of hydraulic components primary side	224
1.2	Total number of hydraulic components secondary side (1 SG only vessel)	21
1.3	Total number of hydraulic components	322
1.4	Total number of hydraulic nodes (meshes) primary side	240
1.5	Total number of hydraulic nodes secondary side (1 SG only vessel)	23
1.6	Total number of hydraulic nodes (meshes)	348
1.7	Total number of heat structures	331
1.8	Total number of mesh points in the heat structures	1356
1.9	Total number of core active structures	3
1.10	Total number of core radial meshes in the active structures	54
2	**NODALIZATION FEATURES**	
2.1	Number of modeled loops	4
2.2	Number of DC tubes modeled	2
2.3	Number of volumes modeling the DC annular region	2
2.4	Number of U-tubes per SG	1
2.5	Number of axial meshes of each SG U-tubes (only one SG)	20
2.6	Length of each SG U-tubes (only one SG), [m]	18.942
2.7	Core model (3-D or 1-D component)	1-D
2.8	N. of hydraulic channels in core region (ring and angular sectors for 3D components)	1
2.9	Crossflow junctions between parallel channels in the core (YES or NO)	NO
3	**CODE OPTIONS**	
3.1	Chocked flow model (e.g. Ramson-Trapp, Henry Fauske, etc.)	Ramson-Trapp
3.2	SEPARATOR or DRYER models in SG dome (YES or NO)	YES
3.3	Specific models activated in PRZ (YES or NO)	NO

The studied scenario consists in a MSLB transient divided in two phases the first is based on the 0.1A BRK (from the start of the transient to 1030s) the events observed in this phase are a sharp pressure/temperature decrease and boil-off in affected SG followed by an increase of the heat transfer from primary to secondary side and a cool down transient on the primary side in the affected loop. The second phase is the HPIS injection in loop

number 1 and number 4 (from 1030s to the end of the transient), the events observed during this phase II are an Increase of the primary pressure and the PZR fill level and PZR safety valve opens and limits primary side pressure at about 42 bar. Finally the general boundary conditions consist in a 0.1 A break inside containment; Hot stand by conditions; All MS-isolation valves closed before start of test (unaffected SG's are isolated from the break); All SG's are isolated from feed water system; RCP's are shut off at start of test (coast down); No 100K/h cool-down procedure of SG secondaries; Safety injection pumps in operation during phase 2. Table 2.2 show general information on the nodalization and the code option of the Technical University of Catalonia developed model. It is to mention, that for the choked flow model Ramson-Trap [59], *0.55* was used as a sub-cooled discharge coefficient and *0.14* as a Two-phase discharge coefficient. Figure 2.9 and 2.10 show the nodalization of the broken loop main steam line. A fine nodalization was performed in order to simulate with more accuracy the discharge phenomenon occurred in the broken main steam line. The line was divided in 43 nodes before break valve and a time dependent volume was modeled after the valve. A discharge coefficient of 0.58 was used to adjust the full clearing of the broken Steam Generator with experimental time trends. Also, PRZ safety valve was modeled with PI values suggested in given documentation. Butterfly valves were implemented in each loop seal and HPI system was performed using Pressure/Mass flow rate curves in order to ensure good agreement with experimental data. They take into account the two phases of the test. Pressurizer safety valves nodalization is shown in figure 2.11.

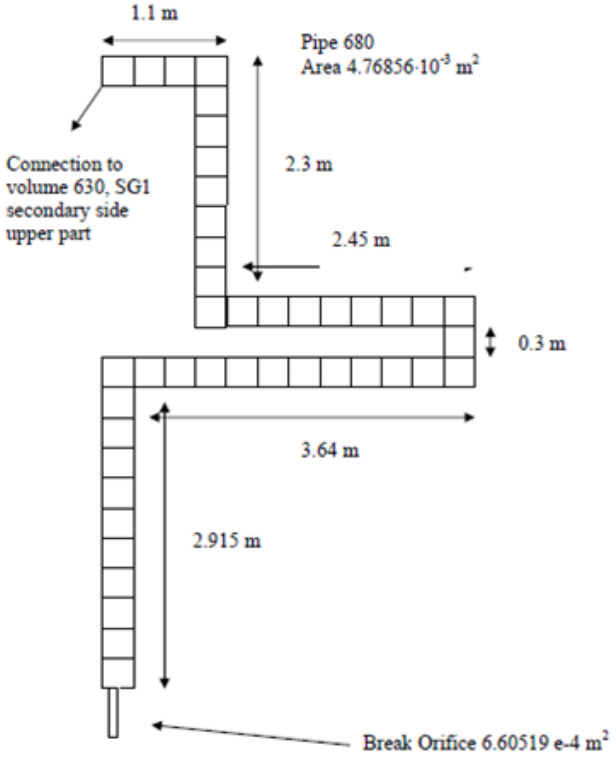

FIGURE 2.9: PKL-2 test G3.1 . Main Steam Line SG1, UPC upstream nodalization.

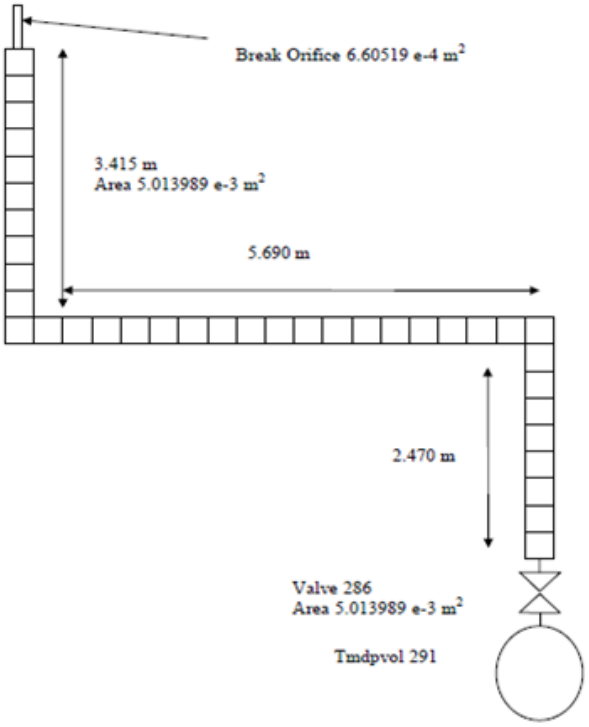

FIGURE 2.10: PKL-2 test G3.1 . Main Steam Line SG1, UPC downstream nodalization.

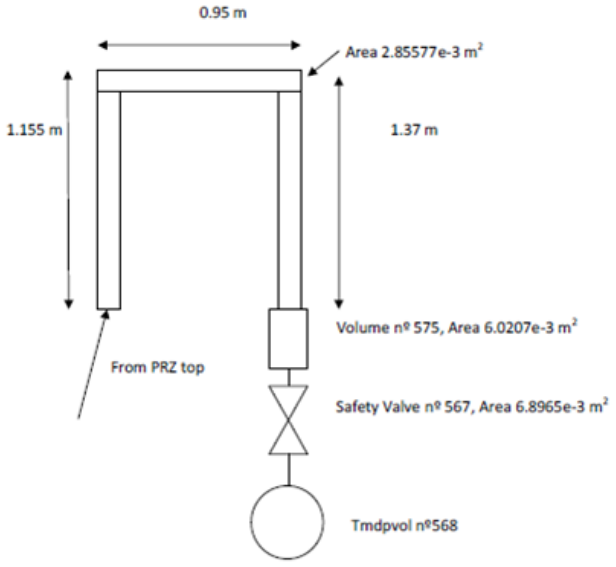

FIGURE 2.11: PKL-2 test G3.1 Pressurizer SV, UPC nodalization.

Next lines summarize the effort made in order to model that scenario and the following figures compare the obtained results with the test facility data supplied to the OECD

Table 2.3: PKL-2 test G3.1 sequence of main events.

#	EVENT DESCRIPTION	EXP (sec.)	CALC (sec.)	Note
1	Start of transient (break opening) in SG #1 steam line	0		Imposed
2	Heaters in SG#1 switched off	0		Imposed
3	Trip of the MCP and coastdown	0		Imposed
4	PRZ heaters switched off	0		Imposed
6	Butterfly valves closure	210		Imposed
7	MCPs completed stopped	210		Imposed
8	Affected SG level lower than < 8.0m		6	Delayed 15100 in ASCII data
9	Affected SG level lower than < 5.0m		48	
10	Affected SG level lower than < 2.5m		300	
11	Affected SG level lower than < 1.0m		518	
12	Affected SG level lower than < 0.1m (emptied)		690	
13	Affected SG pressure <3.0MPa		9.8	
14	Affected SG pressure <2.0MPa		61	
15	Affected SG pressure <1.0MPa		188	
16	Affected SG pressure <0.5MPa		464	
17	Minimum PRZ level		660	
18	Minimum mass flow rate		1044	
19	Minimum coolant temperature in CL#1 (Phase 1)		700	
20	Minimum core inlet temperature) (Phase 1)		700	
21	HPIS activated in loop #1 and 4	1030	1030	Imposed
22	Maximum temperature difference across SG #1 (Phase 1)		657	
23	PRZ safety valve 1st opening (steam released)		1478	PRZ pressure equal to 4.2 MPa
24	Water released through the PRZ safety valve		1774	
25	End of calculation		4500	

NEA PKL-2 G3.1 [50, 51] project participants. Table 2.3 show sequence of the main events of the studied transient, and it compare the experimental time with the computed time. Final conditions of the transient where with T core outlet = 213 $°C$ and PRZ pressure = 4.17 MPa. Starting with Figure 2.12, pressurizer pressure, a good experimental data in firstly depressurization can be observed between start of the test and second 11000. Note that the calculated line is slightly superior to the experimental data. This leads to a delay for the HPI injection and this delay will be dragged until the end of the test. Figure 2.13 show the pressure in secondary side of the SG's. The broken loop shows good agreement the experimental data, while intact loops have a slightly faster depressurization rather than experimental data. Safety relieve valve behavior is functioning with the following behavior, pressure is controlled using the pressure in the upper head (*Pcontr. = 41.5 bar*) PZR-SV opens at *42 bar* (*PRZlevel=8.5 m*), PZR safety valve closed because of pressure drop. PZR-SV opens again at 47 bar (PZR top fill level) Thereafter the PZR-SV is controlled at 42 bar. Parameters of the PI-controller for pressure control: *KP = 0.501*; *KI = 2.661.* Figure 2.14 shows the good agreement for the SG's outlet temperature. Figure 2.15 shows the hot leg temperature results compared with the plant data results. Figure 2.16 shows the Δt in the core, which also has good agreement. Figure 2.17 shows the main steam line discharge flow rate, a discharge coefficient of 0.55 was used to adjust the full clearing of the broken Steam Generator with experimental time trends.

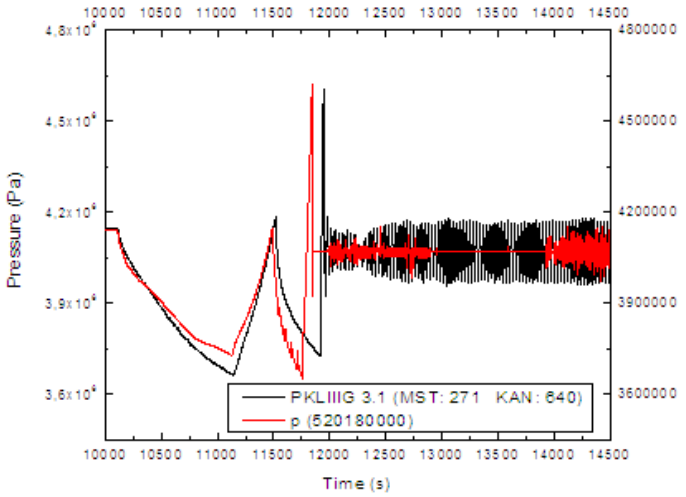

FIGURE 2.12: PKL-2 test G3.1 Pressurizer pressure.

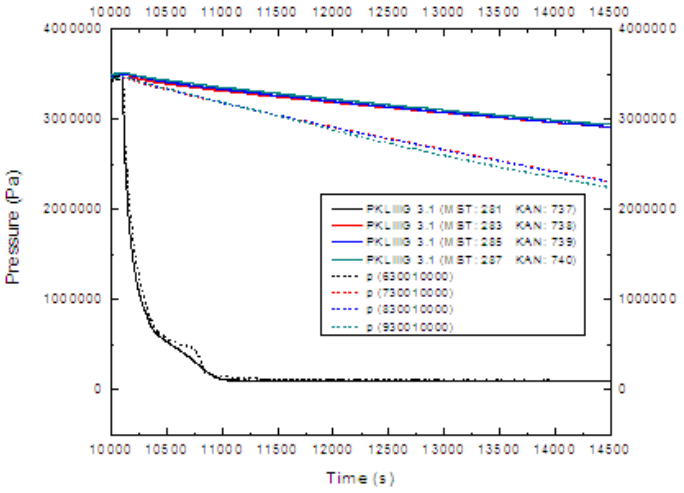

FIGURE 2.13: PKL-2 test G3.1 Steam Generator pressure.

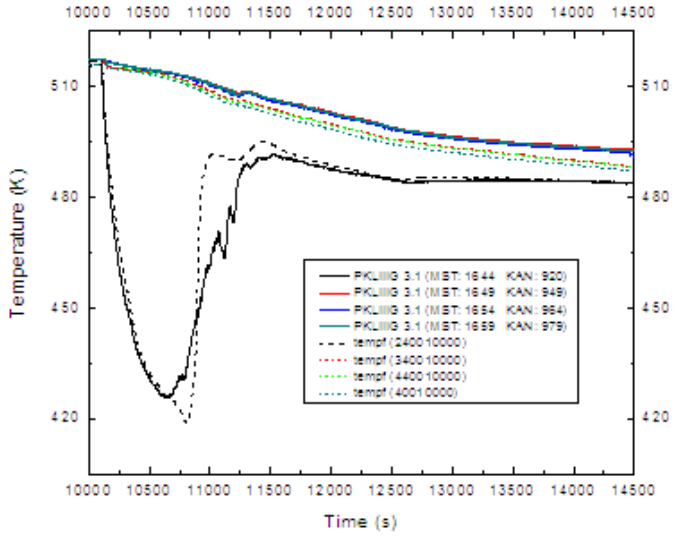

FIGURE 2.14: PKL-2 test G3.1 Steam Generator outlet pressure.

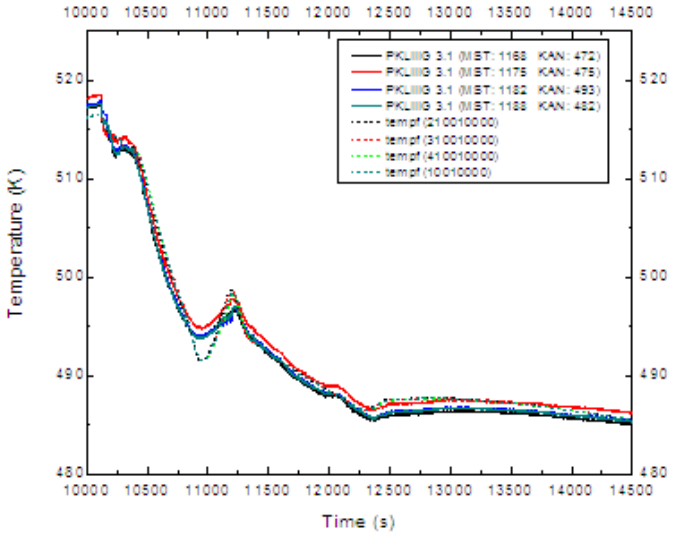

FIGURE 2.15: PKL-2 test G3.1 Hot Leg temperature.

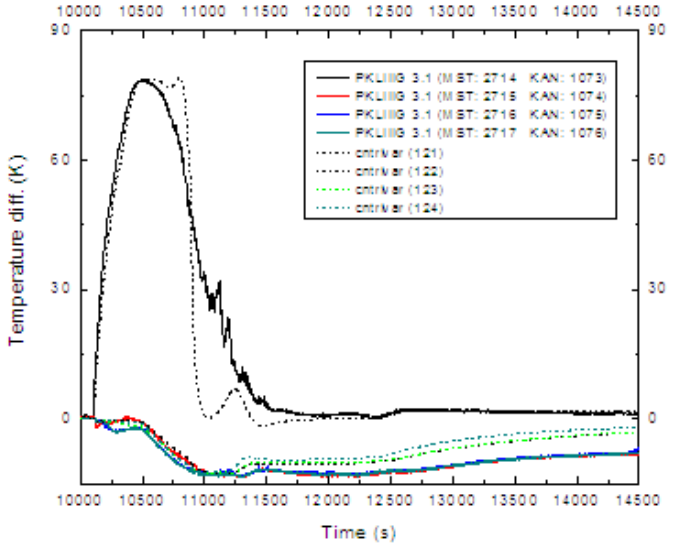

FIGURE 2.16: PKL-2 test G3.1 Delta temperature.

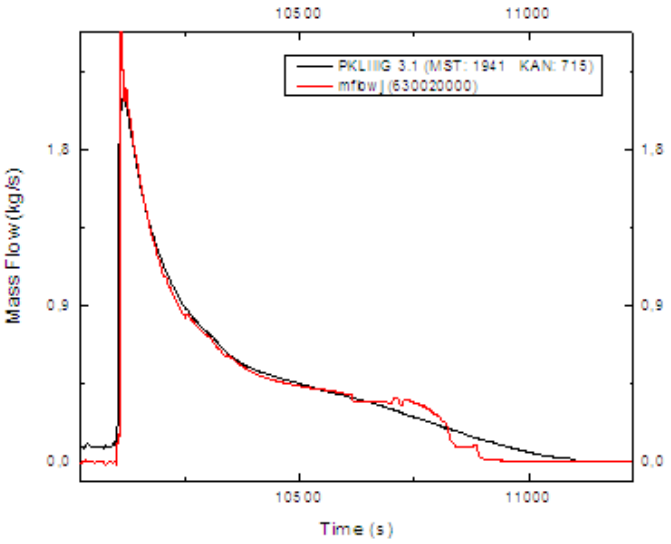

FIGURE 2.17: PKL-2 test G3.1 Break mass flow rate.

By the end of the participation of this test benchmark project, several knowledge was achieved by the author in order to be applied on the future parts of the present thesis report. Within this list we find: Brake modeling issues where applied when modeling the Ascó NPP MSLB scenario; Key parameters here described where also checked and take it into account in the posterior calculations made for this thesis report; Heat transfer (Primary to secondary) mechanism was also well identified and specially studied due its impact to the return to critically behavior for the postulated BEPU MSLB transient; ECCS injection and FW behavior was also specially studied and take it into account in the next calculations.

2.4 CRISSUE project

CRISSUE-S project [20–22] is and international effort made with the collaboration of several institutions and groups in order to establish some guidelines about the actual LWR NPP system modeling. The objectives of the CRISSUE-S project [20–22] can be summarized as follows: To establish a state-of-the-art report on the subject; To provide results of best-estimate analysis of complex transients in existing reactors; To provide recommendations to interested organizations; To identify areas of the NPP design for which the design/safety requirements can be relaxed. CRISSUE-S project [20–22] was divided in three parts:

- CRISSUE-S WP1: Data requirements and databases needed for transient simulations and qualifications
- CRISSUE-S WP2: Neutronics/Thermal-hydraulics Coupling in LWR technology: State of the art report
- CRISSUE-S WP3: Achievements and recommendations report

One of the final targets for CRISSUE-S [20–22] activity consists identify and propose an available list of coupled 3D NK-TH. Once such list is formed CRISSUE-S [20–22] activity will be used to defend "acceptability" (or required precision) thresholds for the results of these analysis. The obtained list of transients is specific to the different NPP types such as PWR, BWR and VVER. The acceptability thresholds for calculation precision are general in nature and are applicable to all LWR's. Finally it is important to remark the creation of a database for the main results of the 3D NK-TH coupled calculations. Following list shows the transients to which under the CRISSUE-S project [20–22] are recommended to be studied with 3D NK-TH tools

- PWR transients
  - **MSLB** Initiation event is a double ended guillotine break in a main steam line. SG depressurization is followed by cold water injection in the primary side, which leads cold water trough the core. As a results positive reactivity is noticed in a core region. Even there is partial mixing at the lower plenum, the cold water is causing positive reactivity in on part of the reactor, causing some asymmetries in terms of radial power distribution.
  - **LOFW-ATWS** Initiating event is in this case the suddenly blockage of the FW pumps. This event leads to a increase of temperature in the primary loop, such increase combined with the modification of moderator density and *Doppler* effect, contribute to a power decrease.
  - **CR ejection** Sudden CR ejection will lead a regional increase of reactivity, which will be a good scenario to be studied with 3D NK-TH coupling techniques due the asymmetries generated for such event.
  - **LBLOCA-DBA** Initiating event in this case is the double ended break in the cold leg in between the reactor coolant pump and the reactor pressure vessel. In this scenario, widely used for licensing, 3D NK-TH connection is justified when appears a need to quantify the conservatism introduced by the highly conservative peak factors (PF) for linear power that cause high values for peak cladding temperature (PCT).

  - **Incorrect connection (start up) of an inactive (idle) loop** In that scenario the *idle* loop is assumed to have de-borated water which might lead to asymmetries into the reactor pressure vessel.
  - **MSLB-ATWS** even this is a classical DBA transient, its recommendation to be analyzed with 3D NK-TH techniques derives from the bounding nature that this transient might have over the input reactivity of the core and the consideration that the core integrity is predicted in these scenarios.
  - **SBLOCA-ATWS** Typical transient (*TMI-type*) which is originated by small break in the primary loop. 3D NK-TH analysis is justified here due the injections of de-borated water which might flow through the core in specific regions if there is no sufficient mixture in the lower plenum.

- BWR transients
  - **TT without condenser bypass available** Initiation event is a positive pressure wave which propagates from the turbine isolation valve to the reactor pressure vessel getting into the core from the top and bottom. This cause the void fraction to collapse and such collapse causes a positive reactivity effect.
  - **LBLOCA-DBA** Rupture of a recirculation line is studied here, same considerations as the ones made for PWR's are valid in here in order to propose this transient to be analyzed with 3D NK-TH techniques.
  - **CR ejection** Sudden CR ejection will lead a regional increase of reactivity, which will be a good scenario to be studied with 3D NK-TH coupling techniques due the asymmetries generated for such event.
  - **FW temperature decrease-ATWS** Malfunction of the FW pre-heaters is supposed here, The cold FW is reaching the core causing some positive reactivity effect.
  - **MCP flow rate increase** A sudden increase of the reactor coolant flow due the malfunction of the main coolant pumps is supposed here.
  - **MSIV closure-ATWS** Also like *TT without condenser bypass available* transient, the closure of the MSIV might lead to a void fraction collapse again like FW temperature decrease-ATWS scenario a positive reactivity effect is caused by such collapse.
  - **Stability analysis** This transient is being widely investigated for the nuclear scientific community during several years. the application of the 3D NK-TH techniques is also being widely proved. the recommended transient for CRISSUE-S program [20–22] can be originated at nominal power and include MCP trip that brings the plant into the exclusion region of the BWR flow map.

  - **Stability analysis-ATWS** Same considerations as the previous scenario but assuming a failure of the SCRAM system.

- VVER transients

  - **MSLB** since the ratios between the SG water and primary circuit in VVER's are large than in PWR's, MSLB scenario is expected to less severe. Nevertheless this scenario is being selected to be studied under 3D NK-TH analysis.
  - **LOFW-ATWS** There is no special different between this scenario in PWR's and VVER's. Also, due the large amount of water, VVER's scenario is less severe than PWR's scenario.
  - **CR ejection** Sudden CR ejection will lead a regional increase of reactivity, which will be a good scenario to be studied with 3D NK-TH coupling techniques due the asymmetries generated for such event. Same considerations as the ones made for PWR's.
  - **LBLOCA-DBA** Sudden CR ejection will lead a regional increase of reactivity, which will be a good scenario to be studied with 3D NK-TH coupling techniques due the asymmetries generated for such event. Same considerations as the ones made for PWR's.
  - **Incorrect connection (start up) of an inactive (idle) loop** Since the VVER's are equipped with main isolation valves in hot leg and cold leg, this might introduce few differences on the scenarios, compared with PWR's
  - **MSLB-ATWS** Its recommendation to be analyzed with 3D NK-TH techniques derives from the bounding nature that this transient might have over the input reactivity of the core and the consideration that the core integrity is predicted in these scenarios. Same considerations as the ones made for PWR's.
  - **SBLOCA-ATWS** Typical transient (*TMI-type*) which is originated by small break in the primary loop. 3D NK-TH analysis is justified here due the injections of de-borated water which might flow through the core in specific regions if there is no sufficient mixture in the lower plenum. Same considerations as the ones made for PWR's.
  - **Isolation of one loop (ATWS)** since VVER's are equipped with main isolation valves, this new transient is also considered to be analyzed with 3D NK-TH techniques. This scenario is also considered as complement of Incorrect connection (start up) of an inactive (idle) loop.

when analyzing any nuclear reactor system transient, there is a list of key parameters to check if they are under the acceptance criteria based on the licensing, experts judgment

and safety requirements. CRISSUE-S program [20–22] also produced a reasonable minimum number of quantities of interest when performing a 3D NK-TH transient analysis. This list of quantities might vary depending on the type of transient performed and the type of reactor analyzed. Nevertheless a minimum common list is showed below. Next list will give a vision of the general quantities and its associated errors.

- **Reactor pressure vessel peak peak of pressure**. Acceptable threshold quantity error is 10% of the nominal pressure of the considered system. Acceptable threshold time error is 100% of the BE value.
- **Time of occurrence of the RPV pressure's peak**. Acceptable threshold quantity error is 2% of the nominal pressure of the considered system. Acceptable threshold time error is 100% of the BE value.
- **Peak total power if applicable**. Acceptable threshold quantity error 100% of the nominal or 300% from the initial, if initial power is smaller than nominal power. Acceptable threshold time error is 100% of the BE value.
- **CHF or DNB occurrence time**. Acceptable threshold quantity error is 20% of the nominal or 100% from the initial, if initial power is smaller than nominal power. Acceptable threshold time error is 20% of the BE value.
- **PCT occurrence time**. Acceptable threshold quantity error is 150K. Acceptable threshold time error is 20% of the BE value.
- **Maximum fuel temperature and occurrence time**. Acceptable threshold quantity error is 200K. Acceptable threshold time error is 20% of the BE value.
- **Total energy released to the fluid during the transient**. Acceptable threshold quantity error is 10% of the energy released to the fluid or 100% of the energy released to the fluid if the initial power is smaller the nominal. Acceptable threshold time error is 20% of the BE value.
- Maximum in % of the core in terms of heat transfer area where at any time rod surface area is bigger than 1000K. Acceptable threshold quantity error is 10% of the heat transfer area. Acceptable threshold time error is 20% of the BE value.
- Maximum in % of the core in terms of the volume occupied by fuel pins where at any time the fuel temperature is bigger than 3000K. Acceptable threshold quantity error is 10% of the volume occupied. Acceptable threshold time error is 20% of the BE value.

Fuel effect is being identified as one of the big contributors to the LWR's 3D NK-TH analysis. There are multiple fuel factors which could effect on the general 3D NK-TH analysis. Among these factors we find: burnup, power distribution, materials; power peaks; history exposure; general thermo-physical properties of the fuel and fuel failure mechanisms. Concerning the thermo-physical properties of the fuel materials, the recommended library to be used is MATPRO. Fuel failure mechanisms are been also identified as a big contributors in 3D NK-TH analysis. Besides the fuel degradation takes place during the life of the reactor, it could also appears some fuel degradation during the transient time. CRISSUE-S program [20–22] identify and explain the effects of the following fuel failure mechanisms: Manufacturing defects, Primary hydriding; Pellet-clad interaction; Corrosion; Dry-out, Cladding collapse; Grid-rod fretting; debris fretting; Baffle jetting and Assembly damage.

The best estimated approach was also made in CRISSUE-S program [20–22]. First a BE versus conservative approach was made in order to evaluate the uncertainties. Once the uncertainties were identified, those were classified in fuel-related uncertainties. These ones where identified as radiolysis in fast reactivity transients; Dynamic sub-cooled boiling; Dynamic CHF; Volume void weighting on heat transfer surface for two fluids; Spacers with mixing vanes. The other source of uncertainties were identified as the uncertainties related to other phenomena or to components. The list for that type of uncertainties is: Valve characteristics; Frictional and discrete pressure losses; Phase separation at tee's; high transient thermal flux and positive pressure pulse propagation. Last type of uncertainties are the ones related to models and codes. The way of the heat transfer inside the pin; the fuel modeling and the use of the neutron diffusion equation and the associated uncertainties due the methodologies used to solve it and the assumptions taken in order to simplify the problem determine this uncertainties type classification. CIAU method was used to determine the uncertainties, besides that in the framework of CRISSUE-S program [20–22] the CIAU method was extended a number of neutron kinetics parameters which contain uncertainties on the basis of a NK-TH calculation. These parameters are: Rod worth ±10% or ±15% (depending on the reference; Fraction of delayed neutrons β ±5%; Doppler coefficient ±20%; Moderator coefficient ±30%; fuel heat capacity ±10% (this is relevant to the TH parameter); Change in the reactivity unit per change in the fuel and moderator temperature when fuel an moderator are ate the same temperature $\pm 3.6x10^{-4}$ $\Delta\rho/^{\circ}C$; Critical boron concentration at 100% of the core power $\pm 50ppm$; power distribution (at intermediate level and at 100% power) ±0.1 *relative power density for each measured fuel assembly.

CRISSUE-S program also identify a list of tools capable to perform the 3D NK-TH analysis. Starting with the thermal hydraulic codes: ATHLET; RELAP5 (NRC version)[41–49]; RELAP5-3D [31–35] (DOE version); CATHARE-2; TRAC-P, TRAC-M; TRAC-B

and POLCA-T. Available neutron kinetics codes: DYN3D; NEM; NESTLE; PARCS [4, 5] and QUABOX. Cross sections generator codes: CASMO, HELIOS and SCALE. Finally some coupled systems like: TRACE-PARCS [1–3] and [4, 5]; RELAP5-PARCS [41–49], [4, 5] and , RELAP5-NESTLE [31–35] and SIMTRAN.

Finally a database with the transient analysis results and qualifications requirements is made. CRISSUE-S program [20–22] sets up a list of requirements that should be taken into account when doing safety analysis with 3D NK-TH codes. These requirements are classified in four points. In the first point the CRISSUE-S program [20–22] gives some guidelines over the level of detail of the input deck. Second point gives guidelines and requirements for the thermal hydraulic nodalization with some acceptability criteria for the thermal hydraulic nodalization at steady state and transient steps. Third step gives the guidelines for the neutron kinetics input deck requirements and qualification. Last point is about the qualification requirements for the coupled input. Once all the qualification requirements are been exposed, CRISSUE-S document [20–22], exposes a list of transient related general acceptance criteria to be used in different transients evaluated during the stages of the program. These general acceptance criteria cover BWR stability transient, ATWS transients and rod ejection event transients. This issue is used as a linkage between the regulatory bodies (licensing works) and 3D NK-TH techniques.

At the end the knowledge achieved from CRISSUE-S program [20–22] is being useful for industry, regulatory bodies and researchers. A base guideline is being setup from the point of view of 3D NK-TH techniques. The present study was based since the beginning over the CRISSUE-S project recommendations [20–22]. Starting with the model development (Thermal hydraulic model, Neutron kinetic model and coupled model) and continuing with the BEPU analysis considerations. Key parameters to be studied in the present report where also selected within the framework of the CRISSUE-S program [20–22]. Finally base case transient used in the present study was also selected according the CRISSUE-S program [20–22] recommendations.

2.5 PIRT's studies

Phenomenon Identification and Ranking Tables (PIRT's) [10–15] technique is a structured process to identify safety-relevant/safety-significant phenomena and assess the importance and knowledge base by ranking the phenomena in order to meet some decision-making objective. PIRT has been applied to many nuclear technology issues including nuclear analysis in order to help guide research or develop regulatory requirements. PIRT methodology was developed in the 1980's and it has been widely used ever since.

Some decisions where taken during the development of the present work specially when selecting the relevant parameters to be uncertainty propagated in the BEPU calculations performed at the latest sections of this study. These decisions where taken over the extensive literature used to identify the relevant phenomenon involved in the studies scenario, but also where taken over the decision of the advisors (i.e. Ph. D advisors in NK and TH parts respectively) and over the suggestions of the current author of the present thesis report. In that way Literature recommendations, expert advice and user experienced tests where the contributors of the PIRT selection presented in the BEPU calculations chapter. In this section a demonstration of a PIRT's methodology is given in order to make clear the selection made when performing a BEPU analysis at later phases of this report. The PIRT's process starts by identifying different phenomena and ranking them by using some criteria which will generate a table from where will be easy to identify the most important phenomenon related to a specific issue. During this phenomena identification, uncertainties associated to each phenomenon needs also to be identified. The selected phenomenon are conditions of a particular reactor, system, component, a physical or engineering approximation, a reactor parameter, or anything else that might influence in the selected analyzed scenario. Each phenomenon is characterized by two three-leveled scales. First three-leveled scale is called *Importance*, which determine the relevance from each phenomenon over the figure of merit (Figure of Merit, FoM: represents the most relevance time trends in the studied scenario). The levels for this scale are *High/Medium/Low*. *High* implies that the ranked parameter has control (i.e. big impact) over the FoM, thus its accuracy should be very high not to introduce big perturbations. *Medium* implies that the ranked phenomenon has a moderate impact over the FoM, and its accuracy is not as critical as the previous group. Finally *Low* tells that the phenomenon has no impact or minimal over the FoM. Second three-leveled scale is called *Knowledge*, which determine the knowledge over the phenomenon. The levels for this scale are *Known/Partially Known/Unknown*. These levels of knowledge are well quantified and *Known* means fully or almost fully known (more than 75% of what we could expect to know). *Partially Known* means knowledge base is moderate (25% to 75% of the knowledge base is established). Finally *Unknown* means knowledge base is low (less than 25% of the knowledge base is established). As a conclusion from the last scale, if there is any phenomenon tag as *Known* there is no suggested research to this phenomenon, on the other way if there is any *Unknown* phenomenon a research over this phenomenon is a priority excluding the case where this phenomenon is being ranked as *Low importance* in the previous scale. Finally a *Partially Known* phenomenon implies the a research over this phenomenon is suggested if in the previous scale the same phenomenon was tag as *High importance* phenomenon. There are several existing PIRT's applications in thermal-hydraulics, severe accidents, fuels, materials degradation, and nuclear analysis. For each case there is a different objective and the

basic, above mentioned, PIRT's methodology is being modified in order to achieve its particular objectives. Some examples of the regulatory bodies supported PIRT's studies are related with: Rod Ejection Accidents for Pressurized Water Reactors; Power Oscillations Without Scram for Boiling Water Reactors; Burnup Credit in Spent Fuel Casks; Coolant Void Reactivity for the ACR-700 Design and Steady State Power Distribution for the ACR-700. The selected figures of merit in the present study where the total power and the total reactivity time trends...to cite some of them, this list is enormous and covers different areas of the nuclear science. The FoM where reduced to two in the present report, since these were the ones with more relevance within the 3D NK-TH coupled analysis. After this process several tables ar built with the specifications from each phenomenon. Table 2.4 shows an example of one of these tables based on the Rod Ejection Accident in a Pressurized Water Reactor analysis, in that particular case, PIRT objective was to understand high burnup fuel behavior under reactivity initiated accidents in order to be able to define research needs and help develop new regulatory criteria.

TABLE 2.4: Example of a PIRT's table

		IMPORTANCE				UNCERTAINTY			
Subcategory	Phenomenon	H	M	L	IR	K	P	U	KR
Calculation of power history	Ejected control rod worth	12	0	0	100	13	0	0	100
	Rate of reactivity insertion	3	5	1	61	10	3	0	88
	Moderator feedback	0	6	2	38	12	2	0	93
	Fuel temperature feedback	12	0	0	100	12	1	0	96
	Delayed neutron fraction	10	1	0	95	13	1	0	96
	Reactor trip reactivity	0	0	10	0	13	1	0	96
	Fuel cycle design	11	2	0	92	12	0	0	100

Where the selected figure of merit was, in this particular case, a calculation of the power history during a pulse (including the width of the pulse). In that shown particular case there where 22 experts in order to determine the importance and uncertainty criteria. The numbers on the table represents the amount of experts which consider the selected

option in each case. Since some experts declined to answer in some selections, a importance ratio ***IR*** and a knowledge ratio ***KR*** was built to measure the real impact of each parameter. These ratios were defined like $100 * (S_1 + S_2/2)/(S_1 + S_2 + S_3)$, where S_n go from the highest importance and the most well known to the lowest importance to the most unknown, 1 to 3.

Since the aim of the present work is to use these PIRT's studies as a tool rather than develop a list of a significant PIRT's which may have impact on the type of analysis in here performed. The selection of the perturbed parameters and its associated uncertainties was taken under thesis advisors and author experience and reviewed literature from PWR MSLB transient analysis. In that way the full methodology (which is the big goal of the present study) was shown and place to its improvement in future works was also left.

2.6 Uncertainties overview

As it has been mentioned previously in this thesis report, the general tendency on the safety analysis in Nuclear Reactors has been moved gradually from a Conservative approximation to the Best Estimate Plus Uncertainties analysis. BEPU analysis are based in considering the different associated uncertainties such: plant uncertainties, representation uncertainties, code uncertainties rather than using a expert limit determination used in the Conservative approach. Wilks studies [52–57] play and important role when performing a BEPU calculation. Basically Wilks [52–57] studies will be used to determine the number of minimum calculations required in BEPU analysis to ensure a quantity level of the analysis. Nevertheless at the present moment, USA Code of Federal Regulation (CFR) 10 CFR 50.46 [54] allows either to use the Conservative approximation or best estimate plus identification and quantification of the uncertainties methodologies when performing such type of analysis. In the past the conservative analysis was used in order to avoid the longer computational costs related to BEPU methodology and also to avoid the cost of developing a more realistic model. The status of the BEPU calculations and its improvements over the classical Conservative approach can be seen in Figure 2.18 which shows the relationship between the Safety limit for a determined value, the acceptance criteria imposed by the regulatory body and the real value. The right side of the picture represents the classical conservative assumption used for years in the Nuclear Industry. On the other hand, the left side from Figure 2.18 represents the BEPU approximation. Where there is a Upper and Lower limit of the calculated uncertainty, which determine the range of that particular uncertainty associated with the studied value. The Margin to acceptance criteria is being reduced but still remains

within the regulatory body acceptance criteria margin. Also in Figure 2.18 situation of the classical Conservative value can be observed. Values in the Conservative approach are expressed in terms of a set of calculated conservative values of parameters limited by acceptance criteria. Values in a BEPU approach are expressed in terms of uncertainty ranges for the calculated parameters. Typically the conservative approach falls closer to the acceptance criteria over the uncertainty range. This type of theoretical situation is the one expected to be found at the end of this report, when performing the comparison between different methodologies results. A good agreement with the theoretical results, here presented, will confirm the roughness of the obtained results.

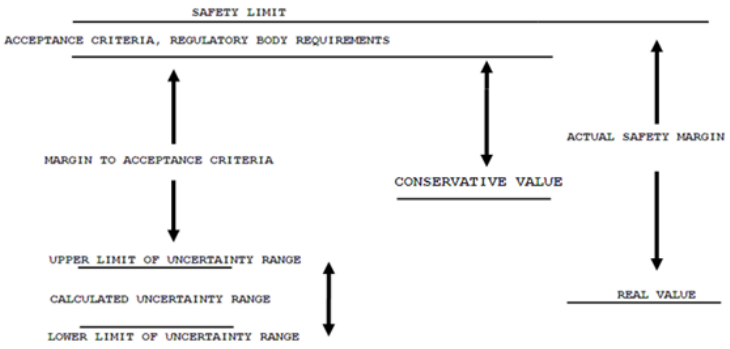

FIGURE 2.18: Safety margins overview.

There are different ways of combining the existing computer codes with data in order to obtain a certain type of analysis. The most common approaches used in Conservative and BEPU methodologies are summarized in Table 2.5. Several options are available besides some of them are not usually used. Starting with *Option a*, this is well known as a fully conservative approach and it was widely used over the 70's. The use of this methodology is no longer supported by the international community since some deficiencies such prediction of unrealistic behaviors was detected. *Options b* and *c* are the most common used at the present moment and they are the chosen ones in the development of the present thesis report. they combine the use of a Best Estimate computer code with conservative assumptions or with uncertainties associated with the input data requirements. Finally *Option d* combines the use of a Best Estimate computer code with the system's availability deduced form the probability safety analysis assumptions.

Source of uncertainties need also to be identified within the framework of any BEPU calculation. The source of uncertainty can vary from the code or model uncertainties which represents those uncertainties associated with the incorporated solutions within the used code (i.e. flow regimes, velocities, field equations, material properties...) and

those ones related to the models used in the code (i.e. heat transfer model, GAP conductance model, fission product release model...). Another identified source of uncertainties is called the representation uncertainties, these deal about the way the system is being represented (i.e. nodalization, mesh, cells...). Scaling related uncertainties are another type to consider and they deal about the scaling laws used when doing a full scale system. Plan effect uncertainties also need to be considered, these represents the uncertainties associated with the values measured from the plant. Finally there is a user effect source of uncertainties which may also cause some discrepancies and it should be very carefully treated, knowledge achieved from the different international projects and benchmarks should help to minimize this type of source of uncertainties.

TABLE 2.5: Combinations of a computer code an input data

Option	Computer code	Availability of systems	Initial and boundary conditions
a	Conservative	Conservative Assumptions	Conservative input data
b	Best Estimate	Conservative Assumptions	Conservative input data
c	Best Estimate	Conservative Assumptions	Realistic input data with uncertainties
d	Best Estimate	probabilistic safety analysis based assumptions	Realistic input data with uncertainties

When performing a BEPU analysis a tolerance interval and tolerance limits need to be defined. Starting with tolerance interval, this is defined as a random interval that contains with probability (or confidence) β at least a fraction γ of the population under study. About the tolerance limits, this is a sampling methodology to reduce the sample size. There are two types of tolerance limits: First type is a non-parametric tolerance limits where nothing is known about variable's probability distribution functions (PDF's) except that it is continuous; Second type is a parametric tolerance limits where the variable's PDF's is known and only some distribution parameters involved are unknown. The problem in any of the previous options is to determine a tolerance range for a random variable x represented by the observed sample, $x_l, ..., x_n$, and the corresponding size of the sample. By using these two parameters the calculation will give some results inside a desired range of confidence and probability without running thousands of calculations. In that sense, Wilks' formula is needed in order to ensure some quality in the results when performing a BEPU analysis.

When applying the Wilks studies, the required minimum number of calculations n are given by the by Wilks' formula [52–57]. These number n of code calculations depends

on two parameters: First is the requested probability content γ; Second is confidence level of the statistical tolerance limits used in the uncertainty statements of the results β. Wilks' formula can be expressed for one or two-sided statistical tolerance intervals. Equation 2.1 show the relationship between Confidence level, Probability and number of runs for one side statistical tolerance limit and equation 2.2 the same as the previous one but for the two sided statistical tolerance limits.

$$1 - \gamma^n \geq \beta \tag{2.1}$$

$$1 - \gamma^n - n(1-\gamma)\gamma^{n-1} \geq \beta \tag{2.2}$$

From the previous expressions $\beta\times100$ is the confidence level (%), $\gamma\times100$ is the probability (%) and n is the number of runs. Within the framework of the present study, the BEPU methodology in 3D NK-TH was intended to be illustrated thus $\beta = 95\%$ plus $P = 95\%$ was selected since it was found as the minimum required to show the methodology, this ends up with $n = 59$ which are the minimum number of runs required to ensure the 95% of Confidence over the 95% of probability for one sided statistical tolerance intervals. Nevertheless as an example, in Table 2.6, different combinations between 90%, 95% and 99% from β and γ over the one or two sided tolerance limits are shown. It can be observed that number of required runs increase from one sided statistical tolerance method to two-sided ones, and also increase while β and γ increases. In the present study the number of runs was calculated by DAKOTA [6–9] code. The probability distribution functions (PDF's) are used in this method to determine the chances of appearance from each parameter over the uncertainty range, with that method some values are more likely to appear that other. This fact is taken into account with the PDF's. Different PDF's are used for different parameters depending on its nature and its estimated distribution. These PDF's will determine the value for each parameter over the calculated runs. Deviation and mean value are need in order to perform such selection.

TABLE 2.6: Minimum number of calculations n for one-sided and two-sided statistical tolerance limits.

	One-sided statistical tolerance limits			Two-sided statistical tolerance limits		
$\beta\rightarrow/\gamma\downarrow$	0.90	0.95	0.99	0.90	0.95	0.99
0.90	22	45	230	38	77	388
0.95	29	59	299	46	93	473
0.99	44	90	459	64	130	662

2.7 OECD UAM LWR benchmark

Finally OECD UAM LWR benchmark [23] is the latest benchmark started in time and it has been widely used as a reference document within the development of the present thesis report. OECD UAM LWR benchmark [23] objective is to define, conduct, and summarize an OECD benchmark for uncertainty analysis in best-estimate coupled code calculations for design, operation, and safety analysis of the LWR's. Reference systems and scenarios for coupled code analysis are defined to study the uncertainty effects for all stages of the system calculations. Measured data from plant operation are available for the chosen scenarios. GET group is actively participating in this benchmark, nevertheless actual stage of the benchmark is some stages before than what is proposed in this report, the general idea of the benchmark is used as a guideline for the development of the present thesis report. Besides that, GET group is actively participating in OECD UAM LWR benchmark [23] in different stages in parallel. The benchmark is very ambitions and it could not be feasible few years ago due the level of the computing tools, nowadays the computational capacity has increased and a full scope uncertainties propagation is feasible to be accomplished. The general ideas of the OECD UAM LWR benchmark [23] projects are: To subdivide the complex system/scenario into several steps (also called exercises); To identify input, output and assumptions for each step; To calculate the uncertainty in each step and to propagate the uncertainty for the evaluation of the overall system/scenario. Also there is a list of steps to be taken in order to achieve the objectives of the benchmark, the listed steps try to cover the full scope of the Uncertainty propagation.

First step will be to do the derivation of the multi-group microscopic cross-section libraries (nuclear data, selection of multi-group structure, etc.). The second step will be the derivation of the few-group macroscopic cross-section libraries (energy collapsing, spatial homogenization, etc.). On the third step the Criticality (steady state) stand-alone neutronics calculations (keff calculations, diffusion approximation, etc.) will be studied. Fuel thermal properties relevant for transients performance will be studied on the fourth step of the benchmark. Uncertainties over the neutron kinetics stand-alone performance (kinetics data, space-time dependence treatment, etc.) in PWR rod ejection and BWR control rod drop accidents will be studied in fifth place. Sixth step will cover the thermal-hydraulic fuel bundle performance interaction with the OECD/NRC BFBT benchmark and the available experimental data as well as the Uncertainty Analysis Exercises being performed in the framework of the BFBT benchmark. Seven steps will discuss over the coupled neutronics/thermal-hydraulics core performance(coupled steady state, coupled depletion, and coupled core transient with boundary conditions) interaction with the Peach Bottom Cycles 1, 2 and 3 operating and measured data. Last two

steps will study the uncertainties propagation over the thermal-hydraulics BWR system performance interaction with the Peach Bottom Turbine Trip and BEMUSE-3 experimental data and Coupled neutronics kinetics thermal-hydraulic core/thermal-hydraulic system BWR performance interaction with the Peach Bottom Turbine Trip experimental data and Peach Bottom stability performance interaction with EOC2 and EOC3 experimental data. It is recommended to use as much experimental data as possible when performing each one of the previous mentioned nine steps.

By following the proposed methodology steps at the end of the benchmark it is intend to held a mixture of information from ITF, NPP and analytical data which will be compared with the current uncertainty methods and as a result will produce some benefits in the different approaches to arrive at some recommendations and guidelines. As can be seen for the structure of the above mentioned nine steps, the project is quite ambitious and it intend to cover the full scope of uncertainties sources. To the above mentioned tasks in an effective way the OECD UAM project [23] is structured in the three phases with three exercises within each phase:

Phase I (Neutronics Phase)

- Exercise I-1: Derivation of the multi-group microscopic cross-section libraries (nuclear data and covariance data, selection of multi-group structure, etc.).
- Exercise I-2: Derivation of the few-group macroscopic cross-section libraries (energy collapsing, spatial homogenization of cross-sections and covariance data, etc.).
- Exercise I-3: Criticality (steady state) stand-alone neutronics calculations with confidence bounds (k_{eff} calculations, diffusion approximation, etc.)

Phase II (Core Phase)

- Exercise II-1: Fuel thermal properties relevant for transient performance.
- Exercise II-2: Neutron kinetics stand-alone performance (kinetics data, space-time dependence treatment, etc.).
- Exercise II-3: Thermal-hydraulic fuel bundle performance.

Phase III (System Phase)

- Exercise III-1: Coupled neutronics/thermal-hydraulics core performance (coupled steady state, coupled depletion, and coupled core transient with boundary conditions)

- Exercise III-2: Thermal-hydraulics system performance
- Exercise III-3: Coupled neutronics kinetics thermal-hydraulic core/thermal-hydraulic system performance

By looking at the previous list it is easy to identify that the present study should be situated at the *phase III (System Phase)*. In this thesis report, the BEPU methodology has being also applied into the system phase and it was omitted when creating the cross section library, due a separate work is held in the GET group in that knowledge area.

Since the project is still going on, there is no general conclusions which could give as some ideas to apply when performing a full scope BEPU analysis. Besides that there is an expected impact and benefits which may come from due the OECD LWR UAM benchmark [23] activity and will contribute to the LWR's safety and licensing. The expected points are: Systematic identification of uncertainty sources; Systematic consideration of uncertainty and sensitivity methods in all steps. This approach will generate a new level of accuracy and will improve transparency of complex dependencies; All results will be represented by reference results and variances and suitable tolerance limits; The dominant parameters will be identified for all physical processes; Support of the quantification of safety margins; The experiences of validation will be explicitly and quantitatively documented; Recommendations and guidelines for the application of the new methodologies will be established. At the conclusion of the present study, the models will be ready to perform a full scope BEPU analysis, for future work it will be left to implement the actual models over the OECD LWR UAM benchmark [23] derived methodologies.

Chapter 3

Codes and Models

Different qualified tools are being used when performing the present study. Some description from all of the nuclear codes used is given in the first part of this chapter. Basic field equations from the lattice physics, cross section generation and treatment, core simulator, thermal-hydraulic and uncertainty propagation codes are given here. The reader can get and idea of how complex are the problems to be solved and which are the assumptions taken by the codes in order to obtain elegant and satisfactory solutions to each phenomena which needs to be simulated. In the second part of this chapter the author's developed models are presented. These models where built from scratch by using the expertise gained in different contributions made in the chapter's two mentioned reference benchmarks, such: OECD LWR UAM benchmark [23]; OECD PWR MSLB Benchmark [16–19]; OECD NEA PKL-2 [50, 51] project and CRISSUE-S project [20–22]. Also Ph.D advisors guidance was an important asset here when building the different models. Finally some trial and error method was also used in order to obtain the best optimized model for each particular case. Some deficiencies where detected and some ways of improving the different models are given at the conclusions chapter. Nevertheless due the complexity of the BEPU calculations, the used models have being proved as the most effective ones with used computing machines.

3.1 Brief description of the codes

This section presents a review of the state of the art tools used for this Ph.D study. In that sense a brief description of the used computer codes is given here. The present study involves several codes. Since the final computation will be a Best Estimate Plus Uncertainties calculation in a coupled 3D NK-TH model, a thermal hydraulic system plant code is required to model full plant specifications. TRACE v5.0 patch 2 [1–3] was

the chosen code for the present study. A core simulator code is also required in order to simulate the code behavior under the 3D kinetics perspective. PARCS v3.0 [4, 5] which is internally coupled and compiled as one executable file, with TRACE v5.0 patch 2 [1–3] is the neutron kinetic code used. The cross section library will be the source of power used for the core simulator code. The cross section library contains all the core specifications along the life cycle of the core. An external code is needed to perform such calculations. HELIOS-1.9 [27–29] is the lattice physics code used for such purpose. Once the cross section library is created, specific code call GenPMAXS v5.0 [30] is used in order to convert data from the HELIOS-1.9 [27–29] output file to the PARCS v3.0 [4, 5] input file. No Uncertainty specifications have been considered at this point. The DAKOTA [6–9] code was chosen to perform the perturbation of several parameters from the thermal-hydraulic code and from the neutron kinetics code. Finally, all those steps have been performed, within the framework of the SNAP v.2.2.1 [60] platform. This is a visual interface that allows the user to build models; change specifications; launch calculations and essentially work with all the above mentioned codes, (except HELIOS-1.9 [27–29]) under same Windows mask.

3.1.1 TRACE

TRACE [1–3] TRAC/RELAP [41–49] Advanced Computational Engine is the selected thermal-hydraulic code for the present study, this section is giving a brief description of the code operation procedures. The version used in the current study was the TRACE v5.0 patch 2 [1–3]. TRACE [1–3] is a Best Estimate code designed to perform analysis over the different scenarios for the different types of the LWR's. As a thermal hydraulic system code TRACE [1–3] is capable to simulate all different thermal-hydraulic phenomena that may occur in test facilities and full scale reactors. The code characteristics which are used to predict different phenomena like multidimensional two phase flow, non-equilibrium thermodynamics, generalized heat transfer, reflood, level tracking, reactor kinetics, comprehensive heat transfer capability TRACE [1–3] system code is organized in cards. Within the cards the user can model the different features of the components. There are several thermal-hydraulic components available when modeling with TRACE [1–3] code: PIPE, VALVE, PUMP, PLENUM, PRIZER, CHAN, TEE, TURB, VESSEL, CONTAN and SEPD by using a combination of these components the user can build the thermal-hydraulic part from a full plant nuclear reactor system. Heat conduction properties are modeled by using: HTSTR and REPEAT-HTSTR. These elements are what we call passive heat structures elements. To produce/release heat to the fluid POWER component coupled to a HTSTR is used. There are also a FLPOWER component which is able to deliver power directly to the fluid as it can happen into waste

transmutation facilities. RADENC component are used to simulate radiation enclosures between multiple arbitrary surface. Finally FILL and BREAK components are used to create boundary conditions to the system such mass flow rates or pressures. Besides the previous list of components the code has a bigger list of CONTROL SYSTEM components which are used to simulate the plant control systems. Control system is organized in *Variables*, *Control Blocks* and *Trip System*. Starting with *variables* there are different types like: *Controlled variables* used for example to know the pressure in a tank; *Manipulated variables* (i.e. modify some conditions to achieve a desired value, valve area for example). Next part is the *control block*. *Control blocks* are functions which operate over the signals to generate a output signal according the selected function. Variables information can be modified from one block to the other with a mathematical function here is where the transfer functions take and important role. Transfer functions are functions which define gain, delays, arithmetic relationships... from one control block to the other one. Usually there is some feedback effect in the flow path where the output signal of one control block is used to feed the input path of itself in order to reduce the produced error. Finally *Trips* are ON/OFF switches that can be used to generate a hardware action (i.e. open/close a valve), to define a signal's status or to define a blocking or coincidence trip. All the previous control system are organized in a system called *control block diagram* which is giving the relationship between the above signals and the flow path of the information in between the control systems.

Thermal-hydraulic system in a LWR is very complex and thermal-hydraulic codes need to reproduce such system with enough accuracy to perform validated analysis over the different plants and scenarios. Several phenomena are involved within a thermal-hydraulic LWR system. Following list gives an idea of all the physical phenomena which are considered in TRACE [1–3] code analysis: ECC downcomer penetration and bypass, including the effects of countercurrent flow and hot walls; lower-plenum refill with entrainment and phase-separation effects; bottom-reflood and falling-film quench fronts; multidimensional flow patterns in the reactor-core and plenum regions; pool formation and countercurrent flow at the upper-core support-plate (UCSP) region; pool formation in the upper plenum; steam binding; water level tracking; average-rod and hot-rod cladding-temperature histories; direct injection of sub-cooled ECC water, without artificial mixing zones; critical flow (choking); liquid carryover during reflood; metal-water reaction; water-hammer pack and stretch effects; wall friction losses; horizontally stratified flow, including reflux cooling; gas or liquid separator modeling; non-condensable-gas effects on evaporation and condensation; dissolved-solute tracking in liquid flow; reactivity-feedback effects on reactor-core power kinetics; two-phase bottom, side, and top offtake flow of a tee side channel; reversible and irreversible form-loss flow effects on the pressure distribution. There are some limitations of use when working with TRACE

[1–3] code. Typically these type of system codes are only applicable in their assessment range of values. Notice that TRACE [1–3] is been qualified to analyze ESBWR design, conventional PWR and BWR Large and Small break LOCA. At this point TRACE [1–3] code is not being validated against BWR stability analysis or other operational transients.

What is needed to model and obtain a realistic solution from thermal hydraulic system:

- Simplified Vapor/Liquid balance equations (energy, mass and momentum).
- State relationships
  - Relationships between thermal hydraulic variables for and specific fluid, for example water or heavy water.
  - Library with all the thermophysical and thermodynamical properties ($\beta, k, C_p, ...$).
- Jump conditions
  - Link to de decoupled balance equations.
  - to express continuity of mass, momentum and energy.
  - $\Gamma_f = -\Gamma_g$
- Closure equations
  - List of correlations that computes independently interphase interactions such mass/heat exchange and dragging as well as wall-to-fluid heat exchanges and frictions.
  - Correlations set empirically through separate effects tests facilities SETS.
  - Validations through SETS's and integral test facilities ITF's.

Best Estimate codes balance equations result from a simplification of *Eulerian* equations. *Navier Stokes* equations (no viscosity) + incompressibility:

$$\frac{\partial(\rho_k \Psi_k)}{\partial t} = -\nabla \cdot (\rho_k \Psi_k \vec{W}_k) - \nabla \cdot \vec{J}_{\Psi,k} + \rho_k S_{\Psi,k} \tag{3.1}$$

First term, left handed, is variation in time, first on the right hand is convection due the fluid motion, second term on the right hand is the diffusion term last term is the volumetric source term. With the following assumptions:

- Mass balance equation $\Psi_k = 1$, $\vec{J}_{\Psi,k} = 0$ and $S_{\Psi,k} = 0$

- Momentum balance equation $\Psi_k = \vec{W}_k$, $\vec{J}_{\Psi,k} = p_k\vec{I} - \vec{\tau}_k$ and $S_{\Psi,k} = \vec{g}$
- Energy balance equation $\Psi_k = u_k + \frac{\vec{W}_k^2}{2}$, $\vec{J}_{\Psi,k} = \vec{q}'' + (p_k\vec{I} - \vec{\tau}_k)\cdot\vec{W}_k$ and $S_{\Psi,k} = \frac{q'''}{\rho_k} + \vec{g}\vec{W}_k$

Simplifications applied to the *Eulerian* equations are:

- Space averaging over the control volume which neglects the turbulent fluctuations.
- 1D motion fluid which implies that local gradients and fluxes are not considered. Besides that, TRACE [1–3] code has a special solution with (3D) equations that can be applied in some components like vessel.
- There are independent de coupled fluid phases which implies that there is no liquid and vapor interactions.
- Hyperbolic solution.
- Time.
- Added artificial viscosity terms on the computations.

the fluid field equations required to be solved in this type of systems are mentioned next. Mass equations 3.2, Energy equations 3.3, Momentum equations 3.4.

$$\frac{\partial\rho}{\partial t} + \nabla\cdot(\rho\vec{v}) = 0 \tag{3.2}$$

$$\frac{\partial\rho\vec{v}}{\partial t} + \nabla\cdot(\rho\vec{v}^2) + \nabla(p) - \nabla\cdot(\overline{T}) = \vec{F}_{ext} \tag{3.3}$$

$$\frac{\partial[\rho(u+\frac{1}{2}\vec{v}^2]}{\partial t} + \nabla\cdot[\rho\vec{v}(h+\frac{1}{2}\vec{v}^2] - \nabla\cdot(\overline{T}\cdot\vec{v}) = Q_{int} + Q_{ext} + \vec{F}\cdot\vec{v} \tag{3.4}$$

Unknowns from the equations 3.2, 3.3 and 3.4 are h enthalpy, p pressure and $\vec{v}$ velocity. Last equations are averaged in time and volume for single phase gas, single phase liquid and combined with interface jump conditions. The fluid at each node is considered with single velocity, single energy and single pressure. Equations must be solved for liquid and gas phase, so the problem ends up with six field equations, three for liquid phase and three for gas phase.

Non-condensable gasses and solute liquid are also considered in TRACE [1–3] code. TRACE [1–3] is capable to model on non-condensable gas as a regular option, but it can

support multiple gas species if required. Equation 3.5 is the non-condensable mixture gas equation and by using it the mechanical equilibrium is assumed this is to assume that the non-condensable gas mixture is in thermal equilibrium with present steam and to move at same velocity.

$$\frac{\partial(\alpha\rho_a)}{\partial t} + \nabla \cdot [\alpha\rho_a \vec{v_a}] = 0 \tag{3.5}$$

$$\frac{\partial[(1-\alpha)m\rho_l]}{\partial t} + \nabla \cdot [(1-\alpha)m\rho_l \vec{v_l}] = 0 \tag{3.6}$$

TRACE [1–3] code also includes a mass-continuity equation 3.6 for a solute moving within the liquid field, where m is the solute concentration (mass of solute/unit mass of liquid water). The solute concentration is not affecting hydrodynamics directly, but its effects over the reactivity feedback could have some effect over the hydrodynamics.

More physics phenomena considered in the code are the *drag models*. The liquid field and gas field momentum equations, include terms of the interfacial shear force and wall drag force. Drag coefficients C_i interfacial; C_{wl} wall liquid; C_{wl} wall gas are required to solve the closure equations. Different values of the coefficient are applied depending on the flow regime, there are different considered flow regimes depending on vertical flow, horizontal flow. Figure 3.1 shows a schematic representation of the different flow regimes. Both the models for interfacial drag coefficient and wall drag coefficient are dependent upon the flow regime.

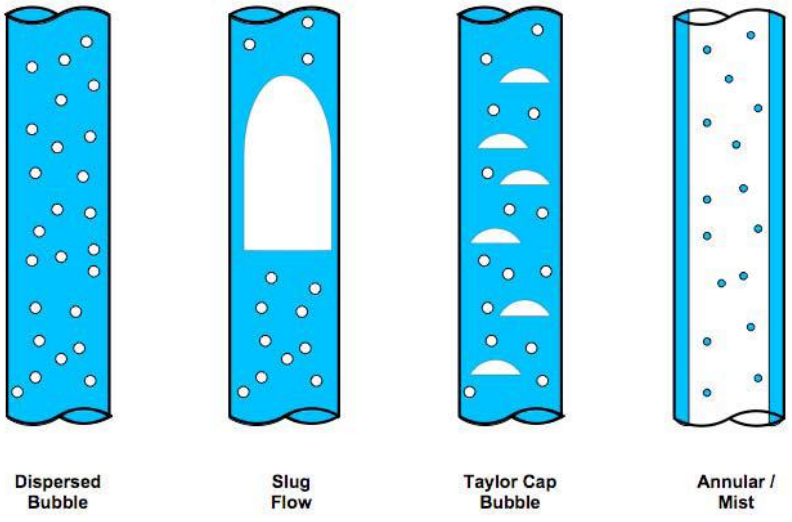

FIGURE 3.1: Schematic representation of the vertical flow regimes.

The general equation which describes the heat conduction process in an arbitrary geometry is the following:

$$\frac{\partial(\rho C_p T)}{\partial t} + \nabla \cdot \vec{q} = q''' \tag{3.7}$$

assuming constant $\rho C_p T$ and expressing the heat flux as temperature gradient by the Fourier's law, 3.8:

$$\vec{q} = -k\nabla T \tag{3.8}$$

Equation 3.7 becomes:

$$\rho C_p \frac{\partial(T)}{\partial t} = \nabla \cdot (k\nabla T) + q''' \tag{3.9}$$

Equation 3.9 its the reference equation for the heat conduction treatment within the TRACE [1–3] code. Besides that, there are different geometries which can contribute to release heat flux to the fluid. Therefore the 3.9 equation, must be applied to those different geometries to find the correct expression in order to determine the coupling of heat conduction field equation to the thermal hydraulic field equation. The geometries included in the TRACE [1–3] code are: Cylindrical walls, slabs and cire fuel rods. TRACE [1–3] code also account for the interfacial heat transfer and for the wall heat transfer. Different models and approximations are used for each geometry. Starting with the interfacial heat transfer, these models are needed for the mass and energy closure equations. In TRACE [1–3] code the interfacial mass transfer rate per unit volume, Γ, is expressed as the following equation:

$$\Gamma = \Gamma_i + \Gamma_{sub} \tag{3.10}$$

Which means the sum of mass transfer rates from the interfacial heat transfer and from the sub-cooled boiling. There are different considerations depending on the type of flow regime and heat transfer stage where the fluid and the wall are encountered. Pre-CHF interfacial heat transfer models which describe the interfacial heat transfer before the CHF occurs. Stratified flow interfacial heat transfer models, which is used for horizontal and inclined pipes where the flow becomes stratifies at low velocity conditions, as gravity and might cause the phases to separate. Post-CHF interfacial heat transfer which describes the interfacial heat transfer for the inverted flow. These situations may happen when the surface temperature is too hot for the liquid phase to contact the wall.

also non-condensable gases effects are considered because its presence effects the mass transfer processes of condensation and evaporation. Also wall heat transfer considered in TRACE [1–3] with different models depending on the heat transfer situation. Wall heat transfer models are required for the mass and energy closure equations. Following equations 3.11 represents the heat transfer rate per unit volume from wall to the liquid and from wall to the gas-vapor mixture.

$$\begin{aligned} q'''_{wl} &= h_{wl} \cdot (T_w - T_l) \cdot A'''_w \\ q'''_{wsat} &= h_{wsat} \cdot (T_w - T_{sat}) \cdot A'''_w \\ q'''_{wg} &= h_{wg} \cdot (T_w - T_g) \cdot A'''_w \end{aligned} \tag{3.11}$$

Where h_{wl} wall to liquid heat transfer coefficient; h_{wl} is the heat transfer coefficient for the direct boiling of the liquid; h_{wg} wall to gas heat transfer coefficient and the wall heat transfer surface area per unit volume is $A'''_w = 4/D_h$. TRACE [1–3] code holds a library of heat transfer correlations plus a selection algorithm which are used to calculate these heat transfer coefficients. By joining all these library correlations and algorithms the code is producing a continuous boiling curve where the more realistic heat transfer coefficient is selected at each step. The models can be divided in the following parts: Pre-CHF transfer (models for wall -liquid convection, nucleate boiling and sub-cooled boiling); CHF transfer (models for peak heat flux in nucleate boiling heat transfer regime and the wall temperature at which occurs); Minimum film boiling temperature (the temperature above which wall liquid contact does not occur); Post-CHF transfer (models for transition and film boiling heat transfer) and Condensation heat transfer (models for film boiling condensation and the non-condensable gas effect).

Finally, after all these balance and closure equations there are some additional *special processes correlations* are added in the system to simulate and compute some local phenomena that might have a significant impact on the global thermal hydraulic behavior of the system. Those *special processes correlations* are representing phenomena that will not be capt in the solution because of the simplifications made on the balance and closure equations. These processes are used depending on the particular fluid conditions at each time step, the user needs to activate the computation of each special process where he (i.e. volume, junction, pump...) thinks it will be required. In that sense experience and knowledge of the problem will tell where and when activate or deactivate such capabilities of the code. Basically these *special processes SP*, are recomputing some particular thermal hydraulic parameters once the system equations are been solved. Following list describes some of the special processes in TRACE [1–3] code:

- Choked Flow
  - Choked flow is by definition a condition wherein the mass flow rate becomes independent of the down stream condition as a consequence, the further reduction in the down stream pressure does not change the mass flow rate. The reason why the choking takes place is due the acoustic signals can no longer propagate upstream. The necessary condition to reach that stage is achieved when the fluid velocity equals or exceeds the propagation velocity. Choking phenomena it is normally related with the flashing phenomena at throats. For certain mass flow rate, the fluid velocity is suddenly increased as a result of the evaporization due that the density is drastically reduced and sound speed is achieved. The choking phenomena usually takes place at breaks or relieve valves since these are places with a great Δp and abrupt area changes. TRACE [1–3] code has a critical flow model which consists in:
    - Sub-cooled liquid choked flow model
      - Determined by the onset of flashing at the nozzle throat.
    - Two phace/two component choked flow model
      - Use Ransom-Trapp model.
    - Single phase vapor choked flow model
      - Based on the isentropic expansion of an ideal gas.

    To activate the choked flow model, the user selects the cell edge where he wants the model to be applied, that is why a good knowledge of those phenomena is required. The model will predict the velocities rather than the momentum equation at the edges where the choked flow is being activated.

- Counter current flow limitation CCFL
  - The idea of the counter current flow limitation is to keep the liquid from flowing in the opposite direction as vapor. The interfacial drag models are used to calculate CCFL for regular geometries. When a irregular geometry is modeled and the flow is not solved fully with the mechanistic method then the CCFL model is used in TRACE [1–3] code to prevent the counter current flow. These situations usually are found in bend pipes or places where there is flow restriction like tie plates. CCFL model can be applied to (1D) vertical models or specific locations from a (3D) vessel component. CCFL TRACE [1–3] implementation supports the models; Bankoff, Wallis and Kutateladze.

- Off-take model

  - When there is a large pipe which contains stratified horizontal flow with small break, where through it the flow is being discharged. Depending on the position of the break the discharged mass flow rate and quality may vary. The Off-take model is used in TRACE [1–3] code to take this situation into account. The Off-take model has three options over the break position, upward position, side position and downward position. Some of the components have the option to activate or not activate the off-take model. Again is an user choice to activate the off-take model in a specific place. Typically the off-take model can be activated in TEE, PUMP, VALVES and PIPE components. The model it self has three assumptions over the geometry:
    * The side tube is required to be either top, bottom or centrally located off the main tube.
    * The angle from the low-numbered side of the main tube to the side tube must be 90 degrees.
    * The main tube junctions must be horizontal.

    The formulation takes into account the critical entrainment height. That height corresponds to the minimum distance for which only one phase is dragged out. This critical entrainment height takes different formulas depending on the location. There are several correlations in TRACE [1–3] off-take model that takes into account the several junction orientations.

- Level tracking

  - A common situation when performing thermal hydraulic analysis is to have stratified levels present in the cells that might compose a pipe. This model tracks the void fractions discontinuities by establishing different values below and above the transition. The level tracking model acts over the closure correlations such drag, wall drag, interfacial heat transfer and gravity head. In the latest versions of the code the the wall heat transfer correlations are not coupled to this model. There are some conditions which are based in empirical observation that are used to determine the liquid and gas interfaces. Once more the model can be activated on components like core up-comer, core down-comer, steam generator riser, steam generator down-comer and steam generator U-tubes.

- Form losses

  - TRACE [1–3] also has a model to deal with the recoverable flow area change loss/gain and irrecoverable contributions to the overall pressure gradient. In the first case recoverable drops sudden contraction followed to the identical

sudden expansion will not introduce any Δp to the system. TRACE [1–3] also includes a special option for removing recoverable Δp in the edges. For the second case, TRACE [1–3] code also incorporates special models for computing irreversible form losses. These form losses are commonly associated to with the creation of turbulence and the deviation of the flow from the smooth straight steam lines. This model es based in factor k.

- Grid spacers
  - On the latest versions of the code there is a Spacer Grid model which computes the convective enhancement effects of the grid spacers and the pressure losses associated with their abrupt area changes. The convective enhancement effect is based on the Yao, Hochreiter and Leech model meanwhile the pressure drops model is based on Yao, Loftus and Hochreiter model [61]. This option is only available with the TRACE v5.0 patch 4 [1–3]. Grid spacers where not modeled in the thermal-hydraulic part of the present study.

There are also some Fuel Rod models in TRACE [1–3] code. TRACE [1–3] holds a temperature dependant extensive library which can be used to model different core structural materials or fuel materials itself. Basically the materials modeled are: Mixed oxide fuel MOX; Zircalloy; fuel-clad and gap-gases and Zircalloy dioxide. The correlations includes phenomena such: mixed oxide fuel thermal expansion; thermal conductivity; specific heat; density and spectral emissivity which will be used in the heat transfer equations. There are also some correlations for the Zircalloy cladding, Zircalloy dioxide; fuel-cladding interaction and gap-gases interactions and reactions are described into the models as well. Some of these features will be disabled automatically since a 3D NK coupled calculation is used, other capabilities will be used to feed the heat transfer equations. The code also has some models for the point kinetics solution of the reactor power. There are various options that the user can apply in order to run the calculations with the point kinetics option enabled. Fixed and table power source was the one used in the present study in order to make the thermal-hydraulic model test in the first part of the steady state problem. Once the thermal-hydraulic system is validated with the point kinetics solution, next step will be to validate it with the 3D NK equations. A multiple comparison between different kinetics solutions is presented at the later phases of the present study. The governing equations for the point kinetics problem are 3.12 and 3.13 which define the first order differential equations for the total fission power P and delayed neutron precursor concentrations C_i as function of time.

$$\frac{dP}{dt} = \frac{R-\beta}{\Lambda} + \sum_{i=1}^{I} \lambda_i C_i + \frac{S}{\Lambda(1-R)} \tag{3.12}$$

and

$$\frac{dC_i}{dt} = -\lambda_i C_i + \frac{\beta_i P}{\Lambda} \qquad for \qquad i = 1, 2, ..., I \tag{3.13}$$

where $R = R_{prog} + R_{fdbk} = (k-1)/k$ is the neutronic reactivity and k is the effective neutron multiplication constant; β is the total fraction of the delayed neutrons and S is the thermal power in watts for an external source of neutrons in the reactor core that are producing power. Subindex i refers to the delayed neutron group. By using the *Kaganove* method to solve the above equation the equation, the next expression, 3.14, is achieved.

$$P_{eff} = P + \sum_{j=1}^{J} \lambda_j^H H_j + S \tag{3.14}$$

Where P is the solution of the equations 3.12 and 3.13; H_j is the energy of the decay heat precursor concentration in group j; λ_j^H decay constant for decay-heat group j and J is the number of decay heat groups. After solving the equation 3.14 for all decay-heat group, the code is computing the total thermal power generated in the reactor core fuel at required time. please notice this equation should be corrected with the elimination of the source term S since the contribution from the external source of neutron has been already included in the 3.12. With last equations TRACE [1–3] code needs the number of delayed neutron groups I; the delayed neutron parameters λ_i and β_i; the number of decay heat groups J; the decay heat parameters λ_j^H and E_j. Then either one of the following information need to be supplied as well: Total fission power history or the initial delayed neutron precursor concentration and decay heat concentrations. Besides that the code holds some default data for delayed neutron groups and decay heat groups. Finally the reactivity feedback can be achieved due three reactivity feedback models available in TRACE [1–3] code. Those are TRAC-P reactivity feedback model; TRAC-B reactivity feedback model and RELAP5 [41–49] reactivity feedback model. The TRACE [1–3] point kinetics model was not used in the present study. TRAC-P reactivity feedback is based on the assumption that only the changes on gas volume fraction α; fuel and coolant temperatures T_f and T_c respectively and solute mass concentration B_m can effect to the neutron multiplication reactivity of the core. The code is averaging by multiplying for a weighting factor for each contribution. There is no averaged parameters for TRAC-B approximation. The reactivity feedback is based on the assumption that for BWR's application more accuracy is needed, thus the sum of the reactivity change per node is applied. Finally the RELAP5 [41–49] model is extracted directly from RELAP5 [41–49] model and includes two models, separate feedback model and tabular feedback

model. First option is taking the contribution to the reactivity as separate effects, there is no interactions in between the contributors to the reactivity, typically: Boron concentration, Moderator density, Fuel and moderator temperature. Second option is taking into account some interaction in between those contributors to the reactivity, some of the above listed parameters might be function to the other ones on the reactivity contribution concerns.

3.1.2 PARCS

The selected (3D) neutron kinetic core simulator code for the present study was PARCS [4, 5]. The Purdue Advanced Core Simulator PARCS [4, 5] is a three-dimensional (3D) reactor core simulator code which solves the steady-state and time-dependent, multi-group neutron diffusion and SP_3 transport equations in orthogonal and non-orthogonal geometries. PARCS [4, 5] is being historically coupled to RELAP5 [41–49] thermalhydraulic system code. Even RELAP5-PARCS [41–49] and [4, 5] coupling is still available and working, nowadays PARCS [4, 5] is being integrated under the TRACE [1–3] package, in the latest versions of TRACE [1–3] released by NRC. Although PARCS [4, 5] code is a completely different code from TRACE [1–3], they had being compiled together under one executable file, in that sense the user will not see any difference when using coupled or non-coupled calculations, when executing the program. Additional files and information will be required when running a (3D) coupled calculation with this system. With one executable file, PARCS [4, 5] is working as a subroutine from TRACE [1–3], and the thermal hydraulic code provides the temperature and flow field information to PARCS [4, 5] during the transient calculations via the few group cross sections. On the other direction, PARCS [4, 5] is giving power to the thermal-hydraulic system. Figure 3.2 shows the total information flow, starting from the lattice physics code to the cross section library to the code simulator code and finally to the thermal-hydraulic system code (only vessel is represented in this picture). The exchange flow of information above explained is represented in the central part of the figure 3.2. In coming sections the other information exchange paths will be explained.

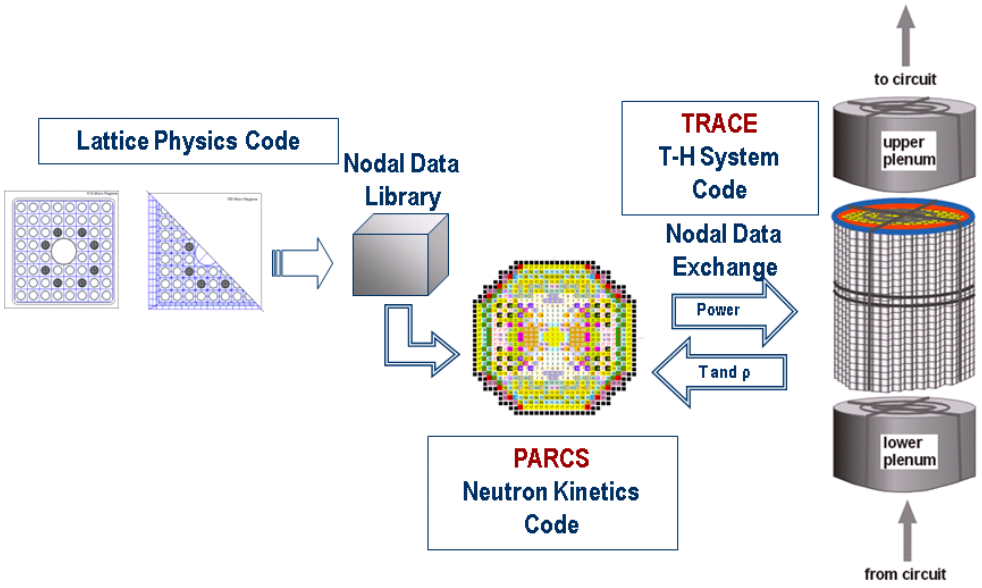

FIGURE 3.2: 3D NK-TH information flow.

As it has been mentioned PARCS [4, 5] is a (3D) neutron kinetics core simulator code which essentially is being used to compute the (3D) power distribution produced by the core fuel assemblies. Beyond this capability PARCS [4, 5] can perform other tasks such: Eigenvalue calculation; Transient (kinetics) calculations; Xenon transient calculations; Decay heat calculations; Pin power calculations and Adjoint calculations. Even the code can be used for different porpoises PARCS [4, 5] has some predetermined geometries that makes the use of this tool very suitable for nuclear reactor and not convenient for other porpoises. There are also some one-dimensional (1D) modeling features available in PARCS [4, 5]. Those ones are used to support faster simulations for a group of transients in which the dominant variation of the flux is in the axial direction. As many of the nuclear code PARCS [4, 5] has an old appearance, with this mean ASCII input files, for the user interaction. Restart capability is also included and becomes very important when running coupled calculations and BEPU analysis with coupled codes. The input file is based in cards like TRACE [1–3] and other nuclear system codes. Using PARCS [4, 5] from SNAP [60] platform becomes more easy and user friendly specially for the novice user. PARCS [4, 5] code have a different list of calculation methods in order to accomplish the various tasks with high accuracy and efficiency. Since the present study is not a Computer Science study I will not go in deeply detail with the solving algorithms integrated in the code. Nevertheless some of the following techniques mentioned are common techniques for neutron flux solver codes. Starting with *CMFD* formulation which provides a means of performing a fast transient calculation. To do that, when there is no strong variation in the neutron flux spatial distribution, the code avoids

expensive nodal calculations during some time steps in the transient. There is also a transient fixed source problem at each time point in the transient. To solve the spatial discretization, there are different solution kernels available like, *ANM* and *NEM* those include the most popular LWR two group nodal methods. In order to minimize the computational time, there are also some well known computational methods for example, the solution of the *CMFD* linear system is obtained using a *Krylov* subspace method. The eigenvalue calculation to establish the initial steady-state is performed using the *Wielandt* eigenvalue shift method. PARCS [4, 5] code is written in *FORTRAN90* language. Its portability has been tested on various platforms and operating systems, to include *SUN Solaris Unix, DEC Alpha Unix, HP Unix, LINUX,* and various *Windows OS*. The following list shows more detailed explanation of the PARCS features, as mentioned above the aim of this work is not in the field of Computer Science, nevertheless a brief description of the capabilities of the code is given.

3.1.2.1 PARCS calculation features

- Eigenvalue problem
  - PARCS [4, 5] code is able to solve two kinds of neutronic problems. Eigenvalue problem and fixed source problem. Neutron flux solver needs to solve the nodal balance equation under the cartesian geometry approximation.

$$\frac{1}{V_g^m}\frac{d\phi_g^m}{dt} = \frac{1}{k_{eff}}\chi_{pg}\sum_{g=1}^{G}\nu_{pg}\Sigma_{fg}^m\phi_g^m + \chi_{dg}\sum_{k=1}^{K}\lambda_k C_k^m + \\ + \sum_{g'=1}^{G}\Sigma_{gg'}^m\phi_{g'}^m - \sum_{u=x,y,z}\frac{1}{h_u^m}(J_{gu}^{m+} - J_{gu}^{m-}) - \sum_{tg}^{m}\phi_{tg}^m \tag{3.15}$$

  and

$$\frac{dC_k^m}{dt} = \frac{1}{k_{eff}}\sum_{g=1}^{G}\nu_{dpk}\Sigma_{fg}^m\phi_g^m + \lambda_k C_k^m \tag{3.16}$$

  where C_k^m is the precursor density, ϕ_g^m is the node averaged flux and $J_{gw}^{m_-^+}$ is the surface averaged net current. The index G stands for the neutron energy group and K index is representative of the delayed neutron group. Finally plus and minus signs determine the flux direction p and d subscripts stand for prompt and delayed neutrons. The eigenvalue k_{eff} it is determined during the steady state process and it is kept it constant during the transient calculation. There is no difference between delayed and prompt neutrons when solving

steady state problem, also all of the derivative parts from equations 3.15 and 3.16 become zero. Thus the new equation can be written as follows:

$$M\phi = \lambda F\phi \equiv \frac{1}{k_{eff}} F\phi \tag{3.17}$$

Where F is the fission matrix and M is the non-fission matrix. Equation 3.17 is solved in the code by using the fission source iteration method. Such solution is achieved via *Wielandt* eigenvalue shift method rather then common *Chebyshev* polynomial method. This is done this way because the *Wielandt* solution will be helpful when solving the transient fixed source problem on the next steps.

- Transient fixed source calculation

  - Fixed source calculation can be used in different occasions, besides that in PARCS [4, 5] code is commonly used for the spatial kinetics problem. Time dependent solution for the equation 3.15 is solved on this step of the calculation. Nevertheless, as mentioned several times, PARCS [4, 5] code is very LWR orientated and there are several approximations which are taken according to that orientation. One of these orientated approximations taken can be seen in transient fixed source calculation where several approximations are made in order to make things more suitable to the problem and to include the use for the two energy groups. The simplifications are the following:

    * $\chi_{p1} = \chi_{d1} = 1.0$ and $\chi_{p2} = \chi_{d2} = 1.0$
    * There is no dependence on the delayed neutron precursor yields on neutron energy
    * There is no up scattering $\Sigma^m_{21} = 0$
    * $\nu_{dgk}\Sigma^m_{fg} = \beta^m_k \nu\Sigma^m_{fg}$ and $\nu_{pg}\Sigma^m_{fg} = (1-\beta^m_k)\nu\Sigma^m_{fg}$ where $\beta^m \equiv \sum_{k=1}^{K} \beta^m_k$

    With the above approximations the two group kinetics equation takes the following form:

$$\frac{1}{V^m_g}\frac{d\phi^m_g}{dt} = R^m_g = \begin{cases} (1-\beta^m)\Psi^m + S^m_d - L^m_1 - \Sigma^m_{r1}\phi^m_1 & g = 1 \\ \Sigma^m_{12}\phi^m_1 - L^m_2 - \Sigma^m_{r2}\phi^m_2 & g = 2 \end{cases} \tag{3.18}$$

and

$$\frac{dC^m_k}{dt} = \beta^m_K \Psi^m - \lambda_K C^m_k \tag{3.19}$$

where from the above equations we have the following definitions; S_g delayed neutron source ; L_g groups leakage; Ψ total fission source term; These definitions take the following forms:

$$\begin{aligned} \Psi^m &\equiv \frac{1}{k_{eff}} \sum_{g=1}^{2} \nu \Sigma_{fg}^m \phi_g^m \\ S_m^d &\equiv \sum_{k=1}^{K} \lambda_k C_k^m \\ L_m^g &\sum_{u=x,y,z} L_{gu}^m \\ L_{gu}^m &\equiv \frac{1}{h_u^m}(J_{gu}^{m+} - J_{gu}^{m-}) \end{aligned} \tag{3.20}$$

The transient fixed source problem is formulated from the two groups kinetic equations by applying temporal discretization methods, in here CMFD formulation and two node nodal method are used to solve the flux equations. At the end the resulting transient fixed source problem will contain only node average fluxes, as the unknowns.

- Numerical solution methods
  - In PARCS [4, 5] the primary solution algorithm is based on the nonlinear Coarse Mesh Finite Difference (CMFD) formulation. In the CMFD method the core is discretized into coarse mesh, typically the size of a fuel assembly. Finite difference discretization is applied between mesh. Each balance equation from each node is coupled to each balance equation of each one of the neighboring nodes using the leakage term. This nodal coupling is solved using a non linear nodal method, where the interface current between two nodes is represented by the average fluxes of the two facing nodes. At the end the PARCS [4, 5] code is solving a matrix system like equation 3.21 where the unknowns are the node average fluxes. The system is called Coarse Mesh Finite Difference Method for a transient fixed source problem. The system can be solved by using any iterative linear system solution method, *Kyrlov* subspace method, *BiCGSTAB*, *GMRES* and *BILU3D* pre-conditioners are used to solve the CMFD matrixes.

$$A_n \phi_n = S_n \tag{3.21}$$

These *Kyrlov* subspace methods are one of the most effective ways on solving linear systems. A consecution of the different above mentioned algorithms constitutes the solution methodology for the CFMD numerical method. The

algorithm methodology goes beyond the scope of the present study and it has only being mentioned here in order to satisfy reader's curiosity. More information can be found in the following references [62, 63]

- Nodal diffusion methods

  – Nodal methods are the primary means used in PARCS [4, 5] to obtain higher order solutions to the neutron diffusion equation. Within the framework of the CMFD formulation the nodal method is used to solve the two node problem and to update the nodal coupling coefficient. The ANM (Analytic Nodal Method) in PARCS [4, 5] has been used most frequently within the Light Water Reactor (LWR) industry to solve the two group diffusion equation. For the previous computational solutions the *CNCC* corrective nodal coupling coefficient was assumed to be known. Besides that *CNCC* should be computed during the nonlinear iteration involved in the process of the *CMFD* and the two-nodes calculation. *CNCC* is determined when the interface current obtained by the CMFD is the same as the nodal interface current obtained from the two node calculation. The two node problem is a (1D) problem, for which the analytic solution is readily obtainable. In PARCS [4, 5] code the (1D) diffusion equation is obtained through the integration of the (3D) steady state neutron diffusion equation over the transverse plane also there is a common approximation used in the all transverse-integrate nodal methods which consists to assume a quadratic spatial variation of the transverse leakage. The NEM Nodal Expansion Method is used to find the solution for the steady state multi-group diffusion equation in cartesian geometry. The principal features of the polynomial nodal method are the quadratic expansions for the (1D) transverse integrated flux and for leakage model for the transversal leakage. The general multi-group neutron diffusion equation is written as:

$$\vec{\nabla} \cdot D_g \vec{\nabla} \phi_g + \Sigma_{tg} \phi_g = \sum_{g=1}^{G} \Sigma_{sgg'} \phi_{g'} + \frac{\chi_g}{k} \sum_{g=1}^{G} v_{g'} \Sigma_{fg'} \phi_{g'} \tag{3.22}$$

  where D_g is the diffusion coefficient in (cm); ϕ_g is the neutron flux in $(cm^{-2}sec^{-1})$; Σ_{tg} is the total macroscopic cross section (cm^{-1}); $\Sigma_{sgg'}$ is the groups-to-group scattering cross section (cm^{-1}); χ_g is the fission neutron yield; k is the multiplication factor (i.e. critical eigenvalue); v_g is the average number of neutrons created per fission and Σ_{fg} is the macroscopic fission cross section (cm^{-1}).

- Xenon/Samarium calculation

– Xenon and Samarium concentrations are also taken into account into PARCS [4, 5] code. Such concentrations will have an important effect in those transients where the power is shifted from upper to lower levels and vice versa. Reactivity variations will occur also due the presence of high concentrations of Xenon and Samarium isotopes. Xenon and Samarium precursors are Iodine and Promethium respectively. Time depletion equations of the fission products of the both chains looks like:

$$\frac{dN_I^l(t)}{dt} = \gamma_I^l \sum_{g=1}^{G} \Sigma_{fg}^l(t)\phi_g^l(t) - \lambda_I^l N_I^l(t) \tag{3.23}$$

$$\begin{aligned}\frac{dN_{Xe}^l(t)}{dt} = \lambda_I^l N_I^l(t) + \gamma_{Xe}^l \sum_{g=1}^{G} \Sigma_{fg}^l(t)\phi_g^l(t) - \lambda_{Xe}^l N_{Xe}^l(t) - \\ - \sum_{g=1}^{G} \sigma_{Xe,ag}^l(t)\phi_g^l(t) N_{Xe}^l(t)\end{aligned} \tag{3.24}$$

Equations 3.23 and 3.24 are for the Xe^{135} and I^{135} decay chain. Equations 3.25 and 3.26 are for the Sm^{149} and Pm^{149} decay chain.

$$\frac{dN_{Pm}^l(t)}{dt} = \gamma_{Pm}^l \sum_{g=1}^{G} \Sigma_{fg}^l(t)\phi_g^l(t) - \lambda_{Pm}^l N_{Pm}^l(t) \tag{3.25}$$

$$\frac{dN_{Sm}^l(t)}{dt} = \lambda_{Pm}^l N_{Pm}^l(t) - \sum_{g=1}^{G} \sigma_{Sm,ag}^l(t)\phi_g^l(t) N_{Sm}^l(t) \tag{3.26}$$

where $N_i^l(t)$ is the nuclei number density of isotope i, $\sigma_{i,ag}^l(t)$ is the group-wise microscopic cross section of the isotope i; γ_i^l is the effective yield (atoms/fission) of isotope i finally λ_i^l is the decay constant of the isotope i. Previous equations are used to calculate the time dependent densities of the Xe and Sm isotopes and its precursors. To obtain the steady state number densities it is necessary to integrate the previous equations which lead to the following ones:

$$N_{I,\infty}^l = \frac{\gamma_I^l \sum_{g=1}^{G} \Sigma_{fg}^l \phi_g^l}{\lambda_I^l} \tag{3.27}$$

$$N_{Xe,\infty}^l = \frac{\lambda_I^l N_{Xe,\infty}^l + \gamma_{Xe}^l \sum_{g=1}^{G} \Sigma_{fg}^l \phi_g^l}{\lambda_{Xe}^l + \sum_{g=1}^{G} \sigma_{Xe,ag}^l \phi_g^l} \tag{3.28}$$

Equations 3.27 and 3.28 are for the Xe^{135} and I^{135} decay chain. Equations 3.29 and 3.30 are for the Sm^{149} and Pm^{149} decay chain.

$$N^l_{Pm,\infty} = \frac{\gamma^l_{Pm} \sum_{g=1}^{G} \Sigma^l_{fg} \phi^l_g}{\lambda^l_{Pm}} \tag{3.29}$$

$$N^l_{Sm,\infty} = \frac{\lambda^l_{Pm} N^l_{Pm,\infty}}{\sum_{g=1}^{G} \sigma^l_{Sm,ag} \phi^l_g} \tag{3.30}$$

To obtain transient concentrations ($t+\Delta t$) is added in the last set of equations. After all these calculations are finished, the resulting number densities are used to update the macroscopic cross section as it is shown in the equation 3.31:

$$\sigma^l_{ag} = \sigma^l_{ag} + \Delta\sigma^l_{Xe,ag} + \Delta\sigma^l_{Sm,ag} \tag{3.31}$$

where:

$$\Delta\sigma^l_{Xe,ag} = \Sigma^l_{Xe,ag} N^l_{Xe} \qquad and \qquad \Delta\Sigma^l_{Sm,ag} = \sigma^l_{Sm,ag} N^l_{Sm} \tag{3.32}$$

If the Xe and Sm contributions are not been calculated by the user, when running the lattice physics code, PARCS [4, 5] code, holds a list of default values for Xe and Sm contribution, either number densities either corrections to be added at each cross section. Also the code has the capability to run different calculations with or without such contribution (i.e. Xe in equilibrium or non-equilibrium, Sm present or not present). In the present study Xe and Sm contribution was included when building the cross section library.

- Neutron Transport Methods

  – Although PARCS [4, 5] code is basically a neutron diffusion code, diffusion equation is not accurate enough for some of the computations required. PARCS [4, 5] code holds a multi-group transport calculation capability. Spherical harmonics method P_N is the most common method used to solve the multi-group transport equation. Equation 3.33 is the steady state Boltzmann transport equation without an external source:

$$\begin{aligned} \Omega \cdot \nabla\Psi(r,\Omega,E) + \Sigma_t(r,E)\Psi(r,\Omega,E) = \\ = \int d\Omega' \int dE' \Sigma_s(r,\Omega' \to \Omega, E' \to E)\Psi(r,\Omega',E') + \frac{1}{4\pi} S_f(r,E) \end{aligned} \tag{3.33}$$

where

$$S_f(r,E) = \chi(E) \int dE' \nu\Sigma_f(r,E')\phi(r,E') \tag{3.34}$$

and

$$\phi(r,E) = \int d\Omega' \Psi(r,\Omega' E) \tag{3.35}$$

Since P_N is referred to one dimensional problem, the generalization of this method to a (3D) problem is known as SP_N approximation. To do that several changes need to be done in the original P_N equations. In that sense, the three dimensional P_1 can be built from the P_1 one-dimensional equations by replacing $\partial/\partial x$ operator in one dimensional $n = 0$ with the divergence operator ∇; replacing $\partial/\partial x$ operator in one dimensional $n = 1$ with the gradient operator ∇; considering zeroth-order Legendre moment of the angular flux ϕ_0 as scalar and considering first-order Legendre moment of the angular flux ϕ_0 as vector. For SP_N the relations between the geometries are extrapolated keeping in mind to replace $\partial/\partial x$ operator in one dimensional for even n with the divergence operator ∇; replacing $\partial/\partial x$ operator in one dimensional for odd n with the gradient operator ∇; considering even-order Legendre moment of the angular flux as scalar and considering odd-order Legendre moment of the angular flux as vector. This methodology is well known process used to solve multi-group transport equation. PARCS [4, 5] code has its own SP_N development and in the actual versions that methodology is truncated at SP_3 for $N > 3$. This ends up with the following SP_3 equations:

$$\begin{aligned}
\nabla \cdot \phi_{1g} + \Sigma_{rg}\phi_{0g} &= S_{0g} \\
\frac{2}{3}\nabla \cdot \phi_{2g} + \frac{1}{3}\nabla \cdot \phi_{0g} + \Sigma_{trg}\phi_{1g} &= 0 \\
\frac{3}{5}\nabla \cdot \phi_{3g} + \frac{2}{5}\nabla \cdot \phi_{1g} + \Sigma_{tg}\phi_{2g} &= 0 \\
\frac{3}{7}\nabla \cdot \phi_{2g} + \Sigma_{tg}\phi_{3g} &= 0
\end{aligned} \tag{3.36}$$

where

$$S_{0g} = \sum_{g'} \Sigma_{sg'g}\phi_{0g'} + \frac{\chi_g}{k_{eff}} \sum_{g'} \nu\Sigma_{fg'}\phi_{0g'} \tag{3.37}$$

Equations 3.36 are the time independent equations resulting for the SP_3 method, for the time dependent solution the equations 3.38 show the addition of the time derivative terms necessary for the time dependent solution.

$$\begin{aligned}
\frac{1}{v}\frac{\partial\phi_{0g}}{\partial t} + \nabla\cdot\phi_{1g} + \Sigma_{rg}\phi_{0g} &= S_{0g} \\
\frac{1}{v}\frac{\partial\phi_{1g}}{\partial t} + \frac{2}{3}\nabla\cdot\phi_{2g} + \frac{1}{3}\nabla\cdot\phi_{0g} + \Sigma_{trg}\phi_{1g} &= 0 \\
\frac{1}{v}\frac{\partial\phi_{2g}}{\partial t} + \frac{3}{5}\nabla\cdot\phi_{3g} + \frac{2}{5}\nabla\cdot\phi_{1g} + \Sigma_{tg}\phi_{2g} &= 0 \\
\frac{1}{v}\frac{\partial\phi_{3g}}{\partial t} + \frac{3}{7}\nabla\cdot\phi_{2g} + \Sigma_{tg}\phi_{3g} &= 0 \\
\frac{dC_k}{dt} = -\lambda_k C_k + \frac{\beta}{k_{eff}}\sum_{g'}\nu\Sigma_{fg'}\phi_{0g'}
\end{aligned} \tag{3.38}$$

where

$$\begin{aligned}
S_{0g} = \sum_{g'}\Sigma_{sg'g}\phi_{0g'} + \frac{\chi_g}{k_{eff}}(1-\beta)\sum_{g'}\nu\Sigma_{fg'}\phi_{0g'} + \chi_{dg}\sum_{k'}\lambda_k C_k \\
\frac{dC_k}{dt} = -\lambda_k C_k + \frac{\beta_g}{k_{eff}}\sum_{g'}\nu\Sigma_{fg'}\phi_{0g'}
\end{aligned} \tag{3.39}$$

Fine Mesh Finite Difference Method, FMFDM is introduced in PARCS [4, 5] for solving the SP_3 equations. This becomes convenient when computing FA with heterogenous conditions. Some inefficiencies in terms of the accuracy of the solution and computational time where encountered when using the FMFDM and that is why PARCS [4, 5] code has an advanced nodal solver method called NEM Nodal Expansion Method.

- Hexagonal modal methods
  - All the analyzed systems in the present study, were based on cartesian geometry solutions, nevertheless PARCS [4, 5] code, holds the capability of solving the neutron diffusion equation for the Hexagonal geometries (i.e. VVER reactors). The hexagonal nodal method needed to solve the neutron diffusion equation is made with TPEN Triangle-based Polynomial Expansion Nodal. TPEN solves two transverse-integrated neutron diffusion equations for a hex-octahedron node. Since this capability goes beyond the aim of the present study it is just mentioned here without getting into much detail than adding it into the list of the capabilities of the code.
- Fuel depletion analysis
  - Depletion capability was added into the code in order to make it able to perform fuel cycle analysis. Burnup history and power needs to be entered to the code to perform such analysis. These information is entered via GenPMAXS [30] and needs to be computed when generating the cross section library with

the lattice physics code. This information was added on the computation in the present study. The burnup capability is structured in steps. Each step is taking the power from each node to compute the advance burnup from each node. With this capability the user is able to run the system through all the stages of the life cycle of the reactor. The user can specify different burnup distributions for different FA and PARCS [4, 5] will compute the advancement step for the cycle of the reactor. This calculation will give as a result a new distribution in terms of burnup and cross section information that the previous one. The user can pick any point from the pre-desired steps to start point of a transient analysis. The burnup distribution is computed using the fluxes provided by PARCS with the following equation:

$$\Delta B_i = \Delta B_c \frac{\frac{P_i}{G_i}}{\frac{P_c}{G_c}} \tag{3.40}$$

where ΔB_i is the core average burnup increment in one step, specified in the depletor input, this is an user decision. G_i is the heavy metal loading in *ith* region. G_c is the total heavy metal loading in the core. P_i is the power in the *ith* region and finally P_c is the total power in the core. History variables needs to be balanced in this section as well, the pass history of each fuel assembly will have an effect on the future burnup distribution. The considered history contributions are: Control rod history (HCR); Moderator density history (HMD); Soluble boron history (HSB); Fuel temperature history (HTF); Moderator temperature history (HTM). All these history variables are defined as weighted quantities as follow:

$$HCR(B_p + \Delta B) = \frac{\int_0^{B_p+\Delta B} \alpha(B)dB}{B_p + \Delta B} = \frac{HCR(B_p) \times B_p + \alpha \Delta B}{B_p + \Delta B} \tag{3.41}$$

where HCR is the control rod history for this example but it could be any one of the above mentioned history variables. B_p is the burnup at the beginning of this step and ΔB is the burnup increment. α is the rodded fraction during this step, this procedure is used for the rest of history variables in order to obtain the burnup and power distribution for the next burnup step. If this feature is used the cross section will have two main contributions:

* Contribution coming from the instantaneous variables, i.e. control rod insertion, moderator density, moderator and fuel temperature and soluble boron concentration.

  - ∗ Contribution coming from the history variables, i.e. control rod history, moderator density history, soluble boron concentration history and finally fuel and moderator temperature.

  The code will produce the resulting cross sections sets in two steps. First it will consider the all the instantaneous values of all dependent variables for a specified history state of a particular region to produce a cross section set depending on the history variables, this job is made by the DEPLETION module. In the Second stage the code will produce the cross section set by taking the cross section generated by the DEPLETION module and correcting it with the current instantaneous variables.

- Decay heat calculation

  – PARCS [4, 5] is also capable of performing core depletion analysis. Burnup dependent macroscopic cross sections are read from the PMAXS file prepared by the code GENPMAXS [30] and the PARCS [4, 5] node-wise power is used to calculate the region-wise burnup increment for time advancing the macroscopic cross sections. Details of the PMAXS file and the GENPMAXS [30] code are provided in the GENPMAXS [30] description section. The amount of computed heat that will be released during SCRAM situation will depend on the burnup history of the FA which conforms the core, different enrichments and FA positions will have its importance in this calculation. Such option is being activated on the present study. Following equation gives the volumetric heat density with the decay heat contributions considered:

$$q_t(\vec{r},t) = (1-\alpha_t)\sum_{g=1}^{G} k_g \Sigma_{fg}(\vec{r},t)\phi_g(\vec{r},t) + \sum_{i=1}^{I} \zeta_i D_i(\vec{r},t) \tag{3.42}$$

  where $D_i(\vec{r},t)$ is the concentration of the decay heat precursors in decay heat group i (J/cm^3); ζ_i is the decay constant of the decay heat group i (sec^{-1}); $\alpha_t = \sum_{i=1}^{I} \alpha_i$ is the total fraction of the fission energy appearing as decay heat where I is the total number of decay heat groups; Finally α_i is the fraction of the total fission energy appearing as decay heat for decay heat group i. After some modifications and simplifications, the concentration of the decay heat precursors $D(\vec{r},t)$ becomes:

$$D_i(\vec{r},t_{n+1}) = D_i(\vec{r},t_n)e^{\zeta_i \Delta t} + \frac{\alpha_i}{\zeta_i}[1-e^{\zeta_i \Delta t}]\sum_{g=1}^{G} \kappa_g \Sigma_{fg}(\vec{r},t_n)\phi_g(\vec{r},t_n) \tag{3.43}$$

- Pin power Calculation

- PARCS code holds the capability to perform a pin power reconstruction calculation. The pin by pin power distribution becomes important in several assets of the nuclear safety, for example when analyzing a DNBR situation. This pin power reconstruction involves some assumptions, the most important takes into account that the pin-by-pin power distribution inside the FA, can be estimated by the product of a global intra-nodal flux distribution and local heterogenous form function. Such form function is taking into account the FA discontinuities such guide tubes, water holes... the form function is generated by the lattice physics code when computing the XS set. Intra-nodal flux distribution is computed by PARCS [4, 5] by its own development and methodologies. When using the nodal option in PARCS, it is necessary to invoke the pin power reconstruction module in order to recover fuel pin powers from the nodal solution. In the present work such capability was not activated on the calculations since it is more required for channel coupled calculations rather than full system calculations.

- Adjoint calculation and Reactivity edits

  - In order to compute the dynamic reactivity during a transient calculation the adjoint solution of the initial eigenvalue problem is required. With this calculation at any time point during the transient calculation the dynamic reactivity is expressed as the following equation:

$$\rho = \frac{\langle \phi_0^*, A\theta \rangle}{\langle \phi_0^*, F\theta \rangle} \tag{3.44}$$

    where A is the net production operator which is defined as $A = F - M$. If the steady state values of the operators and flux vector is used equation 3.44 becomes equation 3.45

$$\rho_0 = 0 \tag{3.45}$$

    Any changes on the production operator $A = A_0 - \Delta A$ can come as a contribution of the following sources: Control rod component *(CR)*; Boron concentration component *(PPM)*; Doppler temperature component *(TDOPL)*; Moderator temperature component *(TMOD)*; Moderator density component *(DENS)*; Xenon/Samarium component *(XESM)* and Nodal leakage component *(NL)*. With those contributions ΔA becomes:

$$\Delta A = \Delta A_{CR} + \Delta A_{PPM} + \Delta A_{TDOPL} + \Delta A_{TMOD} + \Delta A_{DENS} + \Delta A_{XESM} + \Delta A_{NL} \tag{3.46}$$

Adding all these contributions the total reactivity is now a sum of contributions from the other reactivities, equation 3.47 shows the final expression of the total reactivity.

$$\begin{aligned}\rho_{TOT} = \rho_{CR} + \rho_{PPM} + \rho_{TDOPL} + \rho_{TMOD} + \\ + \rho_{DENS} + \rho_{XESM} + \rho_{NL} + \rho_{NULL}\end{aligned} \tag{3.47}$$

where ρ_{NULL} comes from $A = A_0$ from the equation $A = A_0 - \Delta A$ and should be strictly zero, but it is included in the formula due to numerical inaccuracies of the adjoint flux calculation.

- Rod cusping correction
  - When a node is partially rodded, there appears a so called control rod cusping effect. In that scenario the control rod cross section is incorporated using only the volume fraction. This occurs inherently because there is a flux depression in the partially rodded region leading to a smaller control rod worth. The rod cusping problem is addressed in PARCS [4, 5] by solving a three node problem using a fine mesh finite difference method (FDM). The typical rod cusping effect occurs in eigenvalue calculations in such a way that the core k_{eff} varies in a cusp (or wavy) shape as the control rod insertion depth changes. The rod cusping effect is also observed in core power variation during a transient that involves a slow control rod motion. Such option is being tested without success when some discrepancies where found in the 3D NK-TH coupled model validation tests.
- Critical boron concentration and CR position search
  - A common issue when leading with LWR's is to determine the critical boron concentration to make the reactor critical at determined power. PARCS [4, 5] code, holds the capability to determine the critical boron concentration due an integrated algorithm which basically is working with the equation 3.48.

$$ppm = ppm_2 + \frac{1 - k_{eff}^{(2)}}{k_{eff}^{(1)} - k_{eff}^{(2)}}(ppm_1 - ppm_2) \tag{3.48}$$

The code is taking the assumption of two boron concentrations ppm_i with two $k_{eff}^{(i)}$. By using the equation 3.48, the code is determining the boron concentration for the $k_{eff} = 1$ which will be the critical boron concentration for the user problem. The initial boron concentration is determined in the thermal-hydraulic code when performing a 3D NK-TH coupled calculation.

- XS formalism calculation

– Cross section formalism will be more detailed when the use of GenPMAXS [30] code is explained. There are different ways how the code can use the information coming from the lattice physics code. Nevertheless there are some common parts on the way to thread the cross sections sets. Besides the history parameters such burnup, typically a well constructed cross section library will hold dependencies on five state parameters which are:

  * α Control rod insertion
  * Tf Fuel temperature
  * Tm Moderator temperature
  * Dm Moderator density
  * Sb Soluble boron concentration

  Equation 3.49 shows the most common expression used when computing the cross section. The expression involves that the final values of a specific cross section of specific node, will be a contribution of the five variable states above mentioned. Each contribution is added with a partial derivative which essentially corrects the final cross section with a value determined by the deviation (partial derivative) from a computed values of each contribution.

$$\begin{aligned}\Sigma(\alpha, Tf, Tm, Dm, Sb) = \Sigma^r + \alpha\Delta\Sigma^{Cr} + \frac{\partial\Sigma}{\partial\sqrt{Tf}}\Delta\sqrt{Tf} + \\ + \frac{\partial\Sigma}{\partial Tm}\Delta Tm + \frac{\partial\Sigma}{\partial Dm}\Delta Dm + \frac{\partial\Sigma}{\partial Sb}\Delta Sb + + \frac{\partial^2\Sigma}{\partial Dm^2}(\Delta Dm)^2\end{aligned} \tag{3.49}$$

  As mentioned above the equation 3.49 is the basic cross section treatment. On previous versions of the code, 3.49 was the treatment used when considering the cross section variations. Within the actual versions of PARCS [4, 5], the code can be fed by GenPMAXS [30] files. The treatment given to the cross sections by the equation 3.49 is known as a *Partial Derivatives Model*. There are other methodologies to treat the cross sections and to manage the XS library, these are *Multi-dimensional Tables*, *Multiple tables* and *PMAXS model* GenPMAXS [30]treatment, *PMAXS model*, involves much more than the five state parameters contributions mentioned above. With GenPMAXS [30] Assembly discontinuity factors; Corner point discontinuity factors; Local power peaking factors; Power form factors; Groups-wise form factors; Detector information; XE/Sm cross sections; Beta of delayed neutrons; Lambda of delayed neutrons; Spectrum of the delayed neutrons; Decay heat factor; History information and Neighboring effects can be considered or not in the calculation. Also depending on the way that the cross sections are being computed in the lattice physics code. PARCS [4, 5] user can activate or deactivate some of the contributions depending on the type of study and the cross

section library accuracy. The other above mentioned methods are described in the GenPMAXS [30] code description section.

- One dimensional kinetics
  - As it was mentioned above, PARCS [4, 5] code, has also the capability to perform (1D) calculations. Those calculations have not been used in the present study since the (3D) neutron kinetic model was intend to be validated, nevertheless two (1D) modes are available: Normal 1D mode and quasi-static mode 1D. Starting with the first mode, it uses a 1D geometry and pre-collapsed 1D group constants, while the second option of 1D calculation keeps the 3D geometry and cross sections, but performs the neutronic calculation in the 1D mode using group constants which are collapsed during the transient. During the 1D group constant generation, "current conservation" factors are employed in the PARCS [4, 5] 1D calculations to preserve the 3D planar averaged currents in the subsequent 1D calculations.

- Point kinetics
  - The code also holds the capability to generate the point kinetics parameters for a specific point kinetics and also is giving various approximations for the point kinetics equations. Starting from the (3D) time dependent multi-group diffusion equation and the precursors equations are written in a standard way as follows:

$$\frac{1}{V_g(\vec{r})}\frac{d\phi_g(\vec{r},t)}{dt} = \nabla \cdot D_g(\vec{r},t)\nabla\phi_g(\vec{r},t) + \sum_{g'}\Sigma_{g,g'}(\vec{r},t)\phi_{g'}(\vec{r},t) - \\ -\Sigma_{tg}(\vec{r},t)\phi_g(\vec{r},t) + \chi_g(\vec{r})S^F(\vec{r},t) + \Sigma_k \cdot \chi_{dk,g}(\vec{r})(\lambda_k(\vec{r})C_k(\vec{r},t) - \beta_k(\vec{r})S^F(\vec{r},t)) \tag{3.50}$$

with $g = 1, 2...G$ and

$$\frac{\partial C_k(\vec{r},t)}{\partial t} = \beta_k(\vec{r})S^F(\vec{r},t) - \lambda_k(\vec{r})C_k(\vec{r},t) \tag{3.51}$$

With $k = 1, 2...N_d$ where S^F is the fission source term and χ_g is the average fission spectrum. After various approximations the equations 3.50 and 3.51 can be written as the equations 3.52 and 3.53. The time dependent shape

functions can be obtained from the spatial kinetics calculation or by solving the equations 3.52 and 3.53.

$$\begin{aligned}\frac{1}{V_g(\vec{r})}\frac{\partial\Psi_g(\vec{r},t)}{\partial t} = \nabla\cdot D_g(\vec{r},t)\nabla\Psi_g(\vec{r},t) + \sum_{g'}\Sigma_{g,g'}(\vec{r},t)\Psi_{g'}(\vec{r},t) - \\ -(\Sigma_{tg}(\vec{r},t) + \frac{1}{p(t)}\frac{dp(t)}{dt})\Psi_g(\vec{r},t) + \chi_g(\vec{r})\hat{S}^F(\vec{r},t) + \\ +\Sigma_k\cdot\chi_{dk,g}(\vec{r})(\lambda_k(\vec{r})\hat{C}_k(\vec{r},t) - \beta_k(\vec{r})\hat{S}^F(\vec{r},t))\end{aligned} \tag{3.52}$$

with $g = 1, 2...G$ and,

$$\frac{\partial\hat{C}_k(\vec{r},t)}{\partial t} = \beta_k(\vec{r})\hat{S}^F(\vec{r},t) - (\lambda_k(\vec{r}) + \frac{1}{p(t)}\frac{dp(t)}{dt})\hat{C}_k(\vec{r},t) \tag{3.53}$$

with $k = 1, 2...N_d$ and where

$$\hat{C}_k(\vec{r},t) = \frac{C_k(\vec{r},t)}{p(t)} \tag{3.54}$$

Equations 3.52 and 3.53 are almost the same as equations 3.50 and 3.51 except the terms that contains the time derivative of magnitude function. If we look at the ratio of change of the shape function, we will see that it change slower than the flux distribution, that is why larger time steps can be applied to solve the equations 3.52 and 3.53 rather than the ones that were need to solve the equations 3.50 and 3.51 which are the original spatial kinetic equations. With the kinetics conventional formulation see equations 3.55 and 3.56, the time dependent shape functions are not evaluated and the initial shape function is used as a time dependent shape function through the transient shape functions. PARCS [4, 5] holds several point kinetics options for quantifying the error produced when approximate the shape functions. These options are:

* To approximate time-dependent shape functions with the initial shape function.
* To evaluate the reactivity with the core averaged parameters and the pre-computed reactivity coefficients.
* To evaluate the core average with square power weighting.

With the three options the user can quantify the error due the three major approximations made when computing the shape functions.

$$\frac{dp(t)}{dt} = \frac{\rho(t) - \beta^{eff}}{\Lambda} p(t) + \frac{1}{\Lambda} \sum_{k} \lambda_k \zeta_k(t) \tag{3.55}$$

$$\frac{d\zeta_k(t)}{dt} = \beta_k^{eff} p(t) - \lambda_k \zeta_k(t) \qquad with \qquad k = 1, 2...N_d \tag{3.56}$$

Point kinetics option was not used in the present study, but it could be useful for the future parts of the model validation. In that way a point kinetics source generated by PARCS [4, 5] could be tested against the actual RELAP5 [41–49] or TRACE [1–3] models. Some of these models hold more that 20 years of robustness and validation, that is why testing the PARCS [4, 5] point kinetic model against those ones could be a good test to check the validity of the results. Nevertheless this work was little beyond of the scope of the present study.

3.1.3 GenPMAXS

The Purdue Macroscopic Cross Section file, PMAXS, is a computer code which provides an interface between some lattice physics codes such HELIOS-1.9 [27–29] and the PARCS v3.0 core simulator. GenPMAXS v5.0 [30] provides all of the data necessary to perform core simulation for steady-state and transient applications. Principal macroscopic cross sections, the microscopic cross sections of Xe/Sm, the group-wise form functions with several different branch states for the appropriate fuel burnup states, and all of the appropriate kinetics data are included inside the GenPMAXS [30] file. Since HELIOS-1.9 [27–29] is the lattice physics code used in the present study, a brief description of the interaction between HELIOS-1.9 [27–29] and GenPMAXS [30] will be given in this section. Figure 3 shows the general information exchange flow diagram when GenPMAXS [30] is present for a coupled NK-TH calculation.

As it can be seen in 3.3, GenPMAXS [30] is obtains its input files from the lattice physics code HELIOS-1.9 [27–29]. The output file from GenPMAXS [30] will be the input file for the core simulator code PARCS v3.0 [4, 5]. (Big center box on the center of Figure 3.3)Cross section information will be used for the neutronics calculation in order to obtain the power distribution across the core. Depending on the feedback parameters coming from the thermal-hydraulic code, the cross section will take a different value at each time step. The cross section library is containing a scaled list of cross section values with different state parameters values. Obviously it is impossible to pre-compute all the cross section points which will be required for the feedback parameters. A mechanism

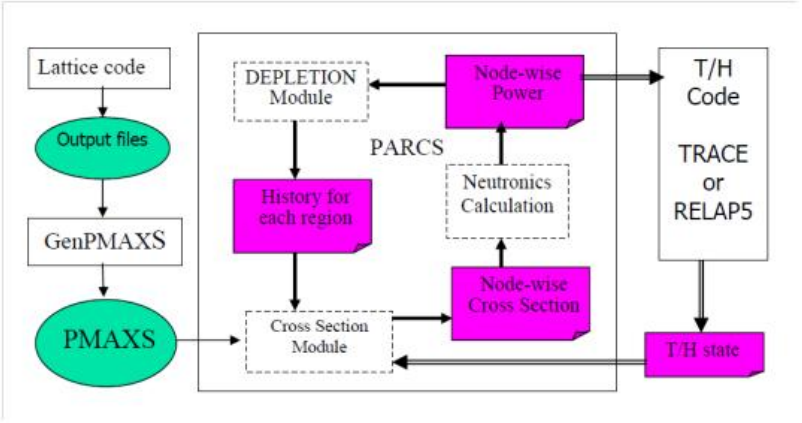

FIGURE 3.3: General information exchange flow diagram for a GenPMAXS code.

to find a intermediate value from a two or more computed points is needed ti interpolate in between the cross section library values. This variation of the cross section typically is treated with the equation 3.49 where the resulting cross section has a contribution of five state parameters, which are: α Control rod insertion; Tf Fuel temperature; Tm Moderator temperature; Dm Moderator density and Sb Soluble boron concentration. This treatment is known as *Partial Derivatives Model*. Beside the *Partial Derivatives Model* there are other cross sections formalisms. *Multi-dimensional Table: Piece-Wise lineal interpolation* is another method based in the following equation 3.57:

$$\begin{aligned}\Sigma(Tf,Tm,Dm,Sb,\alpha) = (1-\alpha)\Sigma^{unrod}(Tf,Tm,Dm,Sb,\alpha)+ \\ +\alpha\Sigma^{rod}(Tf,Tm,Dm,Sb)\end{aligned} \tag{3.57}$$

Where the indexes *rod* and *unrod* are referring to the computed values with and without control rods. If the desired XS value subindex i in the equation 3.58 is a non-existing pre-calculated value, its value will be obtained by the interpolation between Tf^a and Tf^b pre-calculated points in *Multi-dimensional Table: Piece-Wise lineal interpolation* method.

$$\begin{aligned}\Sigma^i(Tf,Tm,Dm,Sb) = \frac{Tf-Tf^b}{Tf^a-Tf^b}\Sigma^i(Tf^a,Tm,Dm,Sb)+ \\ +\frac{Tf^a-Tf}{Tf^a-Tf^b}\Sigma^i(Tf^b,Tm,Dm,Sb)\end{aligned} \tag{3.58}$$

With this method first a generation of the base XS with rodded and unrodded features is needed. Then different XS are calculated for different parameters as it can be seen in figure 3.4. When the required XS is in-between the calculated ones, a lineal interpolation, equation 3.58 is made.

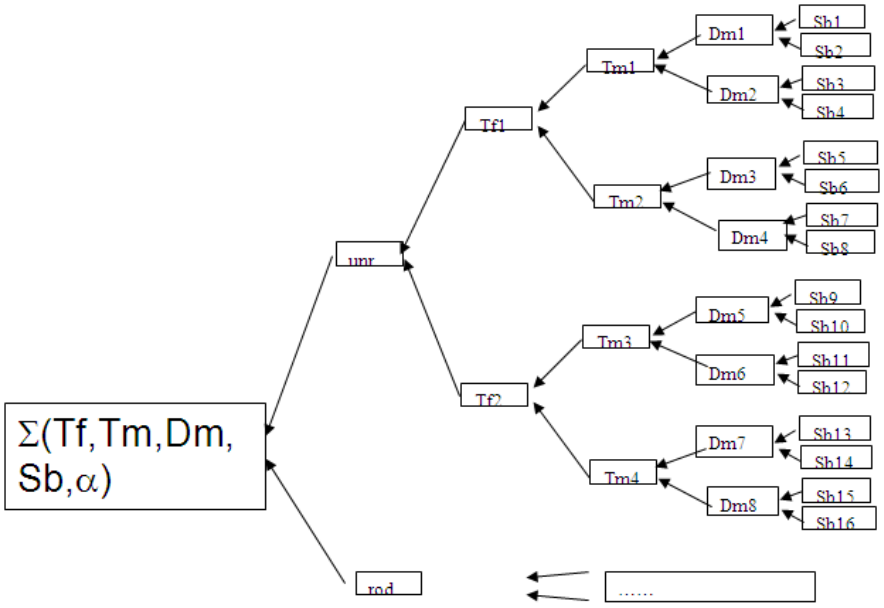

FIGURE 3.4: Multi-dimensional table XS treatment scheme.

Different codes have different approximations and different ways of treating the cross sections, when the desired value is not a pre-computed one. The accuracy of the method used will depend on the number of contributors to the final cross section value and to the type of interpolation used when finding the desired value. other codes might use another methodology named *Multiple tables* method. Where the resulting cross section is a combination of a different parameters including some history effects of the fuel.

GenPMAXS [30] method is a combination of the previous mentioned methods in order to be enough accurate without loosing a lot of time in terms of computational time costs. In GenPMAXS [30] method the cross section will have a contribution of the three main factors such: State variables; History variables; Neighboring contribution all of these factors are considered (with and without control rod). Depletion is also considered in GenPMAXS [30] method. Depletion capacity led burn the fuel assemblies and move along the core reactor life cycle. To burn the different fuel assemblies, historical data from each region is required, once the burnup step is achieved, the historical data will be used to recalculate the new power distribution. Throughout this process, TH feedback is constantly given at each time step. PMAXS [30] is structured in a macroscopic cross section format to be read by the PARCS [4, 5] depletion routine. The code is structured in state variables, such as:

- The control rod poison (CR)
- Density of Coolant (DC)

- Soluble Poison concentration in Coolant (PC)
- Temperature of Fuel (TF)
- Temperature of Coolant (TC)
- Impurity of Coolant (IC)
- Moderator parameters such density, soluble poison concentration, temperature and impurity (DM, TM, PM, IM)

The cross sections are also functions of burnup (B) and other history variables. The 5 history variables are:

- Control rod history (HCR)
- Coolant density history (HDC)
- Coolant soluble poison history (HPC)
- Fuel temperature history (HTF)
- Coolant temperature history (HTC)

The history variables together with the fuel burnup determines the history state, $H = [h_1, ..., h_{nh}, B]$, where nh is number of history variables used in PMAXS [30]. Cross sections can also vary depending on the conditions of the neighboring assemblies. Because the absorption cross sections of Xenon and Samarium are considerably larger than for other isotopes and are strongly dependent on the flux level of each node, the absorption cross sections for Xenon and Samarium are represented by their microscopic cross sections and number densities. The representation of the macroscopic cross section at a certain state is given by:

$$\Sigma^l(C,S,N,H) = \Sigma^{E,l}(C,S,N,H) + N^l_{Xe}\sigma^l_{Xe}(C,S,N,H) + N^l_{Sm}\sigma^l_{Sm}(C,S,N,H) \quad (3.59)$$

The above macroscopic cross section expression can be used for absorption, fission, transport and scattering respectively. But does not include Xenon and Samarium and that is why they are added in the two extra terms on the right side of the equation. Superscript l and the various subscripts denote the node index and isotope name respectively. C, S, N and H are 4 sets of state variables. C concerns about the insertion fraction for each node and is provided for each control rod composition, $C = [c_1, ..., c_{Nc}]$. If the

c_i is flux weighted then the control rod effect is non-linear. If flux weighting is not available or not used, then the control rod effect is linear. PARCS [4, 5] provides for flux weighting by solving a"3-node" problem with very fine mesh for the node with the partially inserted control rod. This is the standard method for treating the "control rod cusping" effect. Alternatively, for special cases where the standard method is not possible, flux weighting is provided by using several branches for the control rod compositions in which different rod fractions are used to represent the non-linear effect of a partially inserted control rod in a node. In this treatment, PMAXS [30] would contain branches for $0 < c \leq 1$ for the first control rod composition and for other control rod compositions if necessary. S represents the state variables of the current nodes except for the control rod state. Those state variables are: Density of Coolant (DC); Soluble Poison concentration in Coolant (PC); Temperature of fuel (TF); Temperature of Coolant (TC); Impurity of Coolant (IC); Moderator parameters such density, soluble poison concentration, temperature and impurity (DM, TM, PM, IM). The N index contains information for 4 pairs of neighboring assemblies in the plane. H represents the history state which contains history information, these are: Control rod history (HCR); Coolant density history (HDC); Coolant soluble poison history (HPC); Fuel temperature history (HTF) and Coolant temperature history (HTC). The macroscopic cross sections in PARCS [4, 5] are constructed with the assumption of a linear superposition of the partial cross sections on a base reference state. Such structure is taken into account when computing the cross section library with HELIOS-1.9 [27–29]. Next equation is showing how the code is representing the macroscopic cross-sections:

$$\Sigma^l(C,S,N,H) = c_{01}\Sigma(\frac{C_1}{c_{01}},S,N,H) + \sum_{i=2}^{N_c} c_i\Sigma(c_i,S,N,H) \tag{3.60}$$

c_{01} represents the sum of the unrodded fraction in one node and the first composition fraction in the same node.

$$c_{01} = 1 - \sum_{i=2}^{N_c} c_i \tag{3.61}$$

$$\begin{aligned}\Sigma(Cr,S,N,H) = \Sigma^r(H) + Cr\frac{\partial\Sigma}{\partial Cr}\bigg|_{(Cr/2,H)} + \sum_{j=2}^{N_S}\Delta S_j\frac{\partial\Sigma}{\partial S_j}\bigg|_{(Cr,S_j^m,N^r,H)} + \\ + \sum_{j=1}^{4}\left(\sum_{k=1}^{N_n} n_{j,k}\frac{\partial\Sigma}{\partial n_k}\bigg|_{(Cr,S,N_{j,k}^m,H)}\right)\end{aligned} \tag{3.62}$$

Here the reference cross section will receive contributions from the control rod insertion in different nodal locations; This is the second term on the right side, from the previous equation 3.62. The next term on the right side, considers the contributions of the other independent variables such density of the coolant, soluble poison concentration in coolant, temperature of fuel, and the temperature and impurity of coolant. The last term considers the four neighboring nodes to the computed one. This is where the state variables for the neighboring nodes contribute to the modification each cross-section. As can be seen from the previous equation, each computed cross-section at each node, will be a contribution from a reference state plus control rod insertion; plus independent state variables and finally plus the neighboring nodes independent state variables. Historical variables are taken into account for each of the terms; note the H index at each term from the previous equation. The partial derivatives of cross sections are calculated at the midpoint in between the reference state and the actual state for the current node. These partial are obtained by a piecewise interpolation of the pre-tabulated data using a "tree structure". The variables which can modify the reference cross sections are distributed in three large groups: a) The control rod fractions, b) Variables of the current node and c) Variables of the neighbors. Each group is treated in the following order: a) First a check for the control rod fraction, b) Second to account for the independent variables, c) Third to account for the neighboring independent variables, and d) Finally consideration of the historical contribution. Such order is followed as a response to a study, performed by the code authors in order to check for the impact relevance to the reference cross-sections by the previous mentioned groups. Once the methodology of cross sections correction contributions and computing is described, next is to describe "tree structure". Tree structure is the methodology used in order to store multiple cross sections sets in a proper manner and to be consistent with the interpolation methodology used by the code to finally obtain the desired cross section. At this level PARCS v3.0 [4, 5] reads the branch information provided by GenPMAXS [30] according to the branches computed by HELIOS-1.9 [27–29] and constructs a tree structure, where all branches are present and the partial derivatives are computed, in between each reference pre-computed state. In order to explain the tree structure methodology, first logical step is to describe the branch structure. Branches are used to compute and store information from every state. Essentially at each branch case, the same cross section as the reference state is used, but with at least one parameter modification. This modification gives a different value to the cross section and constitutes a branch. From all the proposed modification ranges for the state parameters, there will be one base branch and then the subsequent branches which compute the cross sections over all ranges for the other variable state parameters. For every branch there is a single modification to each of the previous parameters. The difference between the reference branch and the modified branch is computed and stored

through a partial derivative. Those partial derivatives are the midpoint between branch state and its state. The way to compute them is through following equation:

$$\left.\frac{\partial \Sigma}{\partial x_k}\right|_{X^m} = \frac{\Sigma(X^i) - \Sigma(X^{B(i)})}{x_k^i - x_k^r} \tag{3.63}$$

where:

- $X^i = (x_1^i, x_2^i, x_3^i, ...x_n^i)$ represents the state variables for one state.
- $X^{B(i)}$ represents the variables for the base state from the same previous state.
- X^m represents the variables which are located at the midpoint between the base state and each state constituting the branch.
- x_k are the branch variables for each state.

Figure 3.5 show a common scheme of the GenPMAXS [30] tree structure organization. The different dependence over the historical variables, instantaneous variables and burnup is structured in three levels in this example. Two main branches are clearly identified after the historical dependence level. These two branches are describing with and without control rod states. After this level, several modifications of the other state variables are made. In this particular case density of the moderator, boron concentration and fuel temperature. There is two options for each before mentioned variable state. Finally each branch is computed with a collection of different burnup points. This is a very simplified scheme but useful to illustrate the tree structure scheme. once the scheme is clear is time to illustrate the cross section computation methodology, let's take an example with six states, that means there are six cross sections provided by the lattice physics code, HELIOS-1.9 [27–29] used in the present study. Those states can be "Ref", for the unrodded reference state C_{r1}, which represents the rodded version of the reference state. Then there are two computations for the unrodded side without rods, where the coolant temperatures, TC_1 and TC_2, are modified. Finally two additional temperature modifications, TC_3 and TC_4, in the rodded branch, are made. Figure 3.6 is the representation of the above mentioned structure. In this case Reference cross sections are stored in "Ref" state. The C_{r1} branch stores the difference between the reference state and the rodded state, due the control rod insertion. The cases with modified coolant temperatures are placed in each branch consequently to their modifications and taking into account the control rod insertion. Finally the vertical "TC_{1T}, TC_{2T}, TC_{3T} and TC_{4T} represented by the partial derivative computation are placed in the

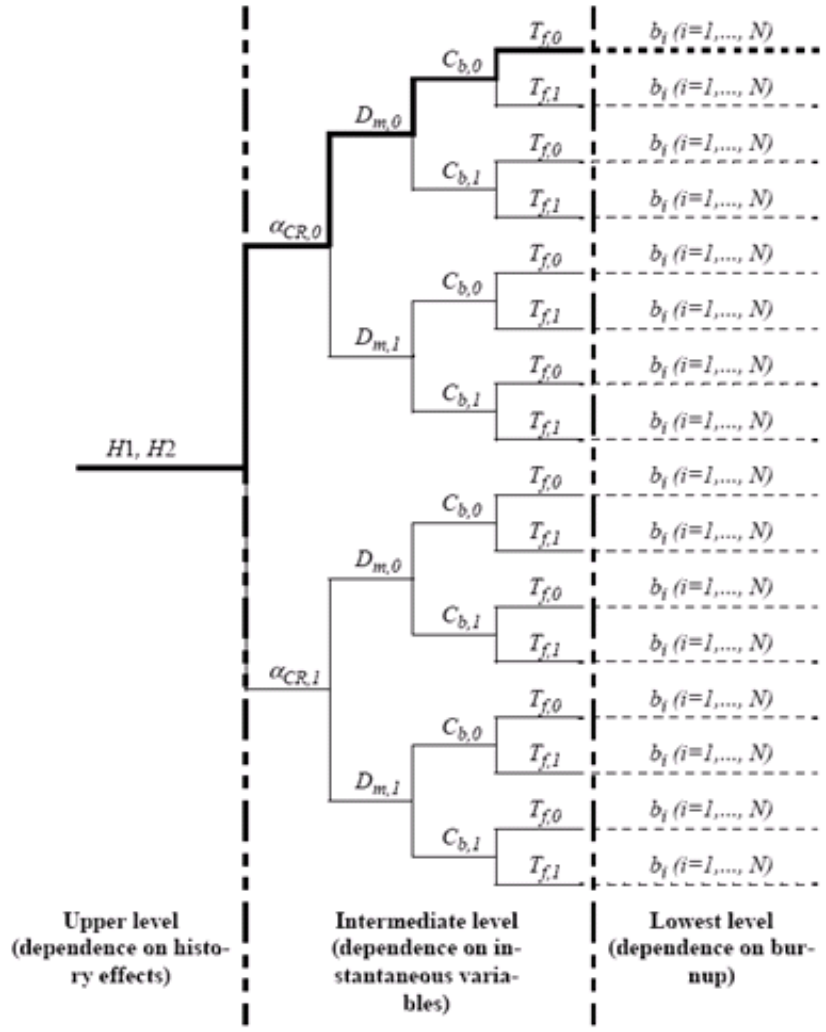

FIGURE 3.5: Example of a tree structure scheme.

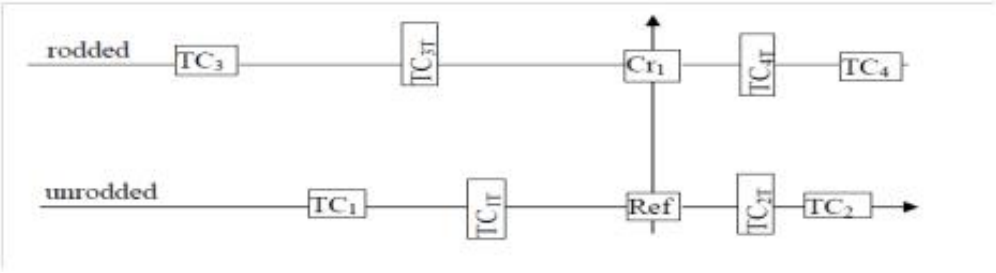

FIGURE 3.6: Branch structure example scheme.

midpoint between the reference state and each modified state. Those partial derivatives are computed using the previous equation 3.63.

Once the branch structure is build, the branches are listed sequentially in the input file. Once PARCS v3.0 [4, 5] has read all the cases it will automatically build the tree structure for the partial derivatives. It is remarkable that there is no need for symmetry in terms of the points at each branch. The misaligned points in figure 3.6, are drawn on purpose to show this fact remarkable. That fact makes the whole thing change the name from branch structure to tree structure, since not all the branches are necessarily forming a regular grid. The example in figure 3.7, explains the steps performed by the code in order to compute the desired cross section. In this case the point 1 is the place (in terms of variable states) where the cross section is required. Note this point is a partially rodded cross section because it is in between the two lines.

$$\Sigma(c,TC) = \Sigma^r + c\frac{\partial\Sigma}{\partial Cr}\bigg|_{(Cr_1/2)} + (TC - TC_r)\frac{\partial\Sigma}{\partial TC}\bigg|_{(c,TC_T)} \tag{3.64}$$

The above equation is the one used to compute the cross section in the desired state 1. The left side term is the desired cross section. First term on the right side from the previous equation is the cross section at the reference state. Second term on the right side, is the control rod contribution. (Note sub index 2 which indicates the position in terms of the control rod insertion where the cross section must be computed.) The last term on the right side is the contribution due from the coolant temperature term. Since first term is has already been computed, the second and third terms still need to be computed. Second term is computed as difference between reference state and control rod state. The results of this computation are point number 2. The key point of the process is to compute point number 3. Essentially, the partial derivative is obtained by a linear interpolation between the four surrounding partial derivatives with respect the coolant .temperatures from the two branches, TC_{1T}, TC_{2T}, TC_{3T} and TC_{4T}, as shown in equation 3.65.

$$\begin{aligned}\frac{\partial\Sigma}{\partial TC}\bigg|_{(c,TC_T)} = w_1\frac{\partial\Sigma}{\partial TC}\bigg|_{(0,TC_{1T})} + w_2\frac{\partial\Sigma}{\partial TC}\bigg|_{(0,TC_{2T})} + \\ + w_3\frac{\partial\Sigma}{\partial TC}\bigg|_{(1,TC_{3T})} + w_4\frac{\partial\Sigma}{\partial TC}\bigg|_{(1,TC_{4T})}\end{aligned} \tag{3.65}$$

Weights for the four points are determined by linear interpolation using following equations:

$$
\begin{aligned}
w_1 &= (1-c)\frac{TC - TC_2}{TC_1 - TC_2} \\
w_2 &= (1-c)\Big(1 - \frac{TC - TC_2}{TC_1 - TC_2}\Big) \\
w_3 &= c\frac{TC - TC_4}{TC_3 - TC_4} \\
w_4 &= c(1 - \frac{TC - TC_4}{TC_3 - TC_4})
\end{aligned}
\tag{3.66}
$$

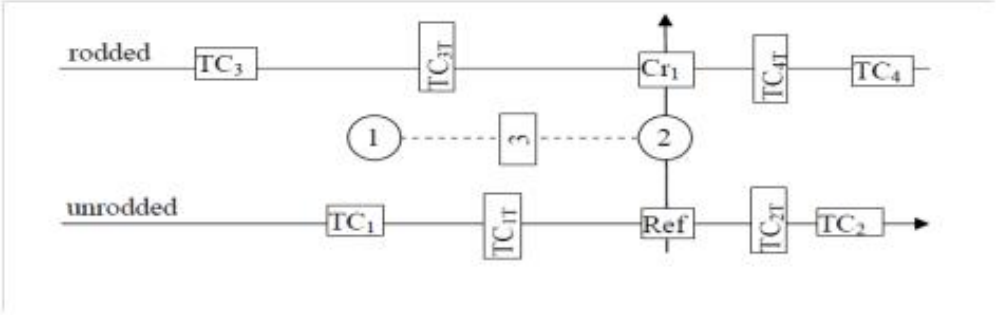

FIGURE 3.7: Cross section computation example with tree structure.

Within GenPMAXS [30] environment, all the history variables, except burnup, are treated with partial derivatives with respect to those history variables. The same type of computations as explained for a regular state variables are used for history variables. In a picture representation of this case a multiple layers represent the different tree structures for the different history variables considered. The code will perform the linear interpolations described above, to obtain the cross section in at a determined point. Burnup dependence of the cross section is treated with a piece wise linear interpolation. The following equation is shows the form of this piece wise linear interpolation.

$$
\Sigma^i(\overline{H}^j, B) = \frac{B_k^{i,j} - B}{B_k^{i,j} - B_{k-1}^{i,j}}\Sigma^i(\overline{H}^j, B_{k-1}^{i,j}) + \frac{B - B_{k-1}^{i,j}}{B_k^{i,j} - B_{k-1}^{i,j}}\Sigma^i(\overline{H}^j, B_k^{i,j}) \tag{3.67}
$$

where:

- Σ^i represents the cross section data in *ith* branch
- $\overline{H}^j$ is history state of *jth* history case
- $B_k^{i,j}$is first burnup point in *ith* branch of *jth* history case which be greater than B

Using these features, the code is able to interpolate and generate a cross section between the pre-computed cross sections which constitute the initial tree structure. Special requirements are needed to make the HELIOS-1.9 [27–29] output file readable by

GenPMAXS v5.0. [30]. Some specifications in the ZENITH-1.9 [27–29] output process are required, other ways the computed cross sections are useless. GenPMAXS [30] reads all the reference cross sections computed by HELIOS-1.9 [27–29] and generates the partial derivatives between the reference states. Generation of the partial derivatives is the first step to needed to generate the GenPMAXS [30] output file. Essentially, the HELIOS-1.9 [27–29] output file has to written in a specific format so that GenPMAXS [30] can read all the characters on the ASCII output file. This step is quite tedious and requires a lot of trial and error methodology since the manuals are not very clear in this section. There is list of required keywords that need appear on the ZENITH-1.9 [27–29] output file so GenPMAXS [30] can identify the following data and process it. Such list of keywords is showed in following tables 3.1 and 3.2.

Table 3.1: ZENITH output keywords for GenPMAXS code

Keyword	Purpose
%FILE_CONT 1	File control flag. It contains number of neutron groups, number of fuel pins, etc.
%FILE_CONT 2	File control flag. It contains the minimum energy bound of each neutron group.
%FILE_CONT 3	File control flag. It contains flow areas for in-channel, by pass and water holes.
%FILE_CONT 4	File control flag. It contains assembly pitch and position for rod array.
%STAT_**** #	Branch state flag. **** will have BRBS, BRCR, BRDC, BRPC, BRTF, BRTM etc. # denotes the sequential number of the same branch state.
%XS_PRIN %****	Principle cross section flag. **** will have KINF, VEL, CHI, STR, SAB, SFI, SKF, SNF, SNU, SDF. KINF = infinite multiplication factor. VEL = group wise neutron velocity. CHI = fission spectrum. STR = transport cross section. SAB = absorption cross section, it includes fission. SFI = fission cross section. SKF = kappa-fission cross section. SNF = nu-fission cross section. SNU = prompt neutron yield per fission. SDF = discontinuity factor. PHW=average flux on west surface PHE=average flux on east surface JNW=average net current on west surface (right as positive direction) JNE=average net current on east surface (right as positive direction)
%XS_SCT %SCT	Scattering cross section flag. Up-scattering is ignored.

Table 3.2: ZENITH output keywords for GenPMAXS code (Continuation)

Keyword	Purpose
%XS_XESM %****	Xe/Sm cross section flag. *** will have YLDXE, YLDID, YLDPM, XENG, SMNG, XEND, SMND. YLDXE = effective yield of Xe-135. YLDID = effective yield of I-135. YLDPM = effective yield of Pm-149. XENG = microscopic absorption XS of Xe. SMNG = microscopic absorption XS of Sm. XEND = assembly averaged Xe-135 number density. SMND = assembly averaged Sm-149 number density.
%XS_SB %****	Soluble boron cross section flag. *** will have SBNG, SBND. SBNG= microscopic absorption XS of natural boron. SBND= number density of natural boron in coolant.
%XS_BETA %****	Effective delayed neutron flag. **** will have DCAYB, BETA. DCAYB = decay constant of delayed neutron. BETA = effective beta.
%XS_PFF %****	Power form function flag. *** will have PAXIS 1, PAXIS 2, PFF. PAXIS 1 = x-axis coordinate of fuel pin. PAXIS 2 = y-axis coordinate of fuel pin. PFF = power form function.
%XS_GFF %***	Group-wise form function flag. *** will have FAXIS 1, FAXIS 2, GFF. FAXIS 1 = x-axis coordinate of pin cell. FAXIS 2 = y-axis coordinate of pin cell. GFF = power form function.

As can be seen from the previous tables 3.1 and 3.2, the required information from GenPMAXS [30] can be divided into several groups. The first group named general information, contains geometry information, group energy information and branch information. The second group of information contains information about the cross sections. The third group contains information about Xe and Sm. The fourth information group contains soluble boron information. The fifth group contains delayed neutron information. Finally the sixth group contains information about power form and Group-wise form. General overview of every quantity which could be used is given in tables 3.1 and 3.2, nevertheless not all the quantities are required, if some information was not computed by the lattice physics code, GenPMAXS [30] is going to use default parameters for those groups which contain no information coming from ZENITH-1.9 [27–29]. Essentially these keywords, in tables 3.1 and 3.2, work as titles, so when GenPMAXS [30] is reading the HELIOS-1.9 [27–29] output file, once it reads any of the previous keywords, the code knows then what to expect in the coming lines. More over the past key words, some extra specifications are needed in order to obtain a proper lecture from ZENITH-1.9 [27–29] output file. In that sense it is required to give: The width of the label at each block; The total width of the ASCII output file; The number of the columns which contains the information and also the width of each column. With this information and the previous keywords, the HELIOS-1.9 [27–29] output is ready to be read by GenPMAXS [30]. This process will end with a GENPMAXS [30] file which contains information about: The job title; Options used by GenPMAXS [30] when computing the partial derivatives; State variables; History state variables; Branch information, such as number and state from all branches; Reference states; Burnup points; Assembly discontinuity factors; Cross sections contents and different optional sections like extrapolation ranges; Incremental cross sections and finally the job ending flag. One GenPMAXS [30] file can also be merged with another GenPMAXS file. This option is known in the code as the PMAXS [30] to PMAXS [30] feature. The code has the capability to merge different GenPMAXS [30] files in one single file. The logical procedure followed by the code begins by reading and checking the logical variables from the both files after the GenPMAXS [30] code has read the both files and checked for the history variables. If the both files have the same history variables, the code will merge the different branches into one unique file. In case the two files do not have the same history variables, the code will merge the histories and obtain a final file which contains the two previous histories. Everything at this level depends on how the cross sections have been computed by the lattice physics code. In the present study, the cross sections are have been computed using the same history variables. The differences between two files, which represent the cross section sets for the same fuel assembly, are due to the control rod insertion, which represents two different branches of the same computation. All the computations have been made with or without the insertion of control rods, in case the fuel assembly

is placed in a zone where control rod banks actuate. In the present study, the merge feature is needed in order to join the rodded and unrodded branches computations in one unique file. Another part that needs to be merged is the fact that every fuel assembly is being computed under low, medium and high reference state conditions. Again the merge feature will be needed in order to join those three calculations for each fuel assembly to a final one. If the fuel assembly has the possibility of control rod insertion, six files will be merged into one. That is three for each reference state conditions and two for rodded conditions. There are up to 27 different fuel assembly types in the modeled core, plus the reflectors. A total of 80 different files are merged into the final 27 fuel assembly plus reflector files. There are more features from GenPMAXS [30] code that have not been described here since they were not used in the present study. Besides merging PMAXS [30] files and obtaining a GenPMAXS [30] file from a HELIOS-1.9 [27–29] computation, the code is capable to read cross sections from CASMO and WIMS which are two different lattice physics codes. Into the newest versions of the GenPMAXS [30] code, the TRITON capability is being added. TRITON is a lattice physics code included inside the SCALE package. This feature was added successfully into GenPMAXS [30] v6.1.1, the newest version to date of GenPMAXS [30] code. This feature will allow performing a full spectra uncertainty analysis, from the cross section calculations through GenPMAXS [30], going over the core simulator code and to the thermal-hydraulic system and finally to the coupled code system. This full methodology will allow visualizing the true effect of the uncertainties since the beginning of each parameter calculation. The general idea is to study how the uncertainties propagate across all the stages of the full coupled study. Such general idea is being studied under an OECD-NEA study called UAM [23], Uncertainty Analysis in Modeling. On side of this full range analysis is being shown in the present study, the other part has already been performed by a different person from the GET (Grup d'Estudis Termohidràulics) from the Technical University of Catalonia in Barcelona.

3.1.4 HELIOS

HELIOS-1.9 [27–29] is a neutron and gamma transport code for a lattice burnup in a general two dimension geometry. The code is divided into different sections depending on the process performed at each time. There is one input processor sub code called AURORA-1.9 which reads, saves and then processes the user input. This information is saved in the HERMES data base. HERMES is an internal HELIOS [27–29] data base which contains information from the input files but also contains information from the computed files. The HERMES data base contains a large quantity of information, which allows the user to decide which part of this large quantity of information is to

be retrieved to form part of the output file. There is also an output processor called ZENITH-1.9 [27–29]. The normal flow of information is showed in figure 3.8.

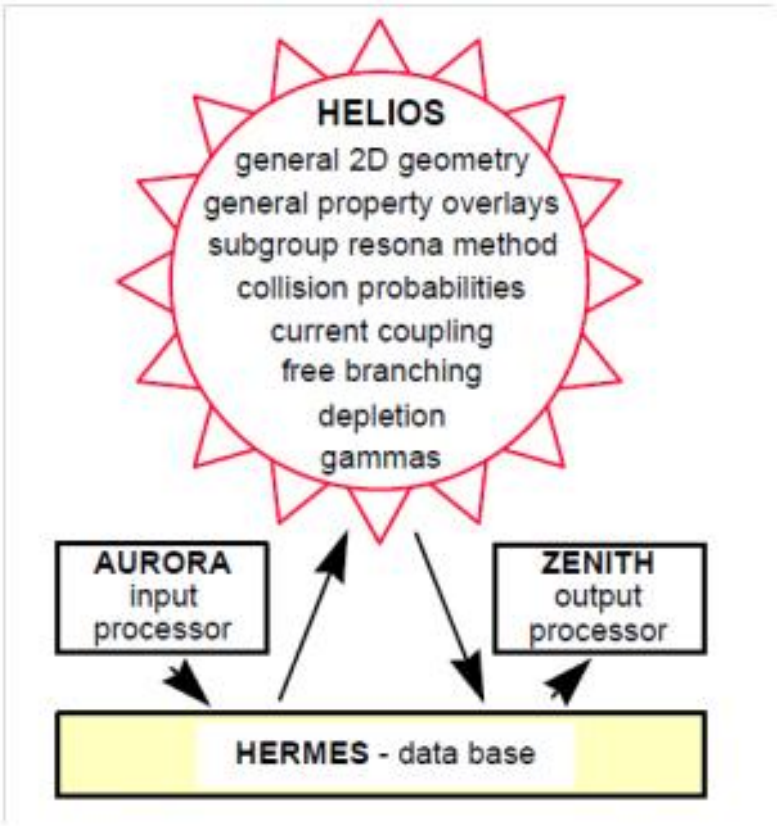

FIGURE 3.8: HELIOS-1.9 sub codes interrelationship.

AURORA-1.9 [27–29] is the input processor. The user is uses this code to define the geometry features from the model, materials compositions and distributions within the geometry, burnup specifications, branch parameters, and structure. This information is saved inside HERMES data base. When running HELIOS-1.9 [27–29], the executable will look inside the HERMES data base and retrieve the information from each input deck saved as a set of arrays. All the calculations specified inside the input deck are performed by HELIOS-1.9 [27–29] in this step. After all the computations have been completed by HELIOS-1.9 [27–29], the output file is also retained in the HERMES data base. This output file usually contains a large quantity of information. Only a part of this information might be required for the cross section library generation. In the same way, in order to form a cross section library that will be understandable by GenPMAXS [30], specific requirements such parameters, names, and quantities order must be accomplished. This task is performed by the ZENITH-1.9 [27–29] input file. The ZENITH-1.9 [27–29] output processor retrieves the exact information in the correct manner to be used in the following steps for the creation of the cross section library. This task could seem very easy but in the way the both codes GenPMAXS [30] and

HELIOS-1.9 [27–29] were made, at least at the moment this task was performed by the author, it was a quite time consuming task since not much information was given in order to make HELIOS-1.9 [27–29] output file readable by the GenPMAXS [30] code. A resume of the general information that the user needs to supply in the input file it is distributed in the following fields:

- Nuclear data library with basic nuclear data. This is the energy group structure. Code holds different energy groups structures starting from 190 energy groups, through 112, 47. Gamma groups can be 48 or 18.
- Isotopes number densities are also contained inside the code. The user has to specify the initial number densities for each isotope. There are also some common nuclear materials specifications and compositions in the library. Such as stainless steel, Inconel ...
- Geometry data for the transport calculation. In here the geometry distribution of the problem has to be entered, including spatial and angular discretization.
- States data. Different states and conditions to be used as branches in the cross section library formation.
- Execution sequences, how the calculations will be performed along all the branches.
- Output data. A list of the output data and its order of appearance in the output file.
- Finally, some specifications relating to accuracy limits, calculus iterations, convergence and methodologies to be used to solve the problem can be entered.

Some extra information might be needed when performing the calculation, besides that, the above list represents basic information needed. Typically at each calculation point, particle fluxes, currents and new material densities at each new burnup step are computed. As mentioned above this suppose a huge amount of information, if we consider multiple groups, and big geometry, that is why the common information retrieved at the end can be two groups homogenized data, with macroscopic cross sections for each fuel assembly. That is why some assumptions are taken at the present moment when performing a cross section library calculation. In future days these assumptions might get reduced to few or zero, but with the present computing machines, there is a big modeling challenge to assume when performing a cross section library computation. Some of these assumptions are explained in the *Cross-section library generation* section.

3.1.5 SNAP

SNAP [60] (the Symbolic Nuclear Analysis Package) its an interface created by NRC. Small definition of its capabilities will be given in this chapter. Since the aim of thesis is to use this software as a working tool, this chapter will not go in deeply detail on the features of the software. In here is intend to show the tool and to illustrate its basic features. More information can be found in [60]. SNAP [60] interface intends to facilitate the task of performing Nuclear analysis with system codes. Those analysis can go from the most common thermal hydraulic analysis (using TRACE [1–3] or RELAP5 [41–49] codes) to the more complex analysis with BEPU metrologies involved. Almost all the nuclear codes from NRC are suitable to be use by SNAP [60] platform. SNAP v 2.2.1 [60] was the version used in the present study. TRACE [1–3], RELAP5 [41–49], FRAPCON, FRAPTRAN, PARCS [4, 5], DAKOTA [6–9], SCALE, MELCOR and CONTAIN are the supported codes for this version. In one side SNAP [60] platform is able to read existing input decks form each one of the above mentioned list of codes. On the other side SNAP [60] is able to create input files from scratch from each one of the above mentioned codes. By using SNAP [60] the user takes the advantage of moving from a ASCII input file to a more comfortable SNAP [60] template. Such template is trying to represent with shapes, colors and figures, whatever is intend to be simulated inside the ASCII file. So if we take as and example TRACE [1–3] or RELAP5 [41–49] which are thermal hydraulic system codes, when using SNAP [60], what is shown to the user is a scheme of pipes, pumps, valves, etc... that represent the system modeled. Figure 3.9 show the typical view of TRACE [1–3] input on SNAP [60] platform.

On this common view from figure 3.9, the screen is divided in four windows. As usual on the top there is a menu where common functions from every computer program are included. Starting on the upper left there is a window that is giving the options from the different parts of the input deck (TRACE [1–3] in this case) Inside there are several menus that are grouping the different features form an input file. In here (keep in talking on TH system code area) the user will find general specifications on time steps, TH components, Control system components, Heat structures, connections between different elements... Second window, left bottom, is showing the inner menu on the above selected option. Lets say the user is looking at one pipe, selected on the above menu, the specifications like dimensions, flow areas, orientations... will be placed here. As a good capability at the end of each parameter to be defined there is a question mark. If the user clicks on this question mark, information from the user's manual (linked previously to SNAP [60]) appears on the screen. This information is saving a lot of time when building a new input file, specially for the beginners. On the right side upper window a representation of the input deck is shown, typically this representation

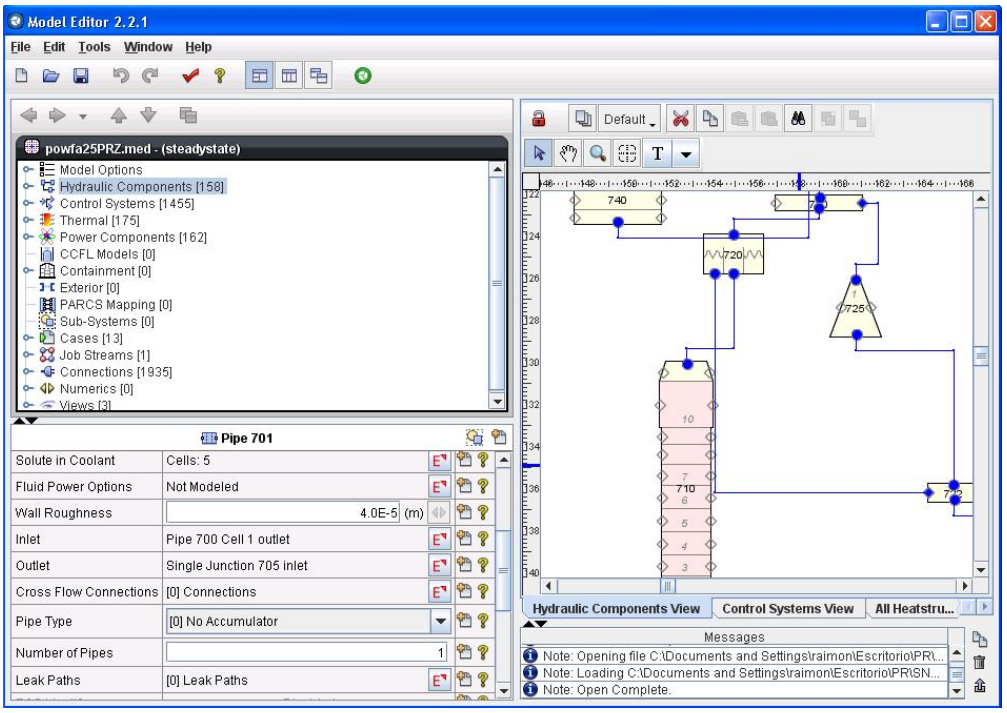

FIGURE 3.9: Example of SNAP window appearance.

is trying to preserve dimensions in the picture it self, also is showing the connection between the elements. This window can hold multiple tabs, for instance in the case of TH system codes, one of the tabs may contain all the TH elements, the next one all the Control system, finally there will be another one which may contain the Heat Structures system. Last window, right en below, its giving some information about the job performed by the user, any errors, misleads, malfunctions etc... are shown here.

SNAP [60] is using a modular plug-in design. This capability is structured in different plug-in connectors between SNAP [60] and the list of available codes for SNAP [60] platform. Once the user have the code and the SNAP [60] platform, the correct plug-in connector will allow the SNAP [60] to read, write, import and export files form a specific code. Beyond those capabilities of working with inputs, SNAP [60] platform is also able to perform restart input files. SNAP [60] allows to launch a calculation by using its own tool called calculation server. This tool is a linkage between SNAP created input and the executable file from each code. This calculation server will take the SNAP [60] developed input file, convert it into ASCII file with all the selected code specifications and it will launch it against the exactable file at the specific folder. This capability becomes very comfortable specially when running BEPU analysis, since a minimum of 59 cases are required. In that case SNAP [60] is taking care of preparing the 59 inputs and executing them in separate folders.

SNAP [60] tool is continuously in development that is why newer versions are coming every couple of months. Meanwhile the supported codes are improving and some bugs from SNAP [60] old versions are reported, new versions with new features are released. In that sense the user needs to be aware on the selected version, and it's clearly impossible to catch up with the newer versions specifications and modifications. That is why in the present study, one version was selected and all the work was performed with that "user frozen" version. Nevertheless a minimum effort will be required at he present to update all the job done to the latest version. There are good and bad consequences of using SNAP [60] tool, as mentioned above good consequences are enormous, in the sense that the user by using SNAP [60], is getting the whole picture of the problem very easy and can self-learn a lot about the used code, just by building its own input file. As a bad consequence the user is loosing a little bit track of the input deck and a lot of selections come by default (typically the user is not paying much attention on those) so in that sense the ASCII user was getting more knowledge since the beginning. Nevertheless SNAP [60] is a wonderful tool that is been used world wide and it has contrasted reliability.

3.1.6 DAKOTA

The DAKOTA [6–9] (Design Analysis Kit for Optimization and Terascale Applications) is the selected code for the Uncertainty propagation with the coupled 3D NK-TH calculations required in the present study. DAKOTA [6–9] an internal research and development activity at Sandia National Laboratories in Albuquerque, New Mexico. A primary goal for DAKOTA [6–9](Design Analysis Kit for Optimization and Terascale Applications) development is to provide a systematic and rapid means to obtain improved or optimal designs or understand sensitivity or uncertainty using simulation-based models. These capabilities generally lead to improved designs and system performance in earlier design stages, alleviating dependence on physical prototypes and testing, shortening design cycles, and reducing product development costs. DAKOTA [6–9] code is a toolkit which provides a flexible and extensible interface between simulation codes and iterative analysis methods. DAKOTA [6–9] contains: Algorithms for optimization with gradient and non-gradient-based methods; Uncertainty quantification with Sampling, Reliability, and Stochastic expansion methods; Parameter estimation with nonlinear least squares methods; and Sensitivity variance analysis with design of experiments and parameter study methods. These capabilities may be used on their own or as components within advanced strategies such as surrogate-based optimization, mixed integer nonlinear programming, or optimization under uncertainty. By employing object-oriented design to implement abstractions of the key components required for iterative systems analysis,

the DAKOTA [6–9] toolkit provides a flexible and extensible problem-solving environment for design and performance analysis of computational models on high performance computers. This chapter about DAKOTA [6–9] It is not intended to be as a comprehensive theoretical treatment. Rather, this section is intended to summarize a set of DAKOTA-related [6–9] capabilities and functions over the uncertainty quantification and optimization. General flow diagram from DAKOTA [6–9] is shown in figure 3.10 .

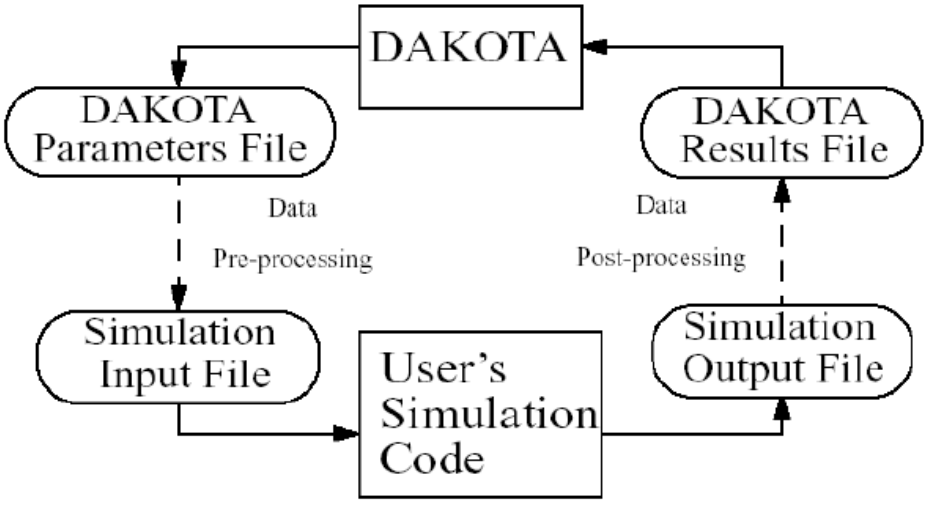

FIGURE 3.10: DAKOTA flow information chart.

DAKOTA [6–9] it is constituted with a big variety of iterative methods and strategies. It also has a lot of flexibility in order to interface with almost any simulation code. The following list explains about the variety of the DAKOTA [6–9] algorithms which compose the code:

- Parametric Studies. Parameter studies employ deterministic designs to explore the effect of parametric changes within simulation models, yielding one form of sensitivity analysis.
- Design of Experiments. Design and analysis of computer experiments techniques are often used to explore the parameter space of an engineering design problem, for example to perform global sensitivity analysis.
- Uncertainty Quantification. Uncertainty quantification methods (also referred to as nondeterministic analysis methods) compute probabilistic information about response functions based on simulations performed according to specified input parameter probability distributions.This feature is the one used from AKOTA [6–9] in the present study.

- Optimization. Optimization solvers built in order to minimize cost or maximize system performance, as predicted by the simulation model, subject to constraints on input variables or secondary simulation responses.
- Calibration. Calibration algorithms are orientated in the way to maximize agreement between simulation outputs and experimental data. They are used solve inverse problems.

As it has been mentioned, all the above features the selected one, which fits the needs for the present study, is the one about the Uncertainty Quantification. At a high level, uncertainty quantification or also known as nondeterministic analysis is the process of characterizing input uncertainties, forward propagating these uncertainties through a computational model, and performing statistical or interval assessments on the resulting responses. This process determines the effect of uncertainties and assumptions on model outputs or results. In DAKOTA [6–9], uncertainty quantification methods specifically focus on the forward propagation part of the process, where probabilistic or interval information on parametric inputs are mapped through the computational model to assess statistics or intervals on outputs. The aleatory Uncertainty Quantification methods in DAKOTA [6–9] include various sampling-based approaches, following list enumerates all the supported sampling-based approaches.

- Latin Hypercube Sampling. In here Monte Carlo (random) sampling and Latin Hypercube sampling methods are supported.
- Reliability Methods. This algorithm includes both global and local reliability methods. Global reliability methods are designed to handle non-smooth and multimodal failure surfaces, by creating global approximations based on Gaussian process models. Local methods include 1st and 2nd order of the Mean value method and most probable point method. Also include first and second order of advanced mean value method.
- Stochastic Expansion Methods. Rather than estimating point probabilities, stochastic expansion methods form an approximation to the functional relationship between response functions and their random inputs.
- Importance Sampling. This method method allows the user to estimate statistical quantities such as failure probabilities in a way that is more efficient than Monte Carlo sampling.
- Adaptive Sampling. The idea of the adaptive sampling is to construct a surrogate model that can be used as an accurate predictor of an expensive simulation.

- Interval Analysis. Interval analysis is often used to model epistemic uncertainty. In interval analysis, one assumes that nothing is known about an epistemic uncertain variable except that its value lies somewhere within an interval.
- Dempster-Shafer Theory of Evidence. The objective of Evidence theory is to model the effects of epistemic uncertainties. Epistemic uncertainty refers to the situation where one does not know enough to specify a probability distribution on a variable.
- Bayesian Calibration. In Bayesian calibration, uncertain input parameters are described by a prior distribution. The priors are updated with experimental data, in a Bayesian framework that involves the experimental data and a likelihood function which describes how well each parameter value is supported by the data.

Several actions need to be taken into account when performing a uncertainty quantification analysis. Within DAKOTA [6–9] framework several options are available. Typically the choice of uncertainty quantification method depends on how the input uncertainty is characterized, the computational budget, and the desired output accuracy. Some user guidelines within DAKOTA [6–9] capabilities are shown in figure 3.11 .

Method Classification	**Desired Problem Characteristics**	**Applicable Methods**
Sampling	nonsmooth, multimodal response functions; response evaluations are relatively inexpensive	sampling (Monte Carlo or LHS)
Local reliability	smooth, unimodal response functions; larger sets of random variables; estimation of tail probabilities	local_reliability (MV, AMV/AMV^2, AMV+/AMV^2+, TANA, FORM/SORM)
Global reliability	smooth or limited nonsmooth response; multimodal response; low dimensional; estimation of tail probabilities	global_reliability
Stochastic expansions	smooth or limited nonsmooth response; multimodal response; low dimensional; estimation of moments or moment-based metrics	polynomial_chaos, stoch_collocation
Epistemic	uncertainties are poorly characterized	interval: local_interval_est, global_interval_est, sampling; BPA: local_evidence, global_evidence
Mixed UQ	some uncertainties are poorly characterized	nested UQ (IVP, SOP, DSTE) with epistemic outer loop and aleatory inner loop, sampling

FIGURE 3.11: Guidelines for Uncertainty Qualification method selection.

DAKOTA [6–9] is also coupled to SNAP [60] platform. This coupling is made due a plug-in communicator. This way make the things easier for the user in terms of sampling and also in terms of input construction. The user needs to selects the desired quantities which are going to be perturbated with uncertainties and apply over them the PDF's, the mean value the standard deviation and the maximum and minimum in case there is any. Also the desired level of confidence and probability is required. By selecting these quantities it will determine the number of cases to be executed. Once this is done

DAKOTA [6–9] is going to apply the input values over the selected sampling algorithm and it will bring as a output a list of a modified inputs to be executed by the code or codes if there is a coupled calculation. Also some statistics information about the parameters and their deviations is printed at the end of the runs. Since the framework of the present study is quite global within the safety analysis, no more details about DAKOTA [6–9] tool will be given in this section. DAKOTA [6–9] has been used as a tool in order to propagate the uncertainties over the 3D NK-TH coupled analysis, its improvement or detailed behavior and algorithms goes beyond the aim of the present study.

3.2 Model description

Nuclear system coupled calculations, involve a minimum of two codes: a Neutron Kinetics (NK) code, for simulating the core behavior, and a Thermal Hydraulics (TH) code for the coolant system modeling. As it has been mentioned, PARCS [4, 5] and TRACE [1–3] are respectively the codes chosen in the present study for representing each model. This section describes the NK and TH models developed for this study plus the coupling assumptions made in the coupled model. This section also describes the methodology learned and used and tagged as a *"Know How"* building a cross-section library. All the required steps are described in deeply details and it leads the reader of how to perform a collection of lattice physics calculations which will lead to development of a *"whole cycle"* cross section library. This paricular sub-section constitutes one of the big achievements of the present report. When building these models different assumptions were taken according to the experience gained on the participation to the Chapter 2 mentioned Benchmarks but also some bibliography of similar works performed previously was consulted see reference [64].

3.2.1 Thermal hydraulic model

Ascó NPP is a 3 loops PWR with 2900 MW at full power. The TRACE [1–3] model completely reproduces the whole NPP system. TRACE V5 patch2 [1–3] is the version of the code used in the present study. The model is been validated against a 50% loss of load transient, typically used at UPC to validate full plant models [36–40], since there is existing plant data from such transient. Also the mentioned models are been used in several fields of thermal-hydraulic research area of study for the GET group such the work performed in scaling field, see: [65, 66]. In a coupled 3D NK-TH code calculation, the most relevant part of the thermal hydraulic model is the vessel. A 3D vessel component model in TRACE [1–3] has been implemented for the present study.

There are different types of vessel models that could be used for the present study. Figure 3.12 shows several different approaches that can be used to model the vessel. On the left side a representation of a parallel channel vessel is shown, in the center a regular single pipe model commonly used for thermal hydraulic analysis is shown and finally on the left side the model is a combination between parallel channels and 3D volumes. The variety of used vessel model used depends on the target of the study. The variety of models can go from 1D vessel, with only 1D volumes, going over to a pseudo 3D model, which is a combination of a parallel channels plus surrounding volumes to active core, to finally real 3D vessel component, which was the one selected for the present study. For a 3D NK-TH coupled calculation with MSLB scenario with high asymmetry in core parameters during the transient a full 3D vessel component was selected as the best option to reproduce with high accuracy and quality the NK-TH feedback and the return to critically event during the late phase of the selected scenario.

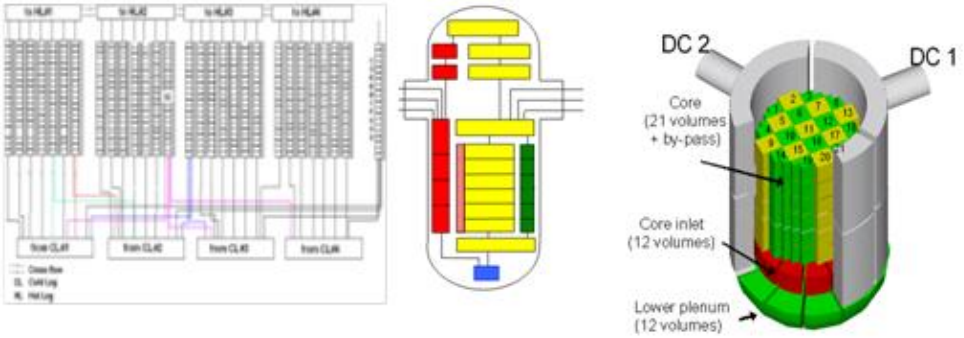

FIGURE 3.12: Different vessel model types.

The chosen vessel model has 15 axial layers, 6 azimuthal sectors and 5 radial rings. The three lower axial nodes represent the lower plenum. The next six axial nodes represent the active core, the center region, the down comer and the bypass for the external regions. The top layers describe the upper head and the upper plenum of the vessel. Figure 3.13 shows an axial cut of the vessel representation. The axial core region (lighter area) is subdivided radially for each layer in 18 TH cells formed by overlapping, three rings and six sectors. As a result there are eighteen TH cells for each axial layer in the active core. The outer rings represent the down comer and the bypass along the active core height. Below and above the active core region, the thirty TH cells formed by overlapping the azimuthal sectors and radial rings have a different meaning as mentioned above. The height of each axial node in the active core is 0.609 m. The total active core axial height is 3.654m. In terms of the thermal hydraulic model, the core region consists of 6 axial nodes and 18 radial cells (nodes) at each axial layer (node). It is important also to note that the real core has Cartesian geometry, due the fuel assemblies, but the used 3D

vessel component has cylindrical geometry, that is why some assumptions were taken when the mapping input decks where developed.

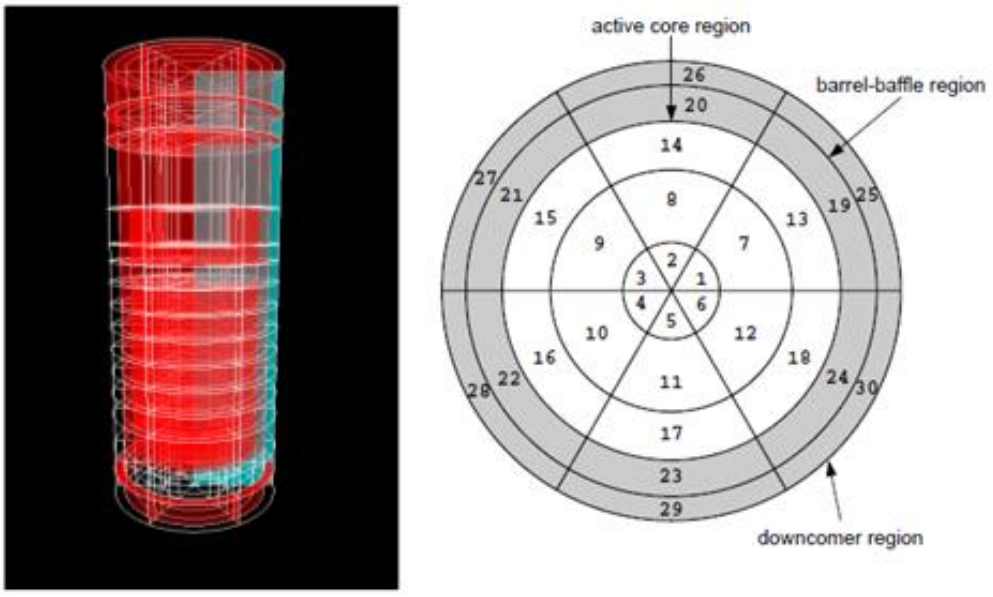

FIGURE 3.13: Used Vessel component scheme.

The rest of the 1D plant model remains the same as for a non-coupled system calculation. The three loops plus the pressurizer are included in the primary circuit representation. Three main steam lines are modeled in the secondary circuit representation. The Main Feed Water and Auxiliary Feed Water systems are also modeled for each loop. In terms of the safety injection systems, there are three accumulators, three LPIS and three HPIS systems, with later six modeled with FILL components. Finally a huge control block system (more than 1400 components) is included based on the developed UPC RELAP5 [41–49] Ascó NPP model, which has been validated and used for more than 20 years for Ascó NPP calculations [36–40]. The aim of the control block system is to reproduce with accuracy the plant response to different transients. The control block system has been increased with the addition of the control rod position control block. Since the model has the 3D capability and the validation of the model has been performed with a loss of load transient, where the control rod position is setup as a response of the thermal hydraulic parameters which pass the information and the position to the core simulator code which places the control rod at the proper position, according the signal coming from the thermal hydraulic code. This feature was not available in the releases NRC version thus some code modifications where need in order to achieve such capability. Code modifications made are presented in next Chapter of the present study in the model validation sub-section. Table 3.3 shows the TH model specifications in terms of the quantities of the used components.

TABLE 3.3: TH model specifications

Component	**Quantity**
Fills	7
Breaks	16
Pipes	94
Pumps	3
Separators	3
Single junctions	15
Valves	19
Vessels	1
Control systems	1455
Heat structures	175
Power components	162

3.2.2 Neutron kinetics model

As mentioned in the previous section, the Ascó NPP is a three loop PWR with 2900MW of thermal power. The core is modeled neutronically with PARCS v3.0 code. There are a total of 157 fuel assemblies in the core with a 17x17 pin array for each fuel assembly. The detail of modeling is one node per assembly in radial plane which results in 157 radial fuel nodes, plus 64 radial reflector nodes, which gives a total of 221 radial nodes for each axial level. Axially the FA is divided in 24 + 2 nodes, 24 for the core active region and 2 for the bottom and top reflectors. The height of the neutronic nodes in the FA's is varying with smaller nodes in the lower and upper regions and larger nodes in the central region. This modeling reproduces with greater accuracy the material and thus cross-section variation along the axial height. in that sense smaller nodes are introduced in the areas where the cross-section variation is larger, while larger nodes are introduced where cross section variation is smaller. There are 6 control rod banks. In terms of the cross-section there are 648 + 2 different compositions, which means 650 nodes where the cross section is evaluated, and they might give different feedback contribution to the thermal-hydraulic nodes. The cross-section library has been generated with the lattice physics code HELIOS-1.9 [27–29] using IDN-Ascó cycle 11, 12 and 13 [24–26] specifications, which are the technical reports coming from the NPP different cycles. Table 3.4 shows the general NK model specifications in terms of the quantities of the used components. Figure 3.14 represents a radial core assembly layout, in here a 27 different types of fuel assemblies can be observed, also the reflector position. Finally table 3.5 shows the core

reference boundary conditions which will be used when computing the cross section library as a reference states.

TABLE 3.4: NK model specifications

Component	**Quantity**
Radial locations	221
Axial planes	26
Nodes X direction	17
Nodes Y direction	17
Planar regions	25
CR bank positions	48
CR banks	6
FA different types	27

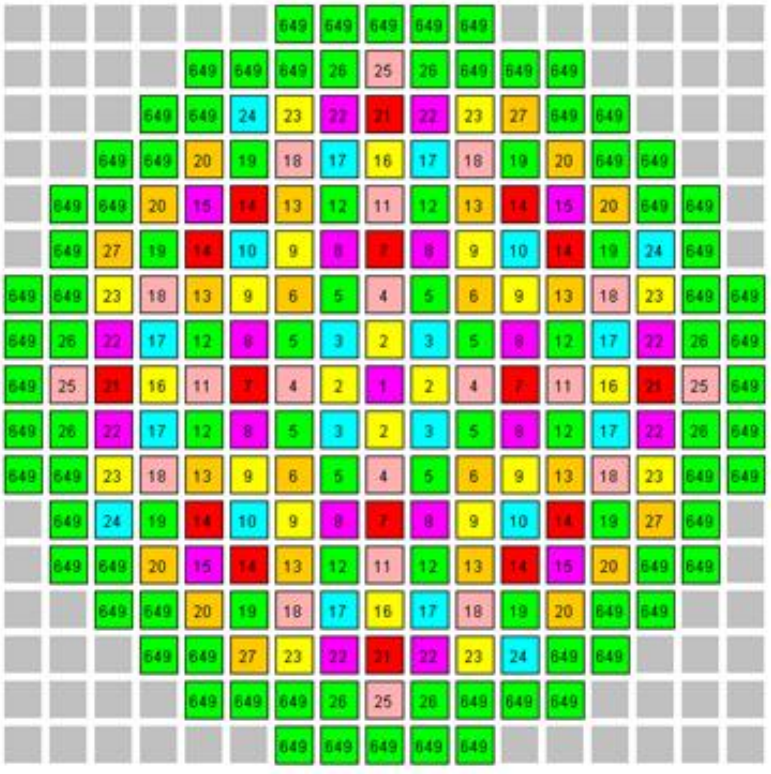

FIGURE 3.14: Example of radial core assembly layout.

The cross-section library contains a two group cross- sections with the 0.625 eV. as an energy group cut-off. Note that there are 27 different types of FA with different enrichments; this can vary between 2.1% to 4.55% of ^{235}U. Also the newest FA's have Gadolinium burnable absorbers with varying Gd_2O_3 concentration from 2.0% to 8.0%

TABLE 3.5: Core reference boundary conditions

Reference core boundary conditions	**Value**	**Unit**
Boron concentration	1728,00	ppm
Moderator temperature	306,50	Celsius
Moderator density	0,70137	kg/cm^3
Fuel Temperature	625,00	Celsius

depending on the FA. Every FA has 264 fuel pins plus 25 Guide tubes. All the cross-section have been generated as function off moderator temperature, fuel temperature, moderator density, boron concentration, control rods insertion, Xe and Sm concentration, history variables and finally over the burnup. Extended ranges of change for the thermal-hydraulic feedback parameters have been selected in order to cover both initial steady-state and expected transient conditions. Table 3.6 shows the NK model length in any direction.

3.2.3 Cross-section library generation

This section describes the methodology developed by the author in order to obtain a reliable cross-section library, which can be used for a wide range of scenarios and is for representing the core parameters and their response with high fidelity. The cross-section library is the most relevant feature inside the neutronic model. A good cross-section library ensures better results. The cross-section library also is the most time consuming in terms of computational time. A good cross-section library is capable to reproduce any point or core status along the reactor cycle life. When such feature is hold by the cross-section library created, "wraparound library" is the adjective used to define itself. This is an author given name which explains the previous features above explained, about the cross section library. The methodology used in the present work, is self-developed and can be used as a guideline for the creation of new cross-section libraries. HELIOS-1.9 [27–29] is the lattice physics code used to perform all the reactor physics calculations in order to obtain the cross sections sets. In previous studies, the author was used a RELAP5-3D [41–49] and [31–35] model coupled with NESTLE [31–35]. This model is described in the section preceding Appendix A, The RELAP5-3D [41–49] and [31–35] Cross section master library creation methodology. In that appendix, the detailed methodology to create a cross section library for the RELAP5-3D/NESTLE [31–35] and computed with HELIOS-1.9 [27–29] is presented. The base line for creating both libraries is very similar, few modifications are made after the computation of the cross sections in order to meet the requirement for NESTLE [31–35] or PARCS [4, 5] (GenPMAXS [30]) at each case. It is very important to have in mind all the considerations that have to

Table 3.6: NK model node length

Node number	Length	Unit
Node length X n1 to n17	21,50364	cm
Node length Y n1 to n17	21,50364	cm
Node length Z n1	100,00	cm
Node length Z n2	5,89	cm
Node length Z n3	6,95	cm
Node length Z n4	9,08	cm
Node length Z n5	9,2	cm
Node length Z n6	9,32	cm
Node length Z n7	9,44	cm
Node length Z n8	9,59	cm
Node length Z n9	24,99	cm
Node length Z n10	27,15	cm
Node length Z n11	24,99	cm
Node length Z n12	27,15	cm
Node length Z n13	24,99	cm
Node length Z n14	27,15	cm
Node length Z n15	24,99	cm
Node length Z n16	27,15	cm
Node length Z n17	24,99	cm
Node length Z n18	27,15	cm
Node length Z n19	11,42	cm
Node length Z n20	4,55	cm
Node length Z n21	5,26	cm
Node length Z n22	5,99	cm
Node length Z n23	5,99	cm
Node length Z n24	5,99	cm
Node length Z n25	5,99	cm
Node length Z n26	25,00	cm

be taken before obtaining the cross section library. Figure 3.15 illustrates in one scheme some of the assumptions considered.

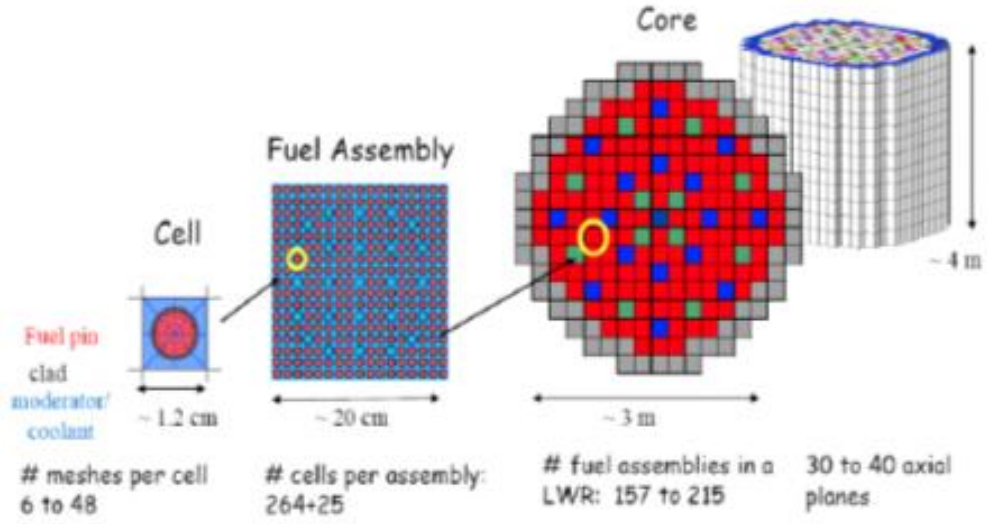

FIGURE 3.15: Cross section library geometry challenge.

Before discussing all the assumptions taken, it is remarkable to say, that some of these assumptions have to be taken because of the computational power of the nowadays computers. Future times might get more precisely results due the increase of the computational power. In terms of the geometry challenge it is important to note that every single fuel pin in our library is represented with a minimum of 16 points, (they can hold up to 48 nodes for the most complicated) which represent the fuel; the gap; the clad and the surrounding coolant. Such grouping of nodes is called a cell. To represent every single fuel assembly, different types of cells will be needed, regular ells, corner cells, side cells. These cells concern the position of the fuel pin across the fuel assembly. Also there are special types of cells, which represents the gadolinium fuel pins, guide tubes, and control rod cells. Control rod cells are essentially guide tube cells, with control rod material inside. Going back to the geometry challenges, it is important to note that 16 nodes are the minimum for each cell with 17 by 17 array of fuel pins in each fuel assembly, 157 fuel assemblies plus 64 radial reflector nodes at each axial level in the core it makes a total of 1021904 computing points in the core, for each axial level at the minimum. This number might be extended along the 24+2 axial levels such addition leads to 26569504 mesh points, in our model. This gives an approximation of the total number of mesh points required to compute the 3D reactor kinetics data for a typical PWR core. As mentioned before, some of the pin cells hold more than 16 meshes, especially those ones on the edges and the ones which are not regular fuel pin cells. This might increase the total number of meshes across the core. Obviously to work with such amount of mesh points requires a large computational time. Figure 3.15 shows the scheme of what

is required to account for all the geometry challenges. Fortunately some good approximations can be made in order to reduce the large quantity of computations required to complete the cross section library. First approximation relates to the pin cells, there is no difference between two identical pin cells. That is each regular fuel pin cell, will hold same number of mesh points and will be identical in terms of the computational treatment. The same applies for the corner cells, side cells, guide tube cell. Also there are some fuel assemblies which are identical in composition and historical burnup. In our model there are up to 27 different fuel assembly types. Every equal fuel assembly is treated same way as their equals. The same type of approximation is made for the reflector cells. Even using all the described approximations, the remaining number of different meshes is extremely large.

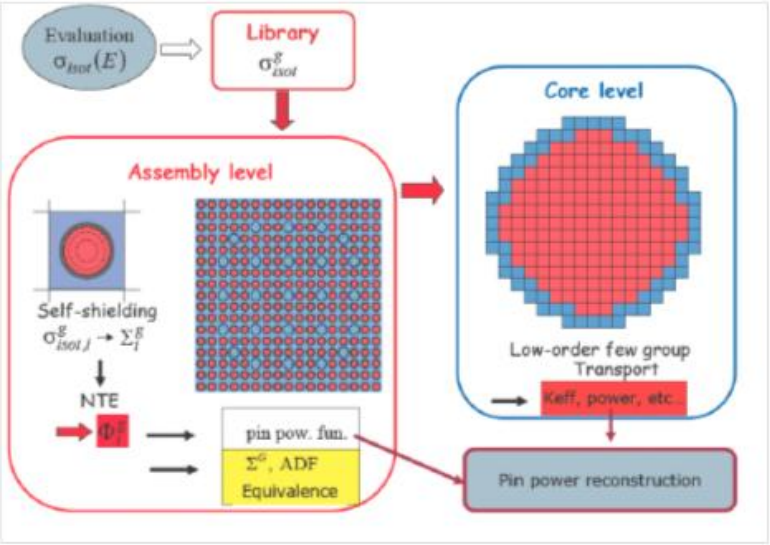

FIGURE 3.16: Approach used in a 3D kinetic core calculation.

There are other considerations that need to be taken in order to model a 3D neutron kinetics core beyond the geometrical considerations and approximations. The first consideration beyond geometry issues concerns the energy groups. A lattice physics code like HELIOS-1.9 [27–29] can hold up to a maximum of 190 energy groups, which is a large amount of groups, but far from a continuous spectra. So in first approximation a reduction from a continuous spectra to 190 group spectra is made. At the end our cross section library will only hold two neutron groups, so the initial computation of 190 groups is finally collapsed into only two groups. Self-shielding is considered in the bounding regions at each pin cell. Also all the macroscopic cross-section resulting from each computation is a homogenization across all the materials conforming each cell. Such homogenization is also made across the fuel assembly, so at the end a single homogenized macroscopic cross section is given for each fuel assembly at each axial level. The

last step is considers each axial mesh point in each fuel assembly together to represent the core. Finally some general quantities like total power or $k_{eff}$are considered. Figure 3.16 shows a schematic of this approximation procedure. At the end a two group cross section library is obtained. At this point no burnup steps, temperature ranges, boron concentrations or coolant density ranges are considered.

The final conclusion from this introductory section about the cross section library creation is to take notice that, despite all the approximations taken which reduce significantly the large initial number of computing points, large numbers are still present. Thus considerable computational time will be required to obtain the cross section library. As an example for the present study, each FA assembly was taking 24 hours non-stop from the computing server, in order to obtain one of the reference state from desired FA. Some FA had up to 6 reference branches. Fortunately the server allowed three parallel calculation at once. On the other hand it is important to have in mind all the approximations made in the process to understand the limitations of this model.

Once the geometry challenges and approximations are defined, the first step in order to start this endeavor is to obtain as much information as possible about the reactor core that is to be represented in the cross-section library. Some of the information needed is geometry information such, fuel dimensions, guide tube dimensions and distributions, control rod tube dimensions and distributions. The fuel pin pitch and fuel assembly pitch are also required. The inner and outer radii from all tubes and the radii from the different materials are needed for the process of building each input deck.

For the next step, compositions of the fuel pellets, such uranium isotopes percentages and uranium enrichment is needed. In the present study the enrichments can vary from 2.10% to 4.55% of ^{235}U and Gadolinium contents can vary from 2.0% to 8.0% of Gd_2O_3. The same information is required for the control rod material composition (Ag-In-Cd in our case). The material composition of the cladding surfaces are also gathered in this phase. Once all the composition information is has been compiled, the description of the fuel assembly geometry description is described. In HELIOS [27–29] input decks, as mentioned above, the fuel assembly description is made by stacking the number of individual cells necessary to conform each fuel assembly. Each cell can contain from 16 to 48 meshes depending on the type of cell represented. In the actual model there are regular fuel pin cells, which represent a regular fuel pin (placed in the center area of the fuel assembly) and its surrounding coolant. There are also corner cells and side cells, which represent fuel pins at the periphery of the fuel assembly. There are also gadolinium fuel pin cells, for the pins which contain gadolinium. Finally there are guide tubes cells and control rod cells, to represent the correspondent elements of each fuel assembly. Once every single cell type has been defined, next the cells are ensambled

conform to the fuel assembly. With the HELIOS-1.9 [27–29] code each fuel assembly is a matrix of different cells. Figure 3.17 shows the typical matrix used for modeling one regular fuel assembly, in between comas, the different nomenclature of each cell can be observed.

```
$FuelPins = PAR(
FC,FS,FS,FS,FS,FS,FS,FS,FS,FS,FS,FS,FS,FS,FS,FS,FC,
FS,F1,F1,F1,F1,F1,F1,F1,F1,F1,F1,F1,F1,F1,F1,F1,FS,
FS,F1,F1,F1,F1,GT,F1,F1,GT,F1,F1,GT,F1,F1,F1,F1,FS,
FS,F1,F1,GT,F1,F1,F1,F1,F1,F1,F1,F1,F1,GT,F1,F1,FS,
FS,F1,F1,F1,F1,F1,F1,F1,F1,F1,F1,F1,F1,F1,F1,F1,FS,
FS,F1,GT,F1,F1,GT,F1,F1,GT,F1,F1,GT,F1,F1,GT,F1,FS,
FS,F1,F1,F1,F1,F1,F1,F1,F1,F1,F1,F1,F1,F1,F1,F1,FS,
FS,F1,F1,F1,F1,F1,F1,F1,F1,F1,F1,F1,F1,F1,F1,F1,FS,
FS,F1,GT,F1,F1,GT,F1,F1,GT,F1,F1,GT,F1,F1,GT,F1,FS,
FS,F1,F1,F1,F1,F1,F1,F1,F1,F1,F1,F1,F1,F1,F1,F1,FS,
FS,F1,F1,F1,F1,F1,F1,F1,F1,F1,F1,F1,F1,F1,F1,F1,FS,
FS,F1,GT,F1,F1,GT,F1,F1,GT,F1,F1,GT,F1,F1,GT,F1,FS,
FS,F1,F1,F1,F1,F1,F1,F1,F1,F1,F1,F1,F1,F1,F1,F1,FS,
FS,F1,F1,GT,F1,F1,F1,F1,F1,F1,F1,F1,F1,GT,F1,F1,FS,
FS,F1,F1,F1,F1,GT,F1,F1,GT,F1,F1,GT,F1,F1,F1,F1,FS,
FS,F1,F1,F1,F1,F1,F1,F1,F1,F1,F1,F1,F1,F1,F1,F1,FS,
FC,FS,FS,FS,FS,FS,FS,FS,FS,FS,FS,FS,FS,FS,FS,FS,FC)
```

FIGURE 3.17: 17x17 HELIOS matrix used to model a regular Ascó NPP fuel assembly.

Different descriptions from the different types of fuel assemblies will be needed in order to completely model the core. After obtaining all necessary information from the nuclear power plant technical report, our core will contain four different types of fuel assemblies. Those are:

- **Norm_FA:** Regular fuel assemblies, no control rod in it, no gadolinium fuel pins, no instrumentation. Only different enrichment grades can be considered in here.
- **Rodded_FA:** Fuel assemblies which contain control rods in the case of the control rod insertion.
- **Gd_FA:** Fuel assemblies which contain a poison material such as Gd_2O_3. Such fuel poisoned pins can be placed in different positions across the fuel assembly matrix. This fact leads to a large variety of this type of fuel assembly.

- **Reflector:** Reflector type contains the reflector elements placed at the periphery of the core. There is no difference between upper and lower reflectors, this means they are modeled with same features.

Once all the different fuel assembly types are represented, the next step is to determine the computing ranges for the different core parameters. This includes determining the fuel temperature, moderator temperature, moderator density and boron concentration ranges. A reference state is declared at this point. Experience, user skills and scenario knowledge are helpful to determine the ranges above and below such reference state. Two important issues are required for such selection. The first is to ensure that the selected range covers at least all the situations to be reproduced. In our model we like to cover all situations from the lower temperatures and conditions found in MSLB scenarios to higher temperatures and conditions found in ATWS scenarios. Nominal conditions are placed in between such range. See figure 3.18.

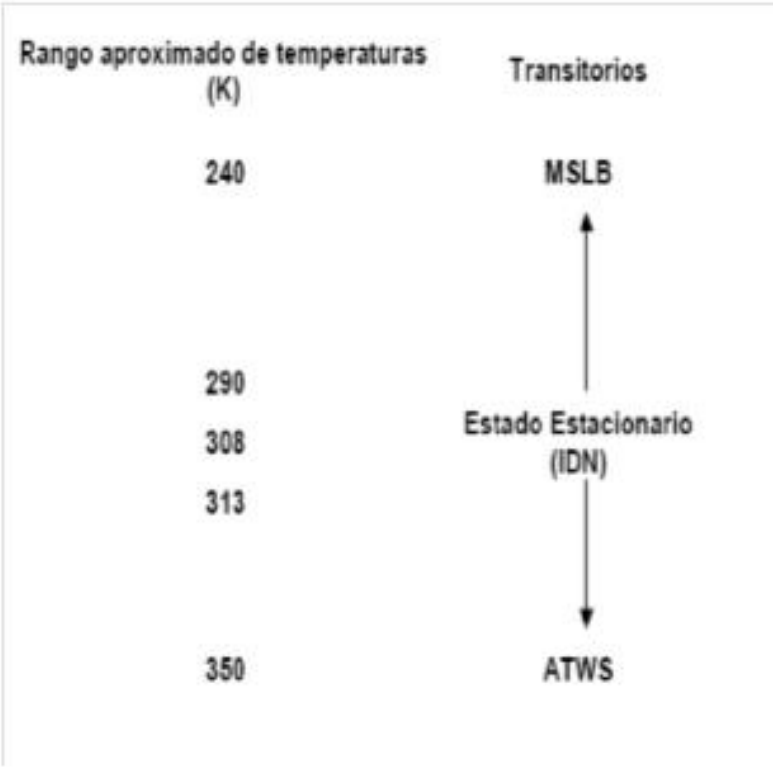

FIGURE 3.18: Purposed range to be covered with the cross sections library values.

The next important issue, when fixing the computational ranges, is to consider when defining the parameter range is the spread the computation points. They should be far enough apart to minimize the computation points and close enough so that large

interpolations between two computed nodes are not needed. Figure 3.7 shows the selected points used in order to compute the cross section library. As mentioned above the selection is made with the users experience and it can be useful for future cross sections libraries. The selection of the computational nodes is one of the most challenging and important parts from the creation of the cross section library. Some trial and error was needed before starting the real calculations in order to have a good balance between computational points (detail description) and computational time (time needed to obtain the cross section library). Once this selection is made, next consideration concerns about the power. The power density at each fuel assembly needs to be taken into account in order to compute the cross sections. 40.106 W/grU is the input power density for the fresh fuel elements, different power densities are considered for old fuel assemblies that came from other cycles. Thus a power increase was applied to the modeled core in previous cycles. Xenon treatment is accomplished by defining three states of Xenon, these states are the non-equilibrium state, equilibrium state and quasi-equilibrium state. Finally burnup steps are defined. To define the burnup steps, several considerations need to be taken. First a small burnup step is required to account for the xenon equilibrium time, in the case reported in this paper is up to 150 MWd/t, The following steps are differently spaced along the fuel assembly life. Again, user experience is the determinant when selecting where the stepwise and again considerations about the interpolation and the maximum allowed burnup are taken in each selection. Same kind of the above mentioned trial and error tests was used here before determining the burnup steps. The selected burnup steps are (0, 150, 500, 1000, 2000, 4000, 10000, 40000, 47000 and 57000) MWd/t. This chain was the one used for regular fresh fuel assemblies. Different burnup steps were taken on the wasted fuel assemblies coming from the previous cycles, due the power increase suffered in the Ascó nuclear power plant.

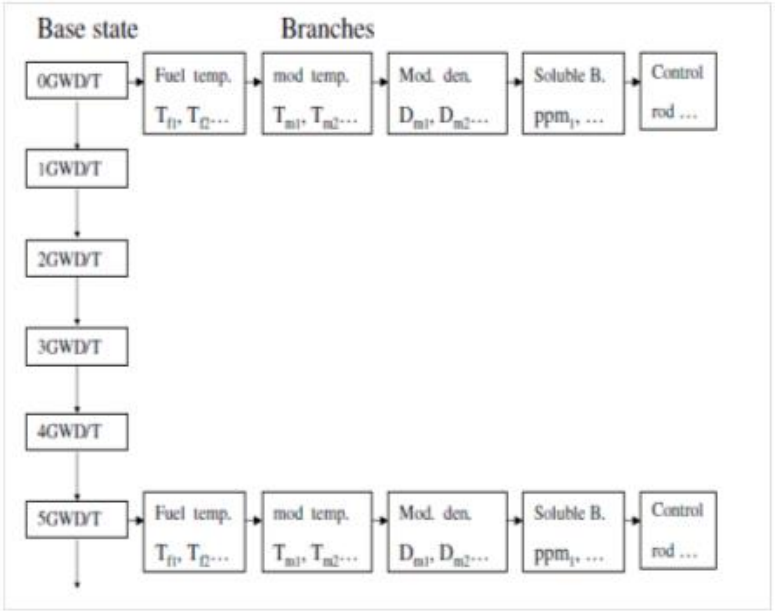

FIGURE 3.19: TREE structure scheme.

Once reference state and the other states (burnup steps, temperature ranges, density ranges, boron concentrations, Xenon, power) are defined, the next step is to build a TREE operator. The TREE operator is a list of all the states to be computed. Figure 3.19 shows the initial part of the TREE structure. Each reference state is considered at every burnup step, and for each burnup step, there is a list of combinations concerning the parameter variations. This structure is prolonged for each reference state along all the burnup steps. Such operation has to ensure that all the possible combinations from all the above listings is taken into account. This ends up with a long list with approximately more than 1000 possible combinations of the previous states. Moreover, three main moderator reference temperatures are selected as a base case for this tree structure, Low, Medium, and High according to that three calculations are performed for each fuel assembly, with more than 1000 states computed inside each case. Every computed state is calculated over all burnup steps. More than one hundred days were need to compute all the cross section sets.

Table 3.7: List of the computed points for each core parameter

Fuel temperature (K)	
Nominal	898.15
TFu1	400.00
TFu2	1400.00
TFu3	1800.00
TFu4	2200.00
TFu5	2800.00
Moderator temperature (K)	
Nominal	579.65
Low	565.45
High	323.00
Cold	600.13
Tmod1	330.00
Tmod2	450.00
Tmod3	525.00
Tmod4	600.00
Moderator density (gr/cm3)	
Nominal	0.70137
Low	0.74264
High	0.66212
Cold	0.99804
Dmod1	0.01
Dmod2	0.3
Dmod3	0.55
Dmod4	0.65
Dmod5	0.75
Dmod6	1.00
Boron PPM (mg/kg)	
PPMN	0.001728
PPML	0.000475
PPMH	0.000533
PPM1	0.00001
PPM2	0.0022

AURAROA-1.9 [27–29] is the input processor subprogram, which inputs all specifications inside HELIOS-1.9 [27–29]. The HELIOS-1.9 [27–29] computing process generates a huge output file with more information than required for the creation of the cross section library. This information is saved in a .hrf file, which contains ASCII codifications and it is unreadable by regular text file reader programs. The user must build another input deck using ZENITH-1.9 [27–29], another HELIOS-1.9 [27–29] subprogram, in order to call all the requested values that will be used to conform the cross section library. Also the ZENITH-1.9 input deck is where all the homogenized cross sections are collapsed in two groups and over the material homogenization. As it has been mentioned in the present study, the common limit of 0.625 eV is being used in order to separate the fast and thermal groups. Also in the ZENITH-1.9 [27–29] processor a list of the output parameters that will appear in the output file must be declared. Figure 3.8 shows such list.

Table 3.8: ZENITH-1.9 output parameters list

Keyword	Meaning
D1	Diffusion coefficient group 1
D2	Diffusion coefficient group 2
SIGA1	Group 1 absorption macroscopic cross section
SIGA2	Group 2 absorption macroscopic cross section
SIGS	Scattering 1 to 2 macroscopic cross section
SIGF1	Group 1 fission macroscopic cross section
SIGF2	Group 2 fission macroscopic cross section
SIGNF1	Neutron produced by fission in group 1
SIGNF2	Neutron produced by fission in group 2
Flux1	Group 1 neutron flux
Flux2	Group 2 neutron flux
ADF1	Group 1 assembly discontinuity factor
ADF2	Group 2 assembly discontinuity factor
VELOC1	Group 1 absorption velocity
VELOC2	Group 2 absorption velocity

After extracting all necessary information from the ZENITH-1.9 [27–29] output file, all the files are saved in a proper manner. In the present study cycle 13 of the Ascó NPP is being reproduced in a core configuration, where up to 27 different fuel assemblies were modeled. Some of the fuel assemblies were fresh fuel, some came from previous cycles, and one fuel assembly came from the first cycle of the reactor core. For each different fuel assembly, there will be up to a minimum of three calculations for each of

the High, Medium and Low reference states. If the Fuel assembly contains control rods, this will add three additional calculations, for the High, Medium and Low reference state assembly configurations. There are 8 different kinds of fresh fuel assemblies, from 15A to 15H, with different enrichments considered in this study. As previously mentioned one fuel assembly came from the first cycle, one fuel assembly came from the 11th cycle, (number 11), one fuel assembly came from the 10th cycle (number 12) and 8 types of fuel assemblies came from the 12th cycle, (number 14). Tables 3.9 and 3.10 show all the calculations performed.

Table 3.9: Fuel assemblies calculations for Ascó NPP cycle 13

CYCLE	Fuel assembly type	Reference state Calculations	Without CR	With CR
13	15A(MAEF+IFM-ZR)	Low	x	
		Medium	x	
		High	x	
	15B(MAEF+IFM-ZR)	Low	x	
		Medium	x	
		High	x	
	15C(MAEF+IFM-ZR)	Low	x	x
		Medium	x	x
		High	x	x
	15D(MAEF+IFM-ZR)	Low	x	
		Medium	x	
		High	x	
	15E(MAEF+IFM-ZR)	Low	x	x
		Medium	x	x
		High	x	x
	15F(MAEF+IFM-ZR)	Low	x	
		Medium	x	
		High	x	
	15G(MAEF+IFM-ZR)	Low	x	
		Medium	x	
		High	x	
	15H(MAEF+IFM-ZR)	Low	x	x
		Medium	x	x
		High	x	x
1	1(STD)	Low	x	
		Medium	x	
		High	x	

As it can be seen from tables 3.9 and 3.10, there are 25 different calculations, each with three reference states, plus reflector input decks which make close to 80 calculations to obtain all the necessary information required to build the cross section library for Cycle 13 of the Ascó NPP using HELIOS-1.9 [27–29] and the following self-developed methodology for building a cross section library. Almost one day was needed for each computation with the used LINUX servers. The described methodology was self-developed for the present study. Once all the computations are finished, the output files will work as input files of GenPMAXS-v5.0 [30]. The idea for making all computations go through GenPMAXS-v5.0 [30] is to be able to provide all needed information to core simulator code PARCS-v3.0 [4, 5]. In this step, all information is collapsed into 27 different files representing the 27 different fuel assemblies in the core, plus 1 file which represents the reflector. First GenPMAXS-v5.0 [30] reads all the information from every ZENITH-1.9

Table 3.10: Fuel assemblies calculations for Ascó NPP cycle 13 (Continuation)

CYCLE	Fuel assembly type	Reference state Calculations	Without CR	With CR
10	12B(AEF+IFM)	Low	x	
		Medium	x	
		High	x	
11	13(AEF+IFM)	Low	x	
		Medium	x	
		High	x	
12	14A(AEF+IFM-ZR)	Low	x	x
		Medium	x	x
		High	x	x
	14B(AEF+IFM-ZR)	Low	x	
		Medium	x	
		High	x	
	14C(AEF+IFM-ZR)	Low	x	x
		Medium	x	x
		High	x	x
	14D(AEF+IFM-ZR)	Low	x	x
		Medium	x	x
		High	x	x
	14E(AEF+IFM-ZR)	Low	x	
		Medium	x	
		High	x	
	14F(AEF+IFM-ZR)	Low	x	
		Medium	x	
		High	x	
	14G(AEF+IFM-ZR)	Low	x	
		Medium	x	
		High	x	
	14H(AEF+IFM-ZR)	Low	x	
		Medium	x	
		High	x	

output file and converts it into a GenPMAXS-v5.0 [30] file. Second the GenPMAXS-v5.0 [30] files can be merged. First the three reference state configurations are merged and then these files are merged with the rodded states. At the end there are 27 files, where some contain control rod calculations and others are without control rods calculations. The PARCS [4, 5] code structure will select a file to represent each different fuel assembly. In case of control rod insertion, nothing needs to be done, since all the fuel assemblies which might contain the control rods already hold the information to correct the cross sections according the control rod insertion. In that sense if there is some node which has a control rod inserted during a transient, the code will pick from the GenPMAXS [30] file the required correction to the control rod insertion and this

effect will lead to a increase of absorption cross section and neutron flux reduction.

Uncertainty deviations have not been considered when building the present cross section library. It is important to have in mind that for a complete Best Estimate Plus Uncertainty analysis in a coupled 3D NK-TH model, uncertainty considerations have to be taken into account since the creation of the cross section library, through over all the steps which compose a coupled calculation. In the present case of study Uncertainties have only been considered over the thermal hydraulic model parameters and neutronic core code parameters. OECD UAM project [23] project intends to carry out the uncertainty propagation over all the phases from lattice physics phase to coupled 3D TH-NK phase. Early phases of the project are still going on. General results (i.e. global Uncertainty propagation) will be discussed in coming years. UPC GET group is actively participating in this international project.

3.2.4 Coupled model

The thermal hydraulic model has been modified in order to meet the neutronics model requirements. In the present model, there are 157 Heat Structures (HS) in the thermal-hydraulic core region. The equivalence is one HS to one FA. There are 18 radial thermal-hydraulic cells in each axial thermal-hydraulic active core layer. Figure 3.20 shows the assignment (mapping) in each axial layer of the active core and reflector TH cells to neutronics nodes. Every color area represents a thermal-hydraulic cell. In terms of the axial nodalization, there are a different number of nodes for each model. Due the axial cross-section variation, there are 24 non-equidistant axial nodes for the HS and for the neutronic models however there are 6 equidistant nodes for the hydraulic model. Consequently the axial mapping between the HS and each of the neutronics nodes is not one to one. Some sensitivity studies about this were made, when validating the model. Essentially a one to one axial distribution model was built and tested. These results are discussed in next Chapter. Notice, in the regular model, the neutronic nodalization is finer than the coarser thermal-hydraulic nodalization. In that sense, it should be taken into account that several neutronic nodes are receiving the same thermal-hydraulic information and vice versa. That is one thermal hydraulic node is receiving and averaging power information coming from different neutronic nodes. All information is contained in a mapping file. This file is responsible for the good agreement and exchange of information between the thermal-hydraulic code TRACE [1–3] and the reactor physics code PARCS [4, 5].

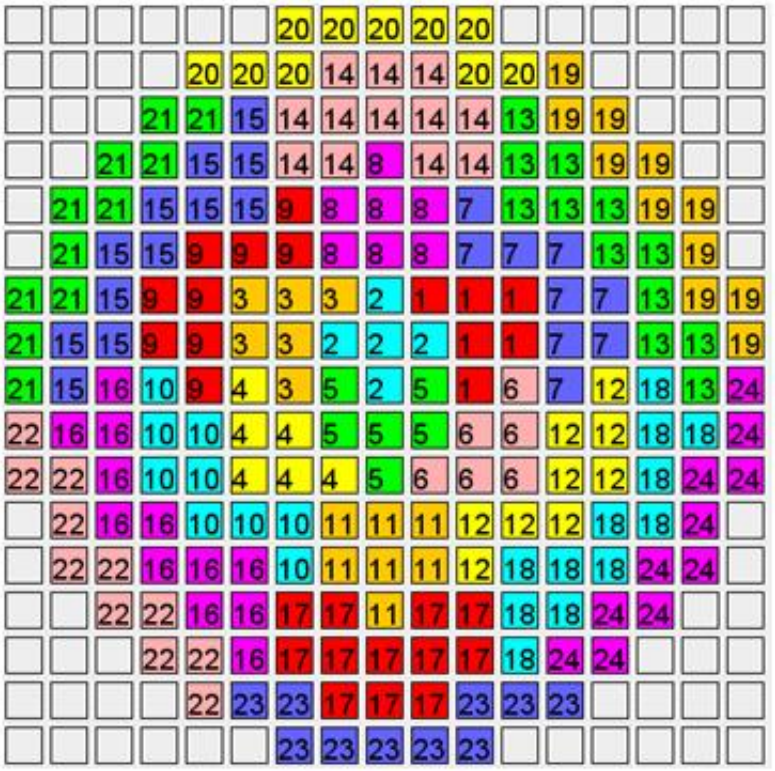

FIGURE 3.20: Core neutronic and Heat structure nodes mapping correspondence to TH cells.

Coupled calculations have a particular way to be performed. This might change depending on the type of codes that are being used for such computations. Usually it is not easy to reach the start point of the transient. In the present study, all the computations are been performed under SNAP v2.1.3 [60] platform. To execute a transient calculation, several previous steps are required. The first step is to run a stand-alone steady-state TRACE [1–3] calculation; using only the thermal hydraulic model. In this case the core power is fixed to 100% by a time table. The aim of this calculation is to stabilize the plant flow parameters. The second step is to perform a coupled restart steady state calculation; restarting from the previous calculation, but adding the 3D neutron kinetics code in steady state mode. In this step, steady state options for both codes are activated as coupled full plant stabilization is the objective of this calculation. Once the plant parameters are in steady-state coupled conditions another restart calculation is launched. In this final run, both codes are in transient mode. For the uncertainty methodology, DAKOTA [6–9] is applied after the completions of the transient computations. Previous to the DAKOTA [6–9] analysis and under the SNAP [60] interface, an Extract Data step is required in order to retrieve data from the coupled calculations and to prepare them to be read and treated by DAKOTA [6–9]. The Extract Data step bridges the gap between analysis code outputs and the DAKOTA [6–9] uncertainty input.

Chapter 4

Model Validation and Improvement

Once the models are built, they need to be validated. This section explains the methodology of validation used in Technical University of Catalonia. This methodology has 14 years of success in thermal hydraulic model validation with point kinetics as a core simulator or power fixed by table model. Nevertheless, has been used few times for a 3D NK-TH coupled calculation validation. The RELAP5-3D [41–49] and [31–35] model, coupled with the NESTLE [31–35] code, was validated by the author using this methodology. Luckily GET group is holding data from a 50% loss of load real event which took place in Ascó NPP. Validation methodology essentially consists on conforming these plant data against code predicted data. Within the framework of the present study, with the existing versions of the coupled codes TRACE/PARCS [1–3] and [4, 5], there is no way to obtain credible results without improving or giving new capabilities to the coupled system. Essentially the coupled package needs to hold the dynamic control rod movement capability, which has been implemented into the source code by the author. In next sub sections a full detailed explanation of the validation process and source code improvement is presented.

4.1 Loss of load transient

As it has been already introduced, Technical University of Catalonia has a specific methodology to validate every model which tries to reproduce the Ascó II NPP. This methodology is based on a real transient which happened in unit 2 of the Ascó NPP on in December 1999. This transient happened during a Start-up test which was performed after the reload process in December 1999 which resulted in a 50% loss of load transient.

The turbine moved from 100% of load to 50% this was the initiating event with a decrease rhythm of 200%/min of the turbine power. There were no more manual maneuvers more over the manual turbine load decrease. There are several issues that make this transient a profitable event to be used as a base line to validate the plant models. First is because University research group holds plant data from such scenario. That will allow to confirm the code predicted data against plant data. According to the accuracy of compared results, the validation process is going to fail or success. Should be noticed that, some of the discrepancies should be explained over the assumptions taken when performing the different models but also over the limitations of the codes in terms of equations or internal models used to reproduce the variety of the 3D NK-TH phenomena. Second is because such scenario represents a transient between two stable zones, the first stable zone is 100% turbine load at full power (steady state conditions), the second stable zone is at the end of the transient at 50% of turbine load and 50% of total power, with some of the control rod banks partially inserted into the core. This particular situation is very useful when testing and validating the different kinetics models. Every validated kinetic model should be able to stabilize around both equilibrium positions without many oscillations in terms of the kinetics parameters. The stability and consistency over the both zones is going to ensure the robustness of the kinetics model.

TABLE 4.1: Main events time table in 50% loss of load transient

Time (s)	**Event**
0.0	Demand turbine load reduction
8.0	Steam dump system open
14.0	Pressurizer spray maximum values
26.0	Shut off pressurizer spray system
761 .0	Start-up pressurizer spray system
1000.0	End of simulation

The above table 4.1 contains a list of the main events on the 50% loss of load scenario.As it has been mentioned the initiating event is the demand turbine load reduction thus time equals 0.0 seconds in that point. Eight seconds later Steam dump system automatically open, the control system should be able to reproduce that event. Fourteen seconds after the initiation of the event the pressurizer spray valves are maximum open, they close after twelve seconds from this point. There is no more actions until 761.0 seconds, where there is a start-up of the pressurizer spray system. Finally the simulation ends at one thousand seconds after the initiation event. The core configuration and the kinetics at the beginning of the event, were set up at BOC for cycle 13 of the NPP. This is important in the present study, since the built XS library has to be able to reproduce the core configuration in order to reproduce with neutronic fidelity the event. The reference neutronic conditions at the beginning of cycle 13 were: 1728 ppm is the Boron

reference concentration; 579.65 K is the moderator reference temperature; 701.37kg/m^3 is the moderator reference density; 898.15 K is the fuel reference temperature. With the scenario described it is important to notice that some features are required in the 3D NK-TH developed model. In that sense, the model has to hold the capability of reproducing some system control actions, but also to reproduce the core at one specific poind from its 13th cycle finally to reproduce with enough accuracy all the thermal-hydraulic and neutronic parameters at steady state conditions and during the transient scenario.

4.2 Dynamic TRACE/PARCS control rod movement

Nuclear system code calculation needs to be validated against plant data transients. In the present study, the 50% Loss of load transient is used to validate the developed 3D NK-TH coupled model. For that purpose a dynamic TRACE/PARCS [1–3] and [4, 5] control rod movement model was needed. With the code versions used, TRACE v5.0 patch2 [1–3] and PARCS 3.0 [4, 5] this feature was not available. In previous TRACE/PARCS [1–3] and [4, 5] 3D NK-TH analysis, for each calculation, the control rod position had to be pre-assigned in terms of time and position of the control rod bank, during the transient. The user has to predict the control rod position in advance, before starting the calculation. This feature did not agree with the methodology where all codes work together like one code, and every side of the computation is receiving feedback from the other code at each time step. Different works are been performed in this field with different coupled codes (i.e. [67]). Similar task performed in [67] with RELAP5 [41–49] and PARCS v 2.7 [4, 5] was intend to be done here with TRACE/PARCS [1–3] and [4, 5] coupled code. Previously to the dynamic control rod movement implementation, the way to validate a coupled calculation was to execute, three separate calculations a stand-alone steady state, a coupled steady state and finally a transient steady state. Finally, the user had to set up all the control rod bank positions in advance. This tells PARCS [4, 5], by use of the MOVE_BANK card, at which position and time control rod bank will be placed. An example is given below:

- *MOVE_BANK 1 0.0 225.0 20.0 225.0 25.0 125.0 30.0 100.0 50.0 50.0*
- *MOVE_BANK 2 0.0 225.0 25.0 225.0 30.0 125.0 35.0 100.0 55.0 50.0*

In the above example the user has set up the following movement for the control rod banks 1 and 2: Bank number 1 is going to be withdrawn at 225 steps from 0.0 seconds to 20.0 seconds then is going to be inserted 110 steps in 5.0 seconds, and 25 steps the

next 5.0 seconds. Final move of Bank 1 is to be inserted 50 steps more in the next 20 seconds and then to stay in this position until the end of the transient. Bank number 2 is going to perform the same sequence, but with a delay of 5.0 seconds. In the case where there are more control rod banks available in the developed input deck, they are going to remain in their initial position during the transient. This feature is all right for some transients, especially those where plant data is held. Also there is not any inconvenient to use the codes during a SCRAM transient. In case of the SCRAM, the codes behave properly. The user can set up the SCRAM features with a SCRAM card in PARCS [4, 5] code. An example follows:

- *SCRAM T 114.0 0.1 1.0*

In the previous example, SCRAM option is been set up as True, and is going to occur when the total reactor power reaches 114.0% of the core power. The control rod banks will start to be inserted with a delay of 0.1 seconds after the target power has been reached. The control rod banks will be completely inserted in 1.0 seconds. The user can set up stuck control rod banks in advance; such control rod banks will not be inserted into the core in response to the SCRAM signal, and will remain completely withdrawn during the transient. In case of SCRAM event the code has already been prepared for that, this means that *MAPPING* file can contain a trip number, which essentially will be the thermal-hydraulic code signal which is going to lead SCRAM situation into neutron kinetics code. Thus there is information exchange between thermal-hydraulics and neutron kinetic code in that particular issue. Same capability is wanted to be achieved, on the control rod position issue. This is what author has named as dynamic control rod position.

Note that the not improved code methodology can solve most of the transients, but still holds some deficiencies. For example, as it is well known that not all the control rod banks will be inserted into the core at the same time. Normally the control rod banks overlap each other, starting with one control rod bank and followed by the others.

TABLE 4.2: Example of Ascó NPP power vs. control rod position in steps

Power (%)	**Bank C (withdrawn steps)**	**Bank D (withdrawn steps)**
0.0	113	0
5.0	114	0
10.0	125	0
13.0	131	0
15.0	136	4
20.0	147	16
25.0	158	27
30.0	168	38
35.0	179	49
40.0	190	60
45.0	201	71
50.0	212	83
55.0	223	94
55.7	225	95
60.0	225	105
65.0	225	116
70.0	225	127
75.0	225	138
80.0	225	149
85.0	225	161
90.0	225	172
95.0	225	183
100.0	225	194

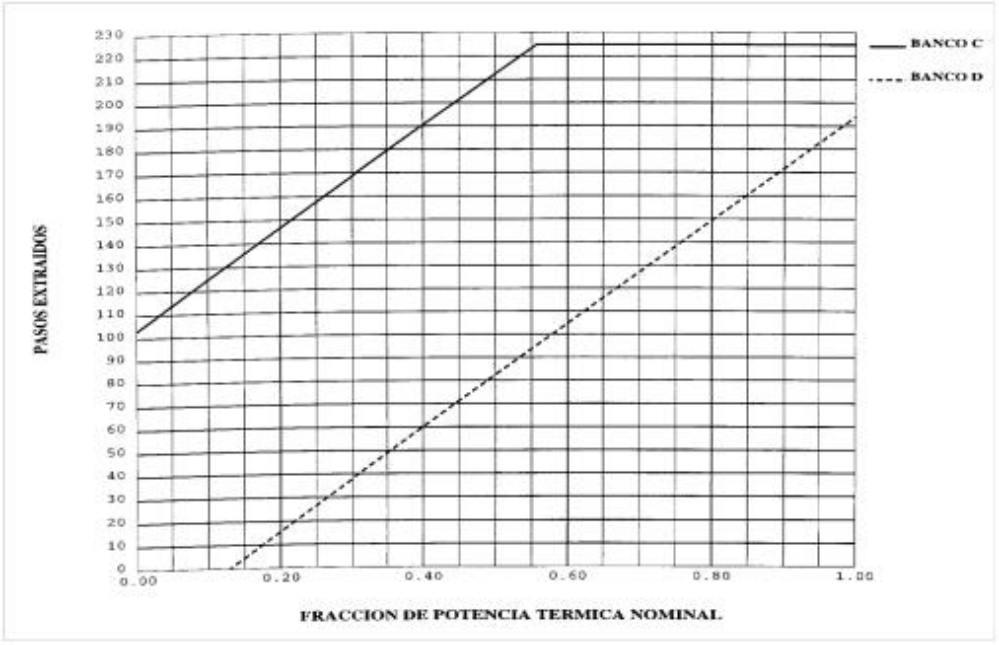

FIGURE 4.1: Example of Ascó NPP power vs. control rod bank position in steps.

In the previous examples, figure 4.2 and figure 4.1 an actual representation from Ascó NPP of the control rod bank overlapping movement which begins with the insertion of Bank D immediately after the power decreases below 1.0 of the nominal power. Note that Bank C remains withdrawn until the power is slightly below 0.6 of the nominal power. Banks A, B, SA and SB start to be inserted consecutively after banks D and C which are the first ones to be inserted. The same behavior can be seen in Table 6 where the total power is represented in terms of the total withdrawn steps. This feature cannot be captured with the card system SCRAM implemented in the PARCS [4, 5] code. Once the SCRAM card is activated all control rod banks get inserted into the core at the same time, just the previously marked as stuck control rod banks, remain completely withdrawn in the transient.

As it has been mentioned before, within the framework of the present study, it is important to have a completely validated model in terms of Thermal hydraulic and Neutronic behavior. To achieve that purpose it has been considered a must, to solve the problem of the dynamic control rod movement between TRACE v5.0 patch2 [1–3] and PARCS 3.0. [4, 5]. What is intended to solve in this endeavor, it is a way to compute or to assign at every single control rod bank a step position against time. Such position must be computed in TRACE [1–3] code as an answer to certain thermal-hydraulic conditions such:

- *Manual stop I.S. manual*

- *High flux. High set point RI*
- *High flux. Low set point RP*
- *High flux. High set point RP*
- *High neutronic flux oscillation*
- *C-3, OTDT*
- *C-4, OPDT*
- *Low mass flow one loop*
- *Low mass flow 2/3 loops*
- *High pressure in pressurizer*
- *Low pressure in pressurizer*
- *High level in pressurizer*
- *Very low level in one steam generator*
- *Automatic safety injection*
- *Turbine trip*

The above list is the actual list from Ascó NPP model which has been used in successful transient analysis and model validations over the last twenty years in Technical University of Catalonia. Some of the previous signals lead the plant to SCRAM status. After considering those signals, the IDN from Ascó NPP [24–26] also needs to be checked, so the position of each control rod bank can be determined in terms of each thermal hydraulic condition above mentioned. With this new feature the coupled calculation there is full feedback, and every transient might be able to be reproduced without considering the control rod position in advance. Notice that a huge logic and control system was required in order to compare different signals and give as a result a final control rod position for each control rod bank.

Both codes are coupled and compiled under the same executable file. Nevertheless an external *MAPTAB*, mapping file, is needed to assign the matrices between thermal hydraulic nodes and neutronic nodes. Also the weighting factors between both side nodes are fixed in this file. some special features are described in the heading part of the file. Such file is structured in several parts, Heading part; Cards part and Assignment part.

```
** PARCS Mapping for V3DcylHS and Cartesian - x[17], y[17], z[26]
*
*
*d: Generated from PARCS model ssAsco2010.inp
*
* Doppler Feedback
%DOPL
LINC   0.7
*
* SCRAM Trip
*%TRIP
*34
*
%CRSIG
9111   1   9112   2   9113   3   9114   4   9115   5   9116   6
*
* Reflector Properties
%REFLPROP
*ctemp   ftemp   cden   cvoid   ppm
584.65   898.15   701.37   0.0   1728.0
*
* Volume Number Table
%TABLE1
  100   20   3   1   1.0
  100   20   3   2   1.0
  100   20   3   3   1.0
.
.
.
.
  100   23   10   5745   1.0
  100   23   10   5746   1.0
*     * Heatstructure Number Table
%TABLE2
   933   1   1    1   0.0
   933   1   1    2   0.0
   933   1   1    3   0.0
   933   1   1    4   0.0
   933   1   1    5   0.0
```

```
   933   1   1    6   0.0
   933   1   1    7   0.0
   933   1   1    8   0.0
  1001   1   1    9   0.0
  1002   1   1   10   0.0
.
.
.
.
  1155   1  24  5736   0.0
  1156   1  24  5737   0.0
  1157   1  24  5738   0.0
   933   1  24  5739   0.0
   933   1  24  5740   0.0
   933   1  24  5741   0.0
   933   1  24  5742   0.0
   933   1  24  5743   0.0
   933   1  24  5744   0.0
   933   1  24  5745   0.0
   933   1  24  5746   0.0
* end of data
```

Above lines constitute an example of the mentioned *MAPTAB* input file. The heading part is related to the specifications and title of the file. The cards part is related to the specific calculations for the Doppler effect, SCRAM trip from the thermal hydraulic code which will begin the SCRAM process into PARCS [4, 5] (Notice, this feature is being disabled with the leading asterisk, this is due the new dynamic control rod feature, will take SCRAM situation into account also. Nevertheless with the modified code, both features can perfectly coexist without any controversy). Next lines give some reflector properties and then there is the card *%CRSIG*, which is the one introduced in order to model the dynamic control rod movement capability. In the final part of the *MAPTAB* file, there are the assignment cards. These cards are structured in two parts, *%TABLE1* cards, where assignment and weighting factors between thermal hydraulic volumes (Vessel nodes, notice vessel component number is 100) and neutronic nodes are given. Second part is *%TABLE2*, where assignments and weighting factors between the heat structures (notice HS start with number 1001 and number 933 is saved for the reflector) and neutronic nodes are given. Notice the neutronic nodes number ascends up to 5746, this equals 221 radial nodes times 26 axial neutronic levels.

As it has been mentioned this new feature is been introduced into the code by using the *%CRSIG* card, which essentially gives in pairs a number of the control signal in TRACE [1–3] and a control rod bank assigned with such signal. Those control rod banks hold numerical names thus in our case banks A, B, C, D, SA and SB have been renamed 1, 2, 3, 4, 5 and 6 respectively. The source codes from TRACE v5.0 patch 2 [1–3] and PARCS 3.0 [4, 5] have been modified. In the following lines a detailed explanation of the all modifications and checks to the source code made are described. Subscript "*Rai!*" refers to some modified lines made in the source code. Other routines have also some modifications, but in the below description only *TdmrErrorCheckM.f90* are showed. Adjustments made:

Source code file: *Pdmr_mapM.f90*.

1. *nfields(line)* modification to meet the number of fields that will be in *%CRSIG* card.

Source code file: *Pdmr_initM.f90*.

1. *initcrp(i)* divide at the end by *ncrbstep*.

Source code file: *Pdmr_timeM.f90*.

1. To check *newcrp(i)* in line 68.
2. To check *crbpos(sgvbank(i))* in line 81.

Source code file: *TdmrInitCalcM.f90*.

1. To check *initcrp(i)* and to check *r8bufn(i)*, line 110.

Source code file: *TdmrTimeCalcM.f90*.

1. To check *newcrp(ii)* in line 79.
2. To check *initcrp(ii*) in line 79.
3. To check *csSig(jj)%presVal* in line 81.
4. To check *r8bufth(1+ii)* in line 83.

Source code file: *TdmrErrorCheckM.f90*.

1. To check the following loops.

   - Check to see if new control rod bank positions are outside range.
   - Line 131 to line 146.

```
      ( ... )
      WRITE (mesg(1), 2109) isgv(ii)
2109  FORMAT (“Processed Signal Variable #”, i5)
      CALL TDMRStatusMesg( mesg, dim=1, status=TDMRSTAT)

      IF (IABS(csSig(jj)%icn1) .NE. sgvbank(ii)) THEN   !Rai
          CALL error(1, 'Fatal* wrong cnt. rod group ID')   !Rai
          RETURN    !Rai
      END IF     !Rai
       IF (initcrp(ii) .LT. 0.0D+00 .OR.
      initcrp(ii) .GT. 1.0D+00) THEN
      crcntl = .FALSE.
      WRITE (mesg(1), 2110) initcrp(ii)
2110  FORMAT (“Initital control rod bank position was out of accceptable
      range: ”, 1pe20.12)
      CALL TDMRStatusMesg( mesg, dim=1, status=TDMRWARN)
      END IF
      GO TO 21
21    CONTINUE
      ( ... )
```

Source code file: *TdmrCommM.f90*.

1. To check the structure value *r8bufn = pbuf%gi2th(nbuf+1: nbuf+dimbuf(6))* line 212.

Source code file: *TransDriveM.f90*.

1. To check the loop.

   - determine current *crbank* .

Source code file: *Pdmr_commM.f90*.

1. To check **SUBROUTINE** *pdmr_comm_copybufto()*.

PARCS [4, 5] input considerations and actions:

1. To add the card CR_AXINFO third field *ncrbstep*, Control rod full insertion position from the bottom of the problem geometry, cm.
2. To consider that in PARCS [4, 5]:
   - 0 steps, means completely inserted.
   - ### steps number of the withdrawn steps.

TRACE [1–3] input considerations and actions:

1. To create a function like:
   - *idcb*, *icbn*, *icb1*, *icb2*
   - Such function has to change the number of the steps and normalize to 1. To consider that in TRACE [1–3]:
     - 1.0 means completely inserted (This is 0 steps in PARCS [4, 5]).
     - 0.0 means completely withdrawn (Maximum number of steps in PARCS [4, 5]).
   - To create a control signal in TRACE [1–3] who reads the above created function.
     - *idsv* = number which will go into MAPTAB file.
     - *isvn* = 16.
     - *ilcn* = (negative) function created before, where the control rod movement is inside, it goes from 0.0 to 1.0.
     - *icn1* = Bunk number which will be moved under the previous parameters.
       * Important: It is not possible to modify this parameter inside the SNAP [60] platform, ASCII modification is required.

MAPTAB file considerations and actions:

1. To add *%CRSIG* card.
2. To add in the under line of *%CRSIG* card the number of the control signal followed by each controlled control rod bank. They come in pairs until the last bank to be controlled.

Final check:

1. To check with the *MOVE_BANK* card.
2. *MOVE_BANK 1 0.0 225.0 20.0 225.0 25.0 125.0 30.0 100.0 50.0 50.0*
3. Double check to be sure that same results appear when:
   - Signal coming from TRACE [1–3].
   - *MOVE_BANK* card from PARCS [4, 5].
4. Same results in both cases.

With all of those checks and modifications the new compiled code which holds, the capability of the dynamic control rod movement, has been developed. Moreover, the *%SCRAM* card in the *MAPTAB* file can be disabled, since the *%CRSIG* gives the position of every control rod bank at each time step, there is no need for the SCRAM feature coming from PARCS [4, 5]. In the new compiled version of the code, the SCRAM signal can be setup in the thermal-hydraulic side of the coupled calculation, as an answer of to the typical signal which leads to SCRAM, (such it is presented at beginning of the actual section) in a non-coupled calculation, replicating the signals in the list mentioned previously.

Before going further, it is necessary to ensure that the modified version of the code is not overlapping any of the previous features. That is why the final check from the above mentioned steps is very important. Once the modifications in the code are solid, and work with any test scenario, it will be necessary to implement a control system into the thermal-hydraulic code. Such system will check the different parameters from the plant model and will assign the control rod bank step position for every time step and for each different control rod bank, depending on the status of the plant. Such control system also has to contain the SCRAM capability, in case of an eventual SCRAM event. At the end what are only by passed to PARCS [4, 5] are the steps for every control rod bank. At the end only the steps for each control rod bank are passed to PARCS [4, 5]. This control block system has been adapted from the one previously developed by the author for RELAP5-3D [31–35] code model. In the following figure and scheme of the control block system build for that porpoise can be seen. As it can be seen in figure 4.2, the control rod logic is quite complicated, because it involves different parameters and different actuation over different system signals. As a basic definition the control logic is looking at the core temperatures, core power and turbine power, to adjust the control rod position of the first inserted control rod bank (Bank D in this particular case) over the pre determined values of position coming from the Ascó NPP specifications.

Some response dead bands are also incorporated into this model in order to avoid some oscillations which might lead to some instabilities. In this way if there is some over power in the steady state conditions, the logic will tell to insert some positions of the control rod bank until the new balance is reached. Vice versa, if there is under full power situation, in steady state conditions, some steps will be required to be withdrawn in order to gain some power production. Control rod movement logic is also linked to the SCRAM signal which might come from different situations (They have been listed in previously). Once the position of the first control rod bank is determined, the other control rod banks position will be determined over the position of the first one. their insertion priority is also determined on the Ascó NPP specifications. Control rod bank position is generated from 0 to 1 value in TRACE [1–3] and it is required in steps for PARCS [4, 5], some conversion from one side to the other "nomenclature" was also needed. With this final step working the coupled TRACE/PARCS [1–3] and [4, 5] model is ready to be validated.

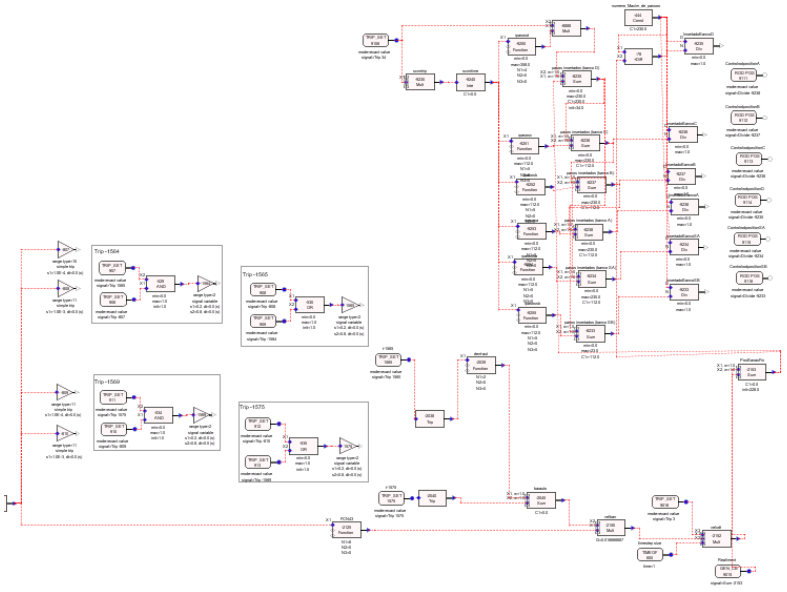

FIGURE 4.2: TRACE control rod bank position control system scheme.

Next figures 4.3, 4.4, 4.5, 4.6, 4.7 and 4.8, show the validation process, between the 50% loss of load of plant data and the calculations from the new compiled version of the code. Typically the transient is computed as a restart file from a 12000 seconds calculation which has been carried out in order to obtain steady state conditions. A general good agreement is shown in all the figures. Even though the agreement is not 100% precise in some figures, what is important to achieve with our model, is the move from one stable region to another. This is in our case, steady state at full power at the beginning off the transient, to 50% of the full power at the end of the transient. Also looking at the

different figures it is noticeable that starting and ending point of each presented time trends is stable and with small discrepancies between plant data and computed results. Also control bank rod movement, shows good agreement with the reality. In figure 4.5 the stabilization level of the control rod bank inserted position has a significantly difference between the plant data and the model predicted result. Such discrepancy is discussed and solved in the coming section. Some discrepancies can be observed in terms of the pressure, figures 4.6 and 4.7 the detail degree of the thermal hydraulic model used and the simplicity from some parts of the logic in the thermal-hydraulic system could explain such differences. On the other side powers and primary levels, figures 4.3, 4.4 and 4.8 show very good agreement.

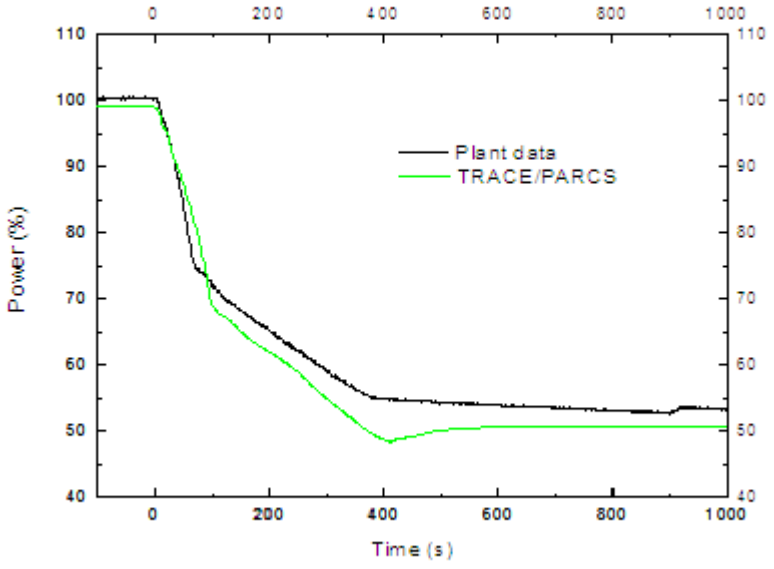

FIGURE 4.3: Total nuclear power 50% loss of load validation.

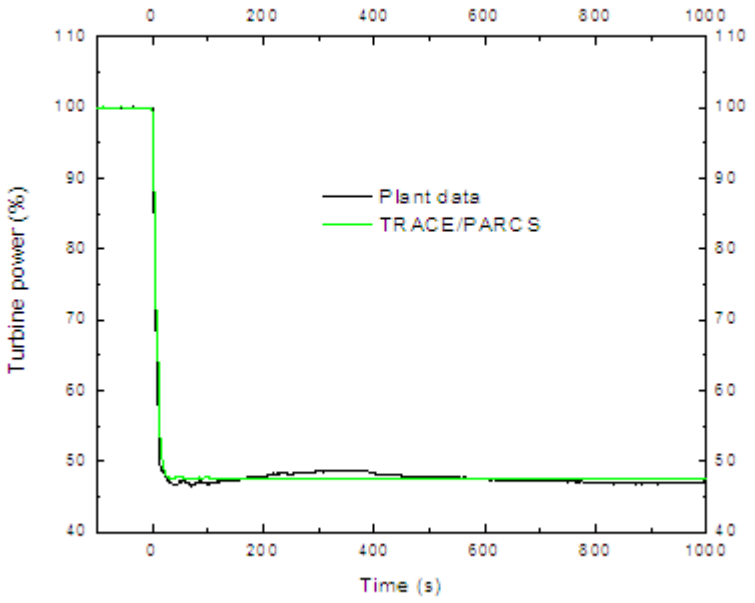

FIGURE 4.4: Total turbine power 50% loss of load validation.

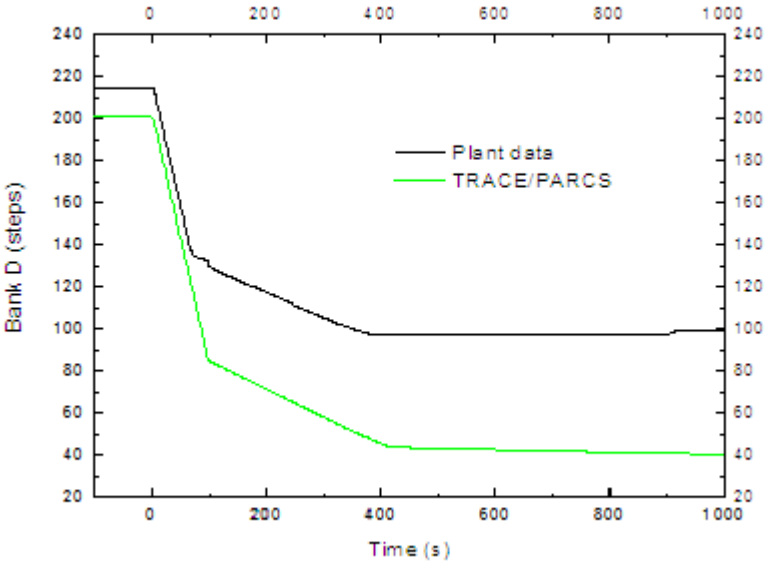

FIGURE 4.5: Control rod bank steps position 50% loss of load validation.

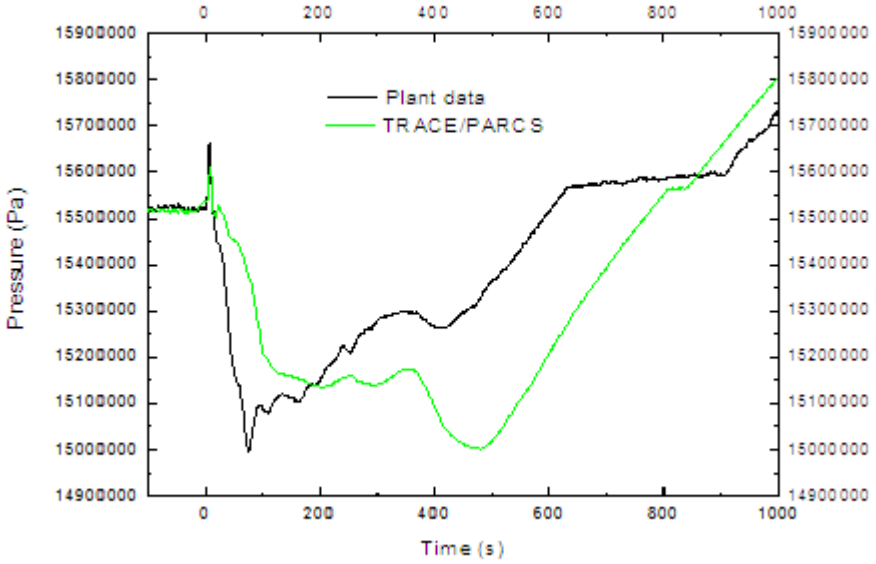

FIGURE 4.6: Primary pressure 50% loss of load validation.

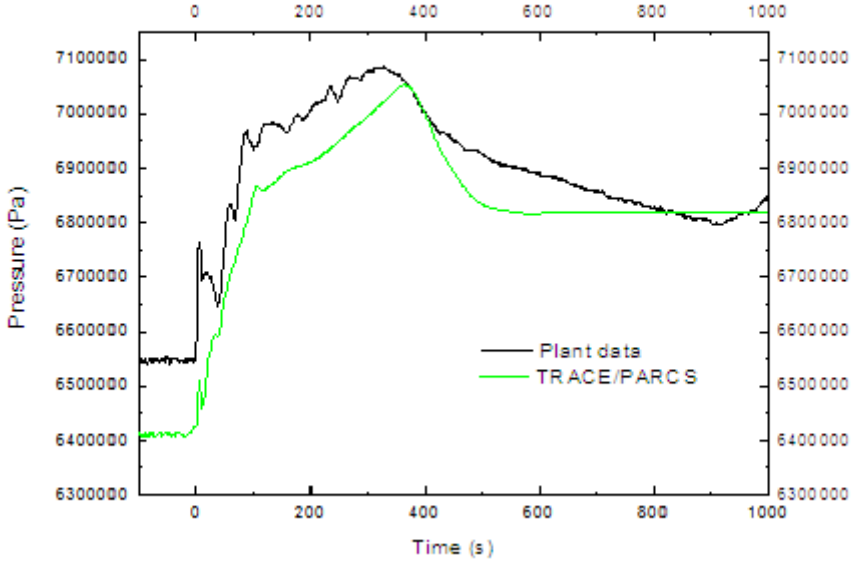

FIGURE 4.7: Secondary pressure 50% loss of load validation.

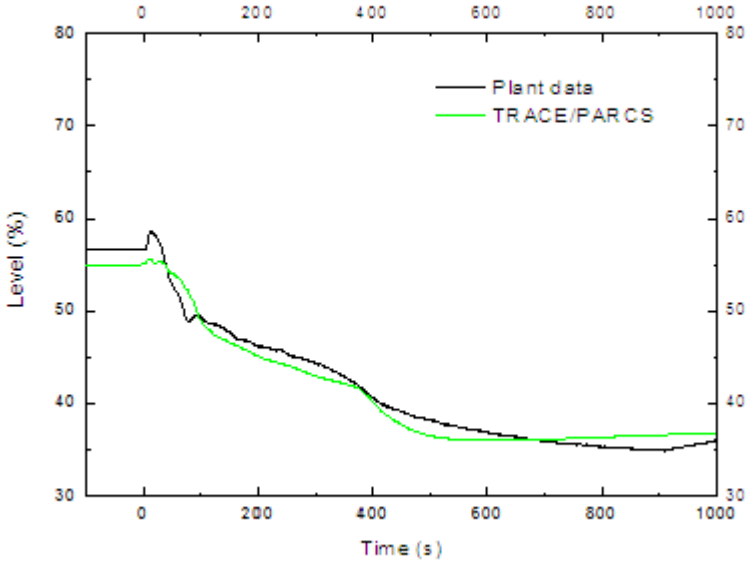

FIGURE 4.8: Pressurizer level 50% loss of load validation.

The 50% loss of load transient can be considered a non 3D Kinetic transient, in the sense that it does not involve real asymmetries in the core which can give an indication of the validity of the results obtained. That is why some actual parameters from the plant have been taken and compared in different areas of the core and at different time steps of the transient, so we can see the agreement with some internal parameters in the core and during the transient. Table 4.3 is showing these results.

TABLE 4.3: Core parameters 50% loss of load validation parameters.

Quantity	**Plant value**	**Calculated value**	**Units**	**Deviation over plant data (%)**
Nuclear power	100,28	98,77	(%)	1,51
Boron concentration	1728,00	1721,00	ppm	0,41
Moderator temperature	306,50	308,29	°C	0,58
Moderator density	0,70137	0,7123	kg/cm^3	1,56
Fuel Temperature	625,00	632,00	°C	1,12

4.3 Model validation

4.3.1 Assumptions

Some assumptions over the logics, models and manual operations over the validation scenario are taken in order to obtain a satisfactory validated model. First assumption is to consider all the safety systems to function properly in the present case of study. As mentioned above since this is a validation exercise it is expected that all the plant modeled systems work properly (according the plant data) during the transient. Beginning of life conditions for the core kinetics were selected in order to reproduce the stage of the cycle of life from the reactor, according to the plant data. A few adjustments were made on the control blocks in the steady state achievement stages in order to achieve steady state, such adjustment where disabled once the transient calculation was launched. This kind of adjustments are very common practices, used in safety analysis, which have the finality to lead the model to stable steady state situation rapidly and easily previously to the start of the transient situation. There are no data from the pressurizer heaters behavior, in the present study it has been considered that fix heaters 1 and 2 stay on since the beginning of the transient. They get compensated with the partial opening of the pressurizer spray valves.

4.3.2 Steady state achievement

Steady state achievement is not an easy task when coupling such a big models like the ones used in the actual study. For the BE coupled TRACE/PARCS [1–3] and [4, 5] calculations the following methodology is used. Since this is a coupled calculation, several prior steps to the transient simulation need to be performed. This previous steps have the aim of adjusting the plant time trends to the steady state conditions with smooth transitions (i.e. temperatures, power, pressures, mass flows and neutron fluxes) from one step to the other. The general idea is to ensure the consistency of the thermal-hydraulic model first, and gradually add the 3D neutron Kinetic capabilities. First step is to run a stand alone calculation with the TH code. Figure 4.9 shows the power steady state achievement with this first stand alone calculation. In here the power is supplied by a table inside the model logic. It is intended to stabilize all the thermal-hydraulic parameters before adding the 3D neutron kinetics as a source of power to the thermal-hydraulic feedback. Other ways the early plant parameters oscillations will be too big and the thermal-hydraulic feedback will lead the calculation to an error, typically a heat transfer error. Second step is to run a coupled steady state calculation. In that case the core power is being substituted for the core code simulator power (PARCS [4, 5]) in

the case of the present study. When running both codes in steady state option, there are several "shortcuts" than thermal-hydraulic code is taking in order to achieve steady state conditions, essentially is making easy the heat transfer convergence criteria. On the neutron kinetics side, the eigenvalue process is taking place, so the code is achieving one stage where all the parameters (fuel and moderator temperature, boron density and moderator density) are the right ones to have the 0.0 reactivity and full power. Since the neutronics solution may not change much over a small time step, a big skip factor is used in this computation so there is no thermal-hydraulic feedback at each time step at this point. This practice speeds up the computation time and smoothes the convergence criteria. The time trend of this computation is shown at figure 4.10. Finally a transient coupled calculation is restarted from the end of the steady state simulation. See figure 4.11. In this calculation a null transient of several seconds has been postulated before enabling the control rod position system. With that we ensure, first, that the transient power is also stable under null transient conditions and second that control rod position is adjusting the power whenever the oscillations of the main parameters from all over the plant are minimal. With other methodologies it becomes more difficult to adjust the control rod positions due the fine sensitivity of the control rod position system. Skip factor is reduced now to one, that means there is information exchange between the two codes at each time step. Finally in figure 4.12 the methodology flow diagram is shown. Table 4.4 shows a comparison between the model calculated values and the plant steady state values. Also a (%) deviation from the plant value is presented in the same table.

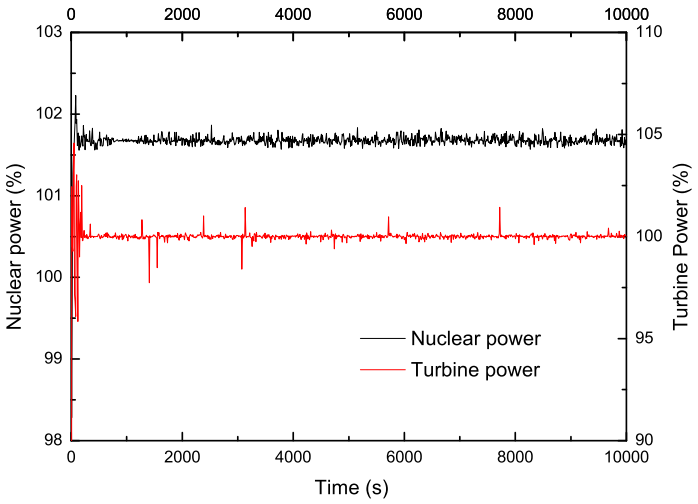

FIGURE 4.9: Standalone power steady state achievement.

TABLE 4.4: Steady state values comparison

Quantity	**Plant value**	**Calculated value**	**Units**	**Deviation over plant data (%)**
Nuclear power	100,28	98,77	(%)	1,51
Turbine power	99,95	99,34	(%)	0,61
Reference temperature	579,58	580,30	K	0,12
Mean temperature	579,75	579,86	K	0,02
Pressurizer level	56,69	55,12	(%)	2,77
Primary pressure	15520136,00	15534774,00	Pa	0,09
Secondary pressure	6560923,00	6435991,00	Pa	1,90
Bank D with drawn steps	214	208	steps	2,80
SG1 narrow level	50,56	53,04	(%)	4,91
SG2 narrow level	50,56	51,62	(%)	2,09
SG3 narrow level	50,54	51,66	(%)	2,23
Steam mass flow secondary loop 1	535,94	538,71	kg/s	0,52
Steam mass flow secondary loop 2	539,16	531,27	kg/s	1,46
Steam mass flow secondary loop 3	537,34	528,54	kg/s	1,64

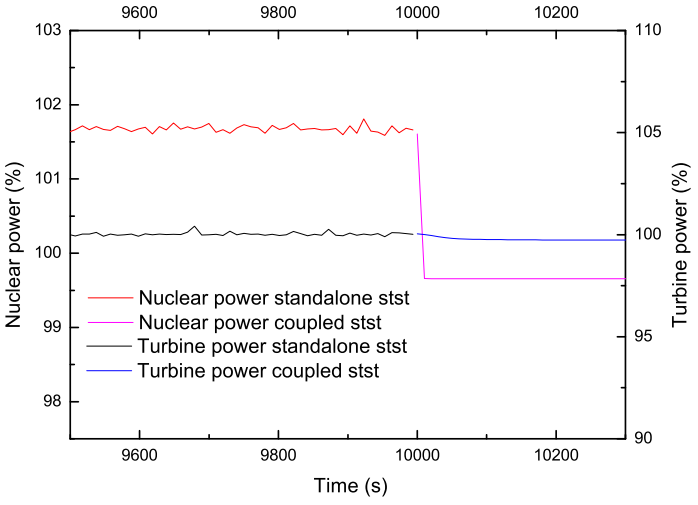

FIGURE 4.10: Coupled power steady state option.

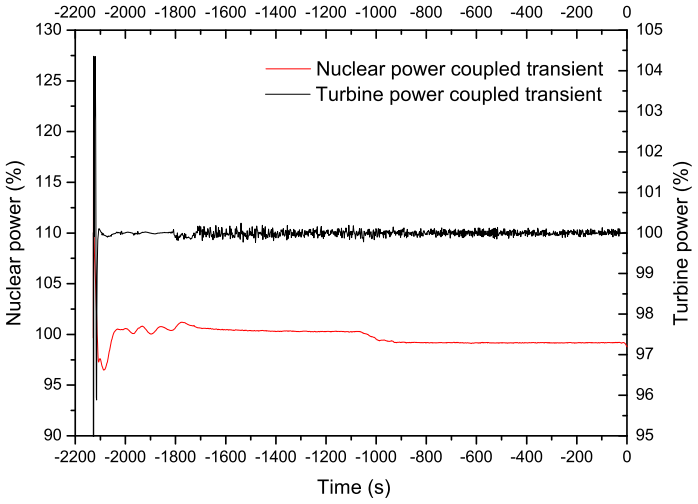

FIGURE 4.11: Coupled power null transient option.

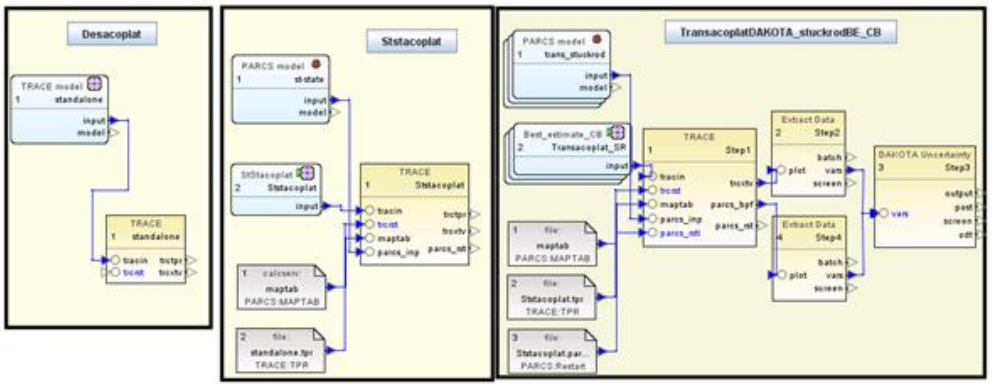

FIGURE 4.12: BE coupled calculation flow diagram.

4.3.3 TRACE/PARCS results

Once the steady state conditions are achieved, and the coupled 3D NK-TH model is stable, next is to perform the transient analysis. Transient starts with a null transient section where the dynamic control rod movement is enabled. Figure 4.13 shows such adjust after 1000.0 seconds of the steady state (i.e. null transient) calculation. The control system which determines the control rod position is quite complex and holds the dual capability of two behaviors one for steady state achievement and the other one for the transient response. Essentially the in and out position of the control rod banks is determined for the same function which holds two forms depending on the

above mentioned situations, a different dead band response determines the control rod position depending on the situation. Such behavior was implemented on the model. In this manner the step function which determines the control rod position is using a small dead band for steady state achievement and big dead band when a transient is happening. An automatic switch of those two functions was implemented in the model. This self made mechanism is also to avoid some non-stable situations during the steady state achievement. After a preliminary analysis some deficiencies in the model were found specially on the determining the control rod position during the transient scenario. Some delay on the control rod speed rate change was detected after 100 seconds of transient. Such delay can be seen in figure 4.15, such phenomenon was identified as one source of uncertainties in the problem. Such source is small in terms of delay (around 15 seconds) but it can cause a big discrepancy at the end of the transient. Check the green line in figure 4.15. The phenomenon was detected and isolated, several causes were identified as triggers of such discrepancy; Coarse TH nodalization, Malfunction between TRACE/PARCS [1–3] and [4, 5] information exchange; Wrong PARCS behavior when having a small velocity control rod insertion transient and XS set bad prediction. Different tasks were carried out in order to identify the different effects from the above mentioned phenomena and the causes of the deviation from the model prediction and plant data results. In coming figures, two plots compared with the plant data are shown in this section TRACE/PARCS [1–3] and [4, 5] these are tagged XS1 and XS2. Acronym XS1 identifies the original cross section sets meanwhile tag XS2 identify the modified set with modified cross section absorption coefficients. In order to reduce the control rod position discrepancies, absorption cross section coefficients have been modified by increasing 10% their original computed value. The comparison is useful to illustrate how some deficiencies on the cross section set can cause a big discrepancy on the coupled calculations predictions. Nevertheless besides that issue the other TH values are fitting reasonable with the plant data. The coming plots on this section compare the results achieved with TRACE/PARCS [1–3] and [4, 5] model and plant data. Total power time trends can be seen in figure 4.14. Figure 4.15 shows the control rod position from the bank D, which is the first one to be inserted in the core. With figure 4.16 pressurizer pressure is compared against the plant data. Figure 4.17 shows the pressurizer water level. Secondary main features side is compared in figures 4.18 and 4.19. First figure shows the SG2 pressure time trends and finally vapor mass flow is also compared, the other loops, which are not shown, have the same agreement concerning the main parameters of the secondary side. figure 4.20 shows the good agreement between the loops mean temperature. Finally a relative 100% radial power distribution was made in order to ensure the good prediction of the PARCS [4, 5] 3D kinetics model. In figure 4.21 the comparison between the predicted relative power and the data plant obtained from [24–26] is shown, as can be seen the prediction is slightly different from the plant

data, in figure 4.22 the (%) of error over the plant data is shown as a mean value of all the errors, $\pm$ 5.86% was calculated, such difference can explain the modifications made in the XS in order to match with more accuracy the plant data in values such the ones shown in figure 4.15. Last three figures 4.23, 4.24 and 4.25 show a 3D power representation. such representation is the same comparison made in figures 4.21 and 4.22, but with the 3D distribution perspective. This perspective could give some interesting conclusions. Figure 4.23 is the 3D power distribution of one quarter of the core at the beginning of life from Ascó NPP 13th cycle, figure 4.24 is the PARCS [4, 5] calculated 3D radial power distribution. Finally, figure 4.25 is the 3D error radial power distribution, between the plant data and the calculated data. By looking at the figures, it seems the computed values have a sharply shape around the second "*ring*" surrounding the center of the core. Since all the fuel assemblies are distributed following a concentric pattern, some deviations can be identified and isolated on few fuel assemblies types. This will be a field to be explored for improving the actual results. Generally speaking the main values shows a good agreement between plant data and the model, some small differences on the plots can be explained dues the nodalization approximation of the model.

In the same way that the XS where modified on its absorption coefficients to identify one possible source of error which can explain the difference between the stabilization point of the control rod bank at the stable phase of the transient, other tests were made to identify different possible source of errors for that specific discrepancy. See figure 4.15. In that way re-nodalization calculation was performed in order to see the effect of fine TH nodalization. This option was not available since the beginning due the extremely large computational costs that this fine TH nodalization involve. These large computational times make it not feasible at the moment for the BEPU methodology calculations. The new re-nodalized 3D TH vessel component used was a one-to-one neutronic node association. Each TH cell has the same dimensions as each NK node in here. Even the results where going in the right direction, (i.e. discrepancies between plant data and model prediction where reduced, specially in the stabilization time window, after 400 seconds of transient). The results where not much different from the ones presented in the past figures. Thus the author decided to keep the model as it is for the rest of the calculations. This decision was taken since the computational time needed for this new re-nodalization was increased significatively for one single case. Since in BEPU calculations a minimum of 59 cases are required, it was not considered for the present study but keep it for future endeavors. Vessel re-nodalization is in this way explored. Finally with all the sensitivities and essays made, the source of discrepancy on control rod bank step position time trend is identified from different points. Summarizing, it can be stated that there is a fair agreement between the model and the plant data. Some small differences can be explained by the nodalization approximation of the model.

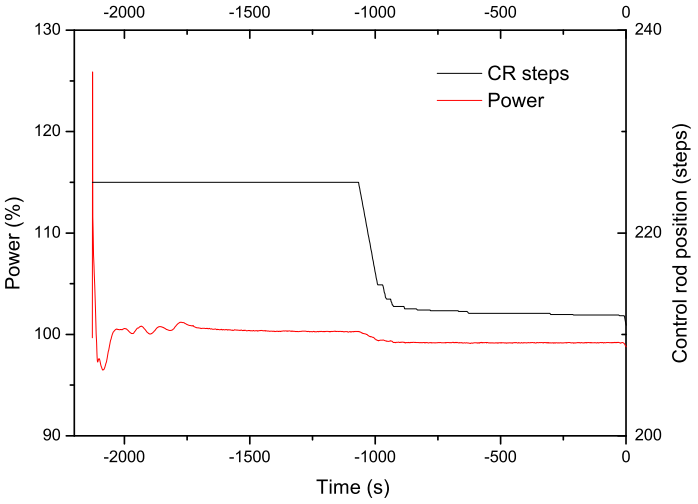

FIGURE 4.13: Control rod steady state adjust position.

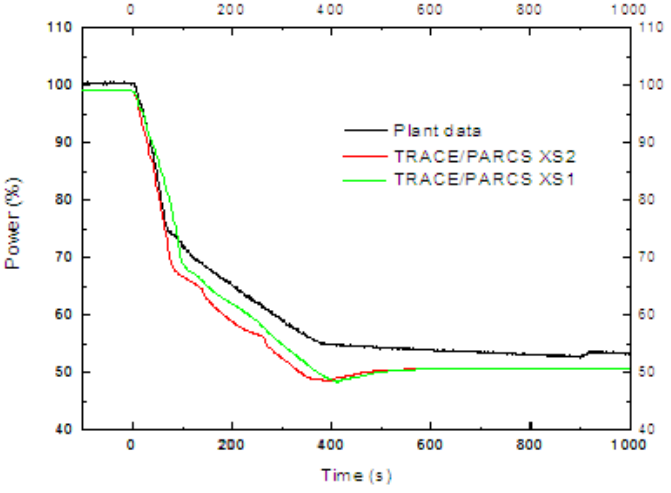

FIGURE 4.14: Total power TRACE/PARCS vs. plant data.

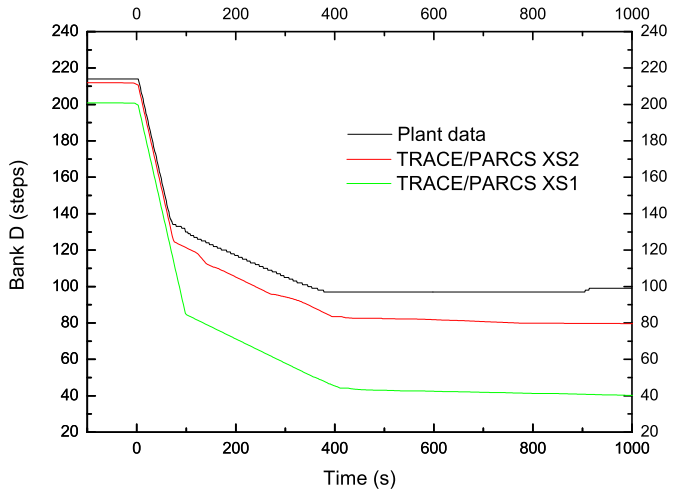

FIGURE 4.15: Control rod bank D TRACE/PARCS vs. plant data.

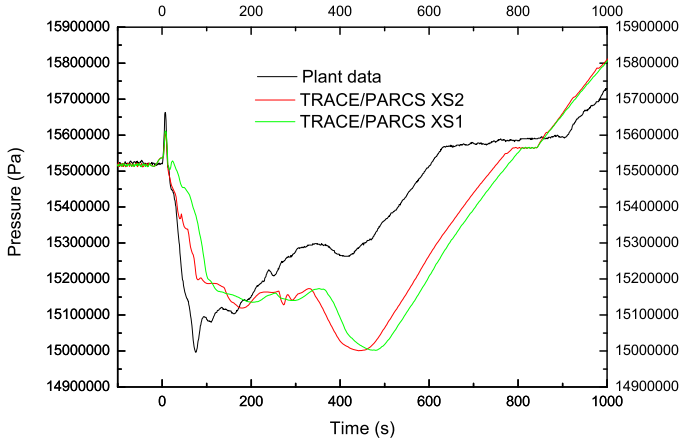

FIGURE 4.16: Pressurizer pressure TRACE/PARCS vs. plant data.

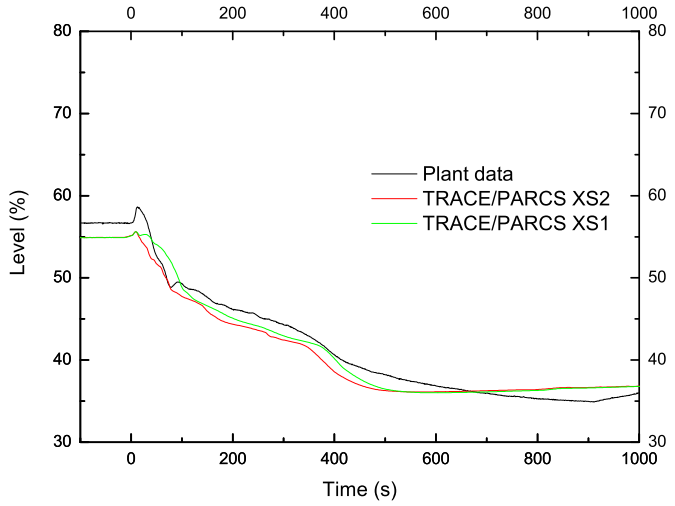

FIGURE 4.17: Pressurizer water level TRACE/PARCS vs. plant data.

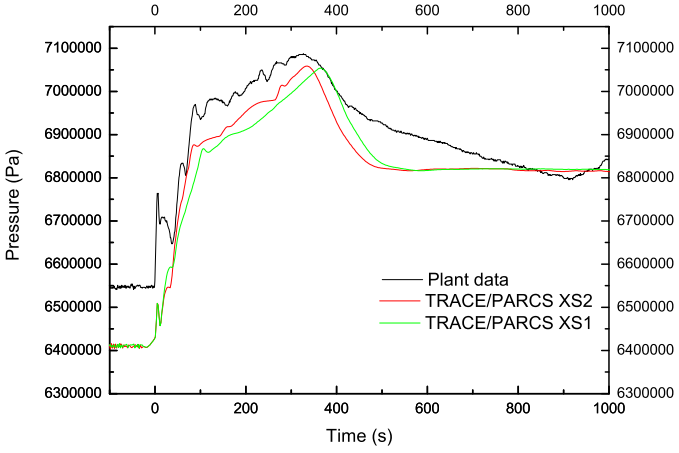

FIGURE 4.18: Secondary side SG2 pressure TRACE/PARCS vs. plant data.

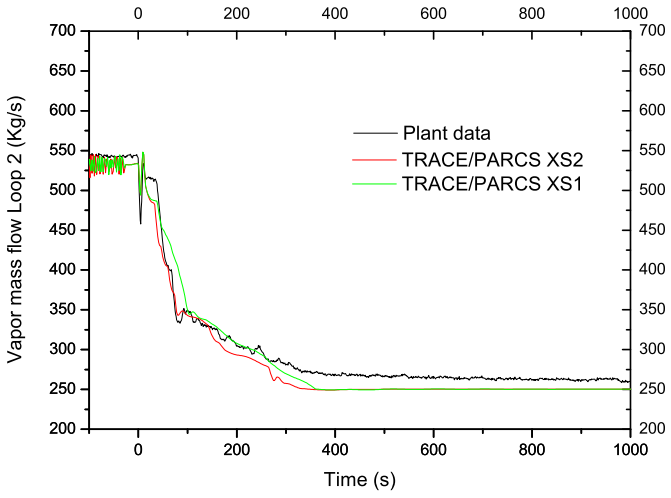

FIGURE 4.19: Secondary side SG2 vapor mass flow TRACE/PARCS vs. plant data.

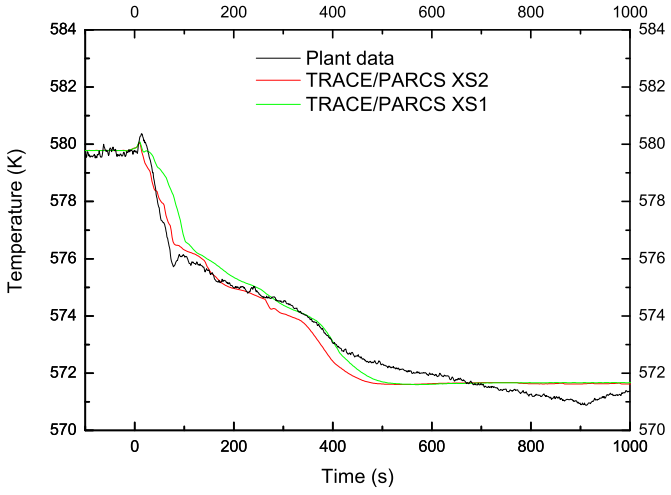

FIGURE 4.20: Loops mean temperature.

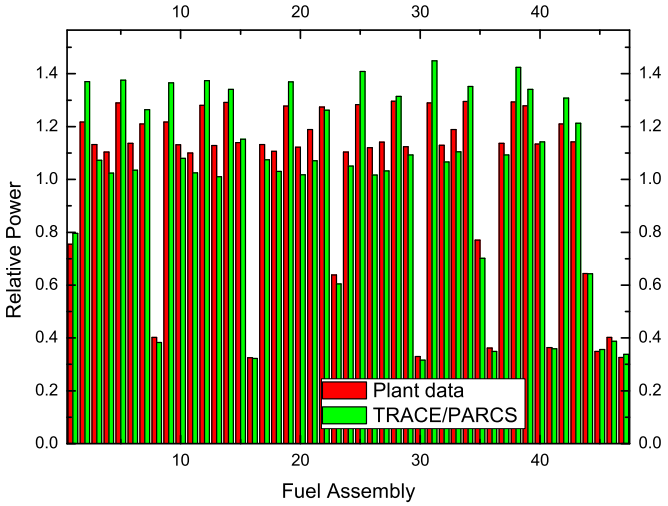

FIGURE 4.21: Radial fuel assembly comparison.

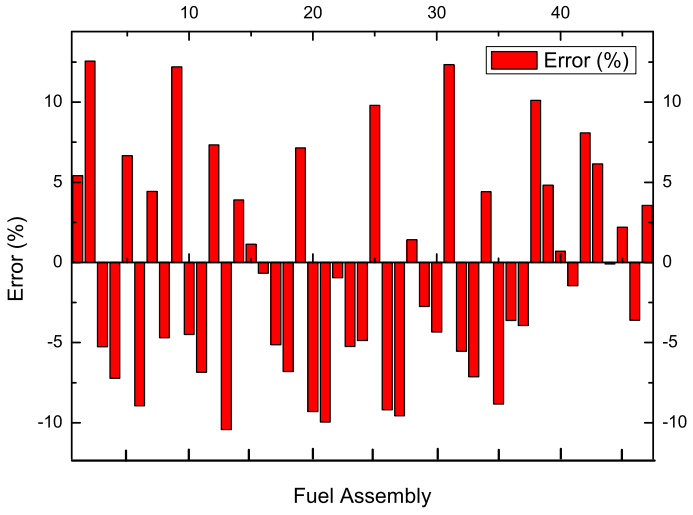

FIGURE 4.22: (%) Error radial fuel assembly comparison.

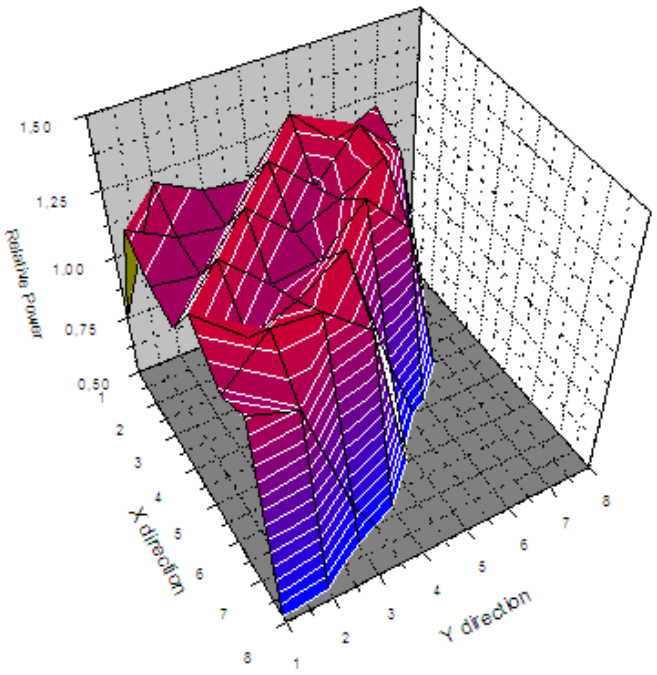

FIGURE 4.23: Plant data BOC, 3D power distribution.

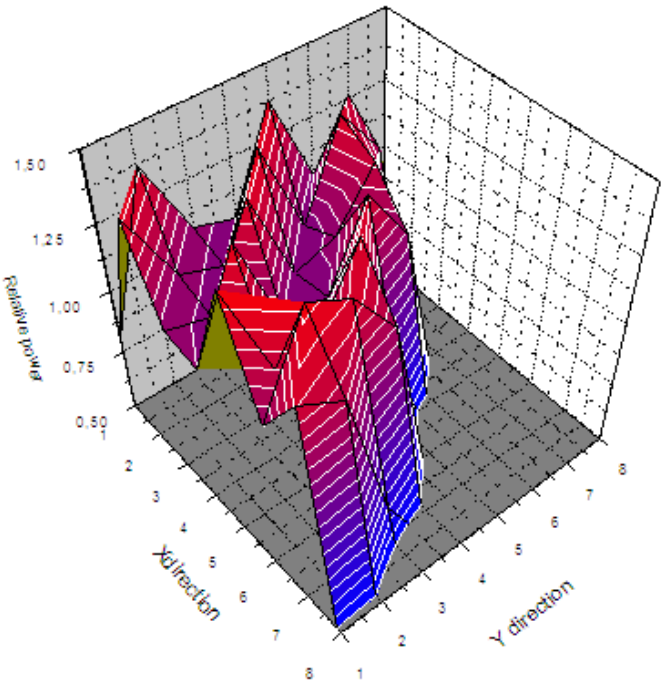

FIGURE 4.24: PARCS computed BOC, 3D power distribution.

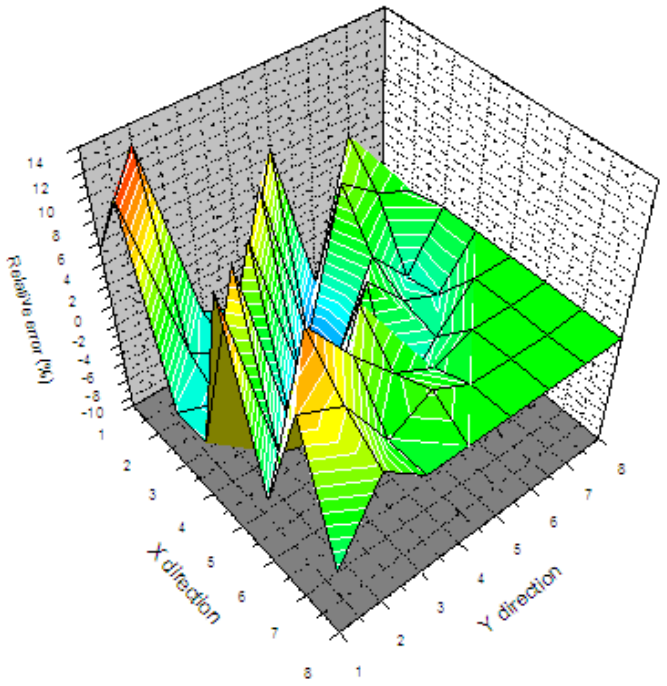

FIGURE 4.25: Relative error comparison, 3D power distribution.

4.3.4 Multiple codes and model comparison

Obtained results were also compared against results with other ASCÓ NPP system plant models from GET group. In the present study, three different calculations plus the plant data is being compared in-between themselves. Two point kinetic calculations plus the 3D kinetic calculation against the plant data will be shown in the next figures. TRACE/PARCS [1–3] and [4, 5] model compared is the one with XS2 cross section set. While TRACE [1–3] point Kinetics model is quite new and barely validated, RELAP5 point Kinetic model has been validated for more than twenty years and it holds a big library of plant transients where the model has shown a very good prediction and agreement with the plant data in a big range of conditions and scenarios.The comparison will provide meaningful information on the quality of the developed model. Figure 4.26 shows the comparison between the total power time trends, where TRACE/PARCS [1–3] and [4, 5] model and RELAP5 are having a lot of symmetry. Control rod bank D position can be seen in figure 4.27, some deviations from plant data are detected in here, and almost same deviation can be attributed to the three models respect to the plant data. Such discrepancies are attributed to the cross section library accuracy and also to the information exchange coding from TRACE/PARCS, more investigation needs to be done in this area. Pressurizer parameters are compared in the next two figures 4.28 and 4.29. Very good agreement is seen in terms of the pressurizer level but some discrepancies are detected in pressure time trends. Such difference is attributed due the detail

degree on the pressurizer control logic also due the pressurizer heaters malfunction with the coupled calculation; again some research over the source code needs to be done here. Also these discrepancies are thought related to some unrecorded manual actions, like valve operation, that were performed at the end of the transient and that have not been simulated. Finally secondary side main features are analyzed and compared in the last four figures; 4.30, 4.31, 4.32 and 4.33. There is a small deviation in the initial secondary side pressure which derives in a small gap between the measured values and computed with TRACE/PARCS [1–3] and [4, 5] values. Nevertheless, main feed water, vapor mass flow rate and steam dump behaviors are very close to the plant data. The non-showed values from other loops hold the same time trend than the values showed here, those plots where avoid in here due the redundant information.

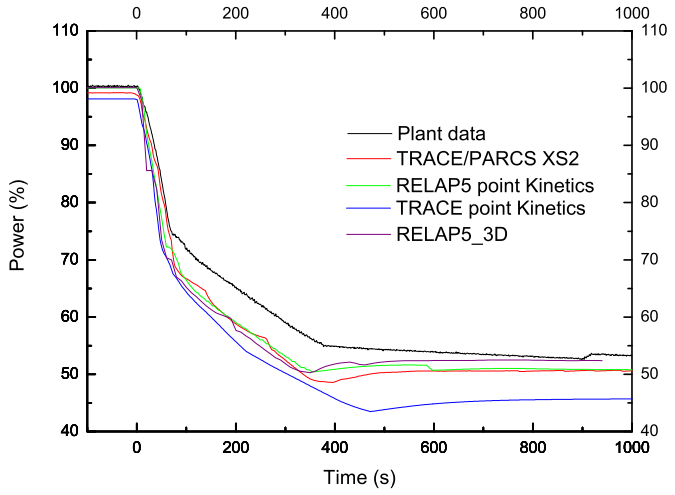

FIGURE 4.26: Total power multiple models comparison.

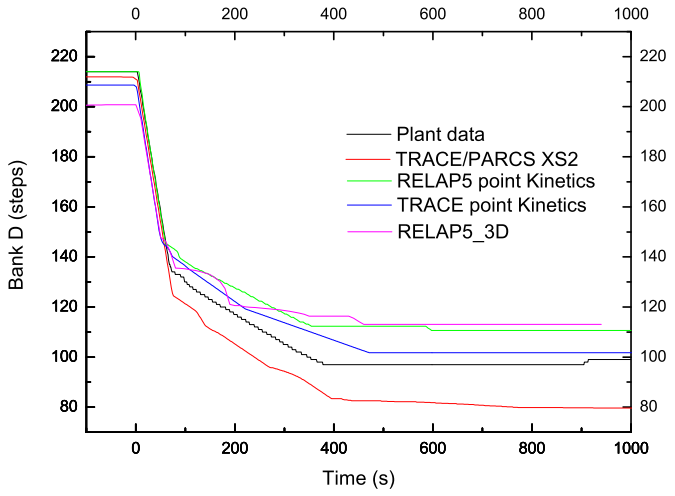

FIGURE 4.27: Control rod bank D multiple models comparison.

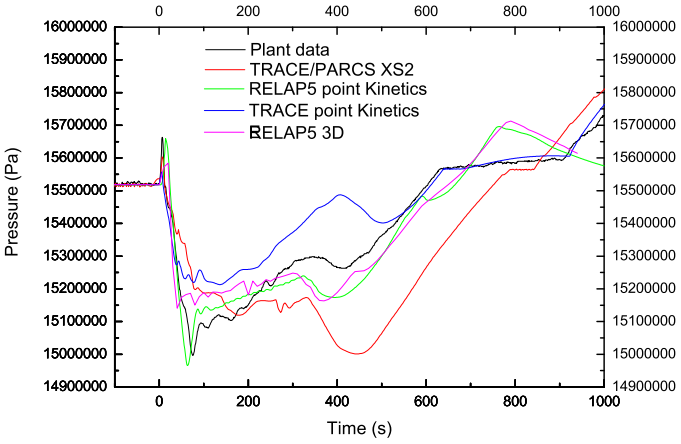

FIGURE 4.28: Pressurizer pressure multiple models comparison.

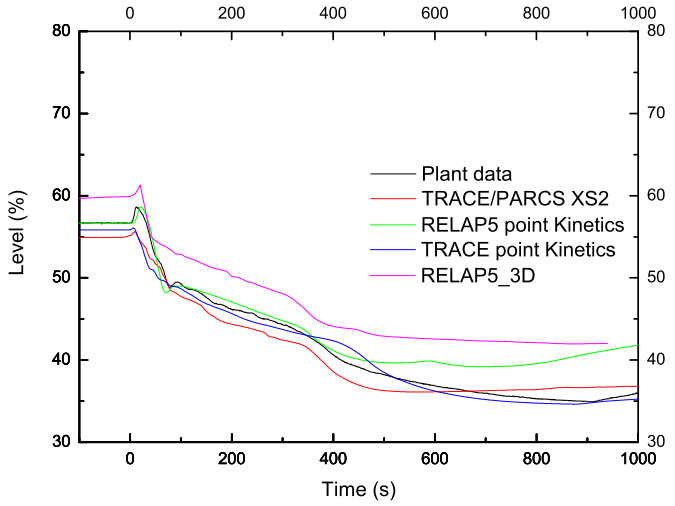

FIGURE 4.29: Pressurizer water level multiple models comparison.

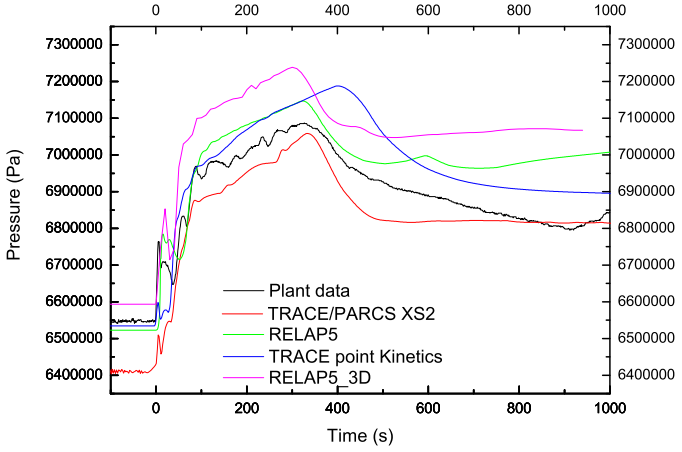

FIGURE 4.30: Secondary side SG2 pressure multiple models comparison.

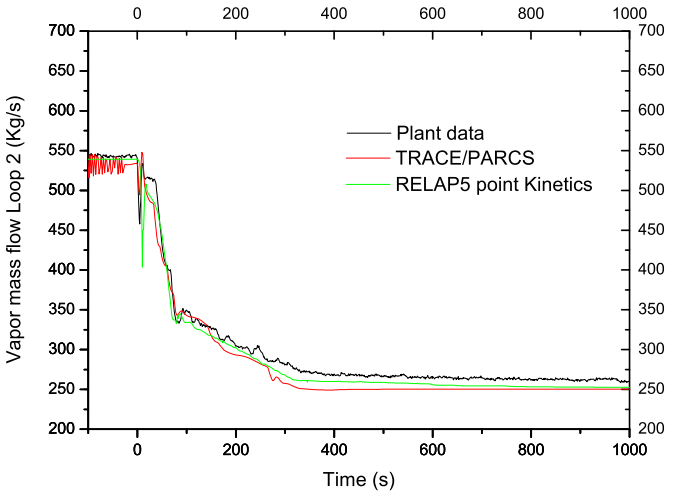

FIGURE 4.31: Secondary side SG2 vapor mass flow multiple models comparison.

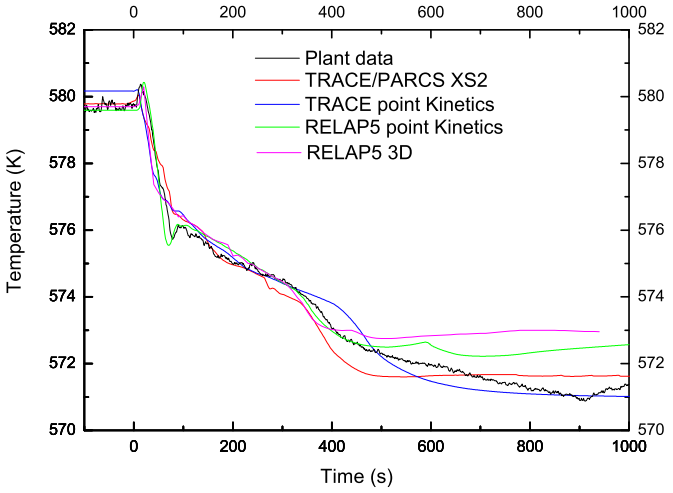

FIGURE 4.32: Loops mean temperature multiple models comparison.

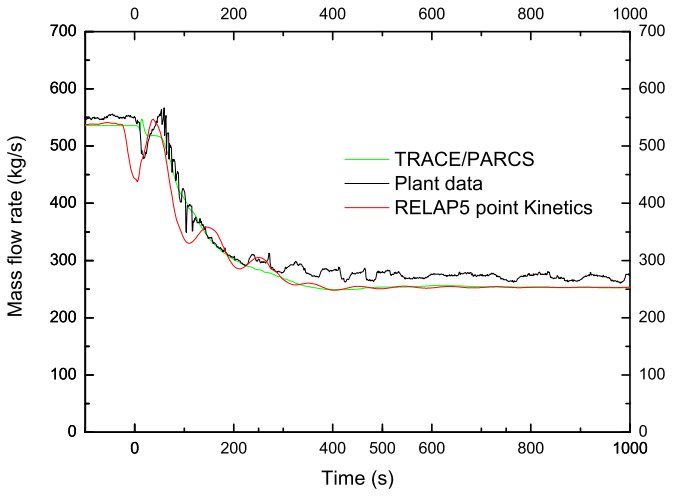

FIGURE 4.33: MFW SG1 mass flow multiple models comparison.

4.3.5 Model validation conclusions

From the calculations performed in this section, some conclusions over the used 3d NK-TH coupled model can be obtained. In general terms the TRACE/PARCS [1–3] and [4, 5] model can be considered validated at the same level as RELAP5 [41–49], RELAP5-3D [41–49] and [31–35] coupled with NESTLE [31–35] and TRACE point kinetics [1–3] models were considered as validated models, against the 50% Loss of load transient. Such affirmation can be done due the general good agreement between TRACE/PARCS [1–3] and [4, 5] model and plant data model. Also the triple and quadruple comparison between TRACE/PARCS [1–3] and [4, 5], RELAP5 point Kinetics, TRACE point kinetics and plant data show good agreement between the calculations. The dimension of the deviations between the plant data at any of the above mentioned calculations are consistent within the acceptance criteria margins. Nevertheless even the TRACE/PARCS [1–3] and [4, 5] model can be considered validated; it needs to be conformed against multiple library of cases as RELAP5 [41–49] GET model has been going through. A good validation process will involve different postulated scenarios for the reference plant such (ATWS, LOCA's, MSLB ...) Obviously these with more relevant 3D kinetics effects will test the model more severely than the ones with less 3D kinetics effects. Each tested scenario can be now compared with the other codes results, since plant data is only hold for the 50% Loss of load transient. In this way the model will gain in roughness and confidence. TRACE/PARCS [1–3] and [4, 5] source code modification also show a good prediction, several tests were performed in order to ensure the code is able to run

in normal conditions even with the modifications made, in this way we ensure the new version is not disabling any of the anterior capabilities. For 3D kinetics validation the dynamic control rod movement has shown to be necessary in order to validate any model and calculation performed. Even the smallest deviation between the measured control rod position and the predicted for TRACE/PARCS [1–3] and [4, 5] model, falls into the acceptance criteria, author has identified some source of possible deviations and set up future work in that sense, in order to improve the model prediction. Those sources are being identified in the following fields; XS library accuracy; Control rod movement logic in the TRACE system; TH vessel nodalization; Rod cusping correction effect and exchange of information between two codes. Some of the previous fields have already been tested and the results of such tests will be presented in future documents. In the control rod bank position the phenomenon can be marked as a source of uncertainties, such source starts with small deviation at the beginning of the transient and end up with a bigger discrepancy at the end of it. Also as it has been said, inside GET group there is another task performed which will be ending with a more detailed XS library that will contain uncertainties over the neutron kinetics parameters used when computing such library. The new library will be computed with the lattice physics code SCALE 6.1. The GET group is expecting to hold more analysis capabilities and more accuracy when such task is done; meanwhile the present XS library (generated by HELIOS-1.9 [27–29]) is being used to perform the model validation. In general terms the modified TRACE/-PARCS [1–3] and [4, 5] code is showing results inside the validation acceptance criteria (i.e. no bigger deviations on the TH parameters are observed, deviations from plant data have equal dimension than the previous accepted models). The implementation conducted in the present work not only allowed the calculation of validation presented, but it also will be useful for future uses in the area of transient analysis involving relevant control rod contribution. Among these transients are: Other tests; Transient startup; and operational transients necessary for the control system adjustment.

Chapter 5

Conservative Model

In order to check the relative adequacy of the Best Estimate Plus Uncertainty (BEPU) methodology, a conservative calculation is performed first to be used as a reference calculation for comparison purposes. Essentially, the conservative calculation is the same as the Best Estimate Base Case Calculation (BEBCC) but with some conservative assumptions in order to ensure the safety margins. The "Conservative" calculation is representative for the use of best estimate computer codes plus conservative initial and boundary conditions. Such calculation is made prior to Best Estimate Plus Uncertainty (BEPU) calculation and after the Best Estimate calculation. In this section a description of the assumptions taken for computing the conservative calculation is given. Such assumptions are taken under the experts criteria (i.e. Ph.D advisors experience and author gained experience) but also over some bibliography research from: USA Code of Federal Regulation (CFR) 10 CFR 50.46 [54]; OECD PWR MSLB benchmark [16–19]; OECD NEA PKL-2 [50, 51] project; CRISSUE-S [20–22] and OECD UAM project [23, 68]. Later some results about the Figures of Merit from the conservative calculations are also shown. These Figures of Merit values time trends are going to be compared with the BE and BEPU calculations in the next chapter.

5.1 Conservative model description and results

As mentioned above a conservative calculation is built is built with the Best Estimate Base Case Calculation as a starting point. Over this input deck several conservative assumptions were taken by using the expertise criteria from the advisors of the present study, the experience gained by the author during the realization of the present work plus the some bibliography research. The main two figures of merit of the MSLB scenario are figure 5.1 and figure 5.2, which represents the total reactivity and the total power

time evolutions for the conservative assumptions case calculation respectively. Such calculation is made prior to Best Estimate Plus Uncertainty (BEPU) calculation and it will be used to set up the safety margins showed in figure 2.18. A lower decrease of the core power in the late phase of the transient (i.e. after 50.0 seconds ±10.0 seconds to the initiating event), plus a higher initial peak of the total power (i.e. after 5.0 seconds ±2.0 seconds to the initiating event) are expected to be found in the total power figure of merit, compared to the Best Estimate Base Case calculation. In the other hand a higher increase of total reactivity parameters, also in the late phase (i.e. after 50.0 seconds ±10.0 seconds to the initiating event) of the scenario compared to BEBCC and BEPU calculations is expected in this case. There are different assumptions that could be taken when modeling the MSLB scenario, with more critical scenario (i.e. higher return to critically event in the late phase of the transient) to a less critical scenario with more smoothly behavior in terms of the total power and the total reactivity.

Nevertheless the present scenario was selected for its simplicity and its robustness in terms of numerical failures of the 3D NK-TH coupled calculation. It should be noticed that with the used code versions, models' detail degree and amount of managed information, any single bug, which delays the calculation, it makes increase significantly the computational time thus it makes it very difficult to used in a Best Estimate Plus Uncertainties calculation framework. Also it should be noticed that at any case, the most critical scenario (which is the one presented in this chapter), it is not becoming critical in terms of nuclear safety, since the postulated actions of the ECCS systems and the non-stuck control rod banks cool down the core in a reasonable time. Also for the same reasons, the total power and total reactivity does not takes critical values as well. Besides that, the conservative calculation must show a more critical behavior of the nuclear power plant essential parameters such total core power and total reactivity time trends. It is not intended to show a conservative case behavior against other calculations in here, that is why comparisons between Conservative case, Best Estimate case and Best Estimate Plus Uncertainties calculations are shown in the coming sections

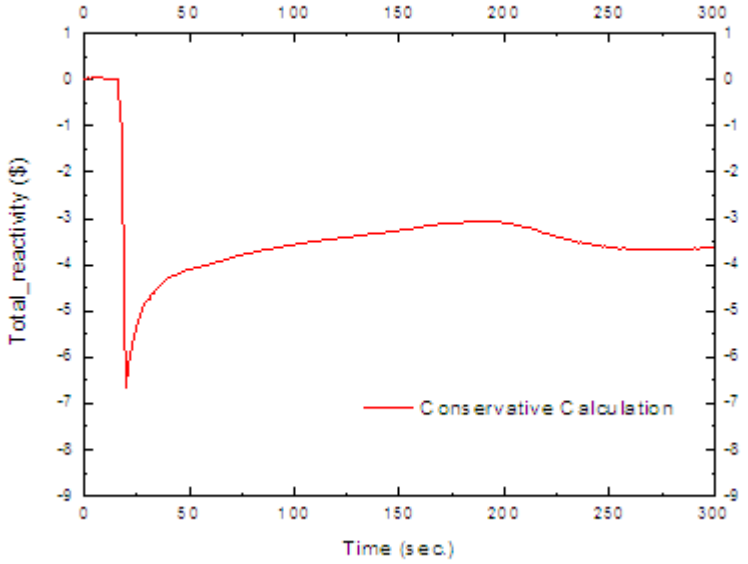

FIGURE 5.1: Conservative Case total reactivity time evolution.

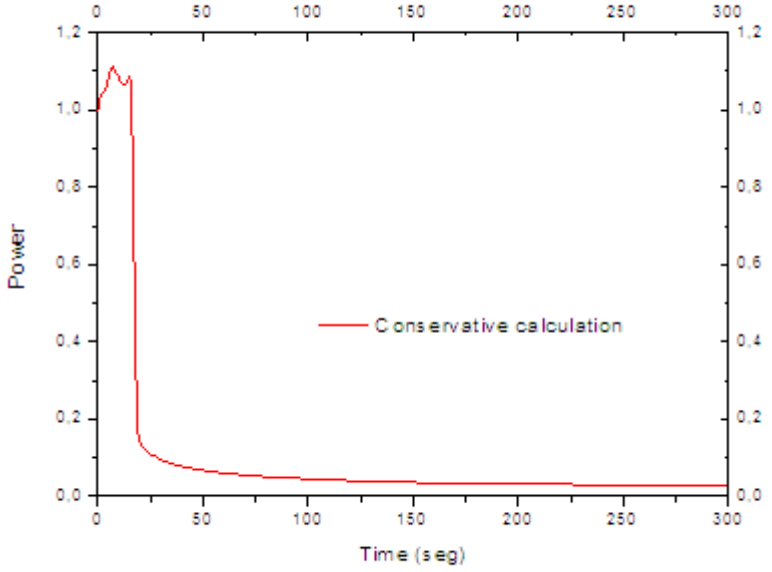

FIGURE 5.2: Conservative Case total power time evolution.

After gathering some information through the extensive bibliography: USA Code of

Federal Regulation (CFR) 10 CFR 50.46 [54]; OECD PWR MSLB benchmark [16–19]; OECD NEA PKL-2 [50, 51] project; CRISSUE-S [20–22]; OECD UAM project [23] and [69] Also after doing some trial and error test calculations, and finally over some experts advice (from the PhD. advisors and author's gained experience) a list of modifications over the Best Estimate case was proposed in order to create the Best Estimate with Conservative Boundary conditions calculation.

The list of the assumptions and modifications made to the Best Estimate model, divided in the modifications made over 3D neutron kinetics and thermal-hydraulic model, is summarized below:

- For the thermal hydraulic input TRACE [1–3]:
  - Small delay on the pumps trip *(+1.0)* seconds.
  - Slightly increase *(+5.0%)* of pressure and temperature of the boundary conditions (*BREAK components*) which receive the fluid from the MSLB.
  - Slightly increase *(+5.0%)* of the OPPENING/CLOSE time from the valves system which are composing the MSLB nodalization.
  - Slightly decrease *(-2.0%)* of the temperature from the ECCS system.
  - Slightly decrease *(-2.0%)* of the temperature from the FW system.
- For the neutronic input PARCS [4, 5]:
  - Initial status of the control *bank D*, *six steps* withdrawn with respect to the BE case.
  - More free space *(+5.0%)* when the control rod is fully inserted.
  - *(+2.64%)* increase in the control rod step size.
  - Increase on the delay of the SCRAM signal by *(+0.05)* seconds.
  - Increase on the delay of the rod insertion time by *(+0.5)* seconds.
  - Increase *powtrip* card, which defines the power level where SCRAM occurs.

Note: All the above (%) values are computed over the nominal values.

In order to emphasize the neutronic conservationism selection and assumptions listed above, the influence from different neutron kinetic parameters in MSLB scenario is described next. In that sense, other considerations over the neutron kinetic are should be noticed in order to perform a conservationism approach of the studied problem. These below mentioned considerations should be enough to explain the above reactor kinetic conservationism parameters value selection. In designing a reactor core, certain

guidelines or limits must be adhered to. Some of these limits for the core modeled in this study are:

- Maximum enrichment in fuel pin = 4.665%
- Total weight percent gadolinium in fuel pin = 8.0%
- Fuel pin radial peaking = 1.45
- Assembly radial peaking = 1.291
- Initial boron concentration = 1728.00 ppm
- Core burnup per cycle = 500 + 32 EFPD

Notice a core that is designed with most parameters at or near the limits can be considered a bounding core design. This means that the fuel configuration and resulting power distribution must be selected to represent the most adverse arrangement expected in future reload cycles. The core power distribution effects the transient results through fuel rod peaking. A conservative power distribution can generally be produced by placing higher enrichment fuel around the stuck rod location. Also, for a MSLB accident, the worst results are obtained by having the most negative moderator coefficient. This can be achieved by modifying the absorption cross-sections as discussed under reactivity coefficients or by designing a core with three consecutive cycles run to 550 EFPD for example, Which is much longer than the design limit of 500 EFPD. Having established a bounding core design, it is further necessary to identify a set of neutron kinetic parameters which are significant and directly affect the results of the analysis. Once these key parameters have been determined, then the impact of variation in the range of values due to a change in the core loading pattern and operating history can be assessed. A conservative or consistent value can then be selected for analysis or several combinations can be analyzed to ensure the transient response is bounded. The most relevant parameters to neutron kinetic field of the problem are discussed below. Notice, on the below development there is some Three Mile Island(TMI) references. This is due the below discussion was applied first on the Three Mile Island core, for example used in [23, 68]. After lessons learned the relevance and impact of the neutron kinetic parameters on the MSLB scenario was determined and thus applied on the model used in the present study.

NEUTRON KINETIC PARAMETERS IMPACT IN MSLB SCENARIO

Reactivity insertion following reactor trip

The reactivity insertion following reactor trip is a combination of a minimum available tripped rod worth and a normalized reactivity insertion ratio. The minimum available

tripped rod worth assumed in safety analysis must ensure, as a minimum, that the shutdown margin in technical specifications is preserved. This shutdown margin assumes that the most reactive rod remains in the fully withdrawn position and that the other control rods banks drop from their power dependent insertion limits. For the point kinetics analysis performed in previous versions of the models, a minimum tripped rod worth of 3.46% ($\Delta k/k$) is used. This typically comprises of a power deficit of 2.3%, a maximum allowable inserted rod worth of 0.16% and a shutdown margin of 1.0%. A criteria for the Three Mile Island core design[23, 68] is that the core should be capable of maintaining a 1% ($\Delta k/k$) shutdown margin at hot shutdown conditions with the maximum worth control rod withdrawn from the core. Consequently, a conservative scram worth would be the minimum shutdown margin of 1% ($\Delta k/k$). For 3D NK-TH simulation, the control rod worth can be decreased to the desired value by decreasing the thermal absorption rodded cross section (*Group 2*). The worth is calculated by running the steady state base case with the rods in, and again with the rods out. The state rod worth (*reactivity*) is defined as the steady state eigenvalue (*rods out*) minus the steady state eigenvalue (*rods in*) divided by the core average delayed neutron fraction (*Beta effective*). It is necessary to iterate on cross section adjustments until the desired rod worth is achieved (*rod worth will decrease monotonically with changes in the Group 2 cross section*). If desired, control rod worth can also be varied by changing both the last and thermal absorption rodded cross sections. The normalized reactivity insertion rate is determined by bounding control rod drop times as determined by plant testing and by developing a conservative relationship between rod position (*% inserted*) and normalized reactivity worth. As an example, the Three Mile Island tech spec acceptance criterion [23, 68] for control rod drop times is 1.66 seconds to 3/4 inserted, which means a very quick insertion time. From here it is concluded, the MSLB scenario is probably not very sensitive to the shape of the scram reactivity insertion versus time variable.

Reactivity coefficients and kinetics parameters

The dynamic behavior of a reactor core during load follow maneuvers, transients and accident conditions can be described in terms of reactivity coefficients. The magnitude and sign of these coefficients affect the reactor stability during transient and accident conditions. Reactivity coefficients are defined as the change in reactivity produced from a change in reactor power, moderator density, and fuel temperature or boron concentration. The moderator density effects are often expressed in terms of moderator temperature. Since these coefficients are a strong function of exposure, they are calculated at several exposure state points during core file. Reactivity coefficients are also influenced by changes in moderator temperature, reactor power and soluble boron concentration. The state points at which reactivity coefficients are evaluated are chosen to ensure that the assumptions made in the specific accident analysis remain bounded. For example,

the main steam line break accident is sensitive to the most negative (*or least positive*) isothermal temperature coefficient. The calculation of the moderator temperature coefficient and fuel temperature coefficients and the state points at which these coefficients are evaluated are discussed in the following sub-sections. These parameters will influence more or less over the studies MSLB scenario. Next discussion is specially focused on the convenience and impact of the discussed parameters in the conservationism approach of studied scenario. The calculation of kinetics parameters follows.

- *Doppler temperature coefficient*
  - The Doppler (*or fuel*) temperature coefficient is defined as the change in core reactivity resulting from a change in fuel temperature. The most and least negative Doppler temperature coefficients are calculated for each reload core considering the core burn up power level. For a MSLB accident, the power increase is exacerbated by assuming a least negative Doppler coefficient. This can be accomplished by decreasing the last absorption cross section derivative for each fueled composition. The Doppler coefficient is calculated by running an un-rodded steady state base case (*rods out*) at cross section reference temperature followed by a case at a lower fuel temperature. The Doppler coefficient is defined as the steady state eigenvalue (*at lower fuel temperature*) minus the steady state eigenvalue (*at reference fuel temperature*) divided by steady state eigenvalue (*at reference temperature*) divided by the difference of the square roots of the absolute fuel temperatures (*non-reference and reference*).
- *Moderator temperature coefficient*
  - The moderator temperature coefficient is defined as the change in core reactivity resulting from a change in moderator temperature. Bounding coefficients (*first and most negative*) are calculated for each core reload. The moderator temperature coefficient is calculated by inducing a change in moderator temperature (*and, therefore, density*) about the average temperature of interest and dividing the resulting reactivity change by the change in moderator temperature. For a MSLB accident, the return to power is exacerbated by assuming the most negative moderator coefficient. This can be accomplished in a manner similar to that described for the *Doppler temperature effect.*
- *Effective delayed neutron fractions and decay constants*
  - The delayed neutron parameters are more important during rapid reactivity excursion transients such as the rod ejection accident. If the transient is

not characterized by a rapid change in reactivity, then the value of beta-effective is not significant. Delayed neutron fractions and decay constants are calculated for six effective delayed neutron groups. The total beta-effective is the sum of the six group effective fractions and is, along with prompt neutron lifetime, calculated at BOC and EOC conditions. For the MSLB accident analysis, the EOC delayed neutron fraction is used. A smaller beta-effective can be calculated by scaling all values of beta in each delayed group of each composition by the same multiplier to get the desired core average beta or by normalizing the total beta in each composition to the desired value of beta. The values of the fractions and decay constants for each delayed neutron precursor group are not key parameters, and typical values are sufficient.

- *Prompt neutron lifetime*
  - The prompt neutron lifetime is mainly important during rapid reactivity excursion transients. This parameter is not a key parameter, and so typically beginning and end of cycle values are used consistent with the limiting core condition for the transient. For the MSLB analysis, the end of cycle value should be used.

THERMAL HYDRAULIC PARAMETERS IMPACT IN MSLB SCENARIO

Same type of discussion above made for the neutron kinetics parameters was made in order to find the relevance of the thermal hydraulic parameters in the MSLB scenario. After finding the impact of each parameter a conservatism approach in thermal hydraulic field was also determined. Same as in the neutron kinetic parameters, these below mentioned considerations should be enough to explain the above thermal hydraulic conservationism parameters value selection. It should be considered the following effects when analyzing the thermal hydraulic part of the scenario. A trip delay of 0.4 seconds is used for the high flux trip. The high RCS pressure delay is modeled as 0.6 seconds. These values represent the delay from the time the trip condition is reached to the limit the control rods are free to fall and bound the actual delays for Three Mile Island. Since the primary-to-secondary heat transfer is the driving force behind the RCS cool down and depressurization, steam generator inventory is maximized to provide the largest cool down capacity. In addition, the feed water between the isolation valves and the affected steam generator is modeled to contribute to the overcooling and depressurization of the RCS. The double ended rupture of one steam line was assumed to occur at the steam generator nozzle. The 0.329 m^2 rupture results in the highest break flow assumption and maximizes the RCS cool down. No credit is taken for pressurizer heater operation. This assumption enhances the RCS depressurization and is therefore conservative.

As a concluding part of this chapter, it can be seen from the modifications made, that the aim of these assumptions was to bring the plant into a worst scenario. Since the selected Figures of Merit for the present study are the total power and the total reactivity, it is expected to see some different time trends on these two variables by applying the above assumptions. More precisely, and starting with the total reactivity, an increase of the return to critically scenario (bring in the system to a worst scenario) it should be observed on the reflooding phase. In total power figure of merit, it is a little bit difficult to see much differences since there is a domination effect created by the all rods in when SCRAM takes place. Nevertheless slightly differences can be observed also in terms of the total power time trends. In this case residual power for conservative scenario is slightly superior. These small differences between the three compared calculations (i.e. Conservative; BE and BEPU) in terms of the total power makes the author to choice as a representative figure of merit from the present scenario the total reactivity instead of the total power. This comparison of BE scenario and BE with conservative boundary conditions can be seen in the *Comparison Results Chapter*.

Chapter 6

Best Estimate Plus Uncertainty model

Best Estimate Plus Uncertainty calculations are presented in this chapter. In here a culmination of the whole report will be exposed. The ultimate goal of the present study was to contribute in to the 3D NK-TH coupled BEPU analysis, thus the results in here will represent the final step of this illustrated methodology prior to the results analysis. The parameters selected, their associated probability density functions, their mean and standard deviation are described in this section. DAKOTA [6–9] code played an important role in this part of the task, since all the selections was made manually (i.e. bibliography, and experts selection), but all the sampling and input files construction was made by DAKOTA [6–9] code under the author's pre-fixed criteria. It is also noticeable that at the present point of the realization of the present study, not all the used computer codes are ready for the uncertainty propagation which will be an ideal case, where uncertainties generated in the first step (i.e. lattice physics code) are taken into account through the final 3D NK-TH calculations. Such Uncertainty propagation is well studied in the framework of the OECD UAM LWR benchmark [23] project. Nevertheless, with the work performed in here, the tools will be ready for GET group when UAM project reaches the Phase III (System Phase) where coupled 3D NK-TH system codes are going to be tested with Uncertainties, which may be generated from lattice physics code and propagated over each step involved in this coupled calculations. In that sense the methodology described here can be used in future calculations when the effectiveness of the computing machines will be higher and the computing time will be smaller.

6.1 Best Estimate calculation

Before performing the BEPU calculation over the models, the following methodology is used. Since this is a coupled calculation, several prior steps to the transient simulation need to be performed. Steady state achievement is described in previous sections, besides that it is to mention as a resume, that the steady state conditions are achieved in three steps. In first step, a stand-alone calculation with the thermal-hydraulic code is done. Second step is to run a coupled steady state calculation. Finally a transient coupled calculation is restarted from the end of the steady state simulation, this is know as null transient calculation. The methodology flow diagram is shown in figure 4.12. Once the input decks are setup and the steady state conditions are archived, next step is to configure the DAKOTA [6–9] sequence. The general sequence of steps for performing an Uncertainty Analysis in a best-estimate model is summarized below:

1. Specify Uncertainty Analysis input such as sampling method, number of samples, etc ...
2. Select the set of input parameters to be modified.
3. Assign probability distributions and range of variation to each input parameter.
4. Generate the sets of random variables.
5. Generate an input file for each set of random variables.
6. Execute each case.
7. Extract response data from each case run.
8. Calculate uncertainty and sensitivity results.
9. Compile a report summarizing the Uncertainty Analysis.

Some of the steps (like the selection of input parameters, definition and assignment of probability distributions, and input requirements given to the DAKOTA [6–9] software such as the sampling method, number of samples, and the random seed) need to be entered by the user. Other steps, from the above list, are internal steps within the code's framework and last type of the previous steps, might be the result of the calculations with the DAKOTA [6–9] Uncertainty package. As mentioned before DAKOTA [6–9] software it really simplifies the task of performing a BEPU calculation, since it generates all the input decks with its modifications according to the above mentioned criteria. SNAP [60] package is the tools which carries out all the executions from all the created cases. In this work, 59 3D NK-Th executions, at the minimum.

The author of the present study has compiled a list of one hundred thermal-hydraulic parameters plus forty neutronic parameters, which are relevant to PWR MSLB analysis, to be used as perturbable parameters in a BEPU calculation. Such list has been reduced based on Phenomena Identification and Ranking Tables (PIRT's)[10–15], CRISSUE [20–22] reports and experts conclusions to a list of twenty two relevant parameters. Twelve thermal-hydraulic parameters and ten neutronic parameters are representative of the most relevant parameters to the MSLB transient in a PWR. The table 6.1 and table 6.2 show the list of the twelve thermal-hydraulic parameters and ten neutronic parameters. Each table contains mean values for each parameter, Probability Density Functions (PDF's), standard deviations, Maximum and Minimum values in case there are any. In addition the reference [70] has also been used to determine the parameters and their associated probability density functions. This parameters reduction follows the philosophy of all the present study to contribute to the validation of best estimate plus uncertainties coupled codes for the analysis of NK-TH nuclear transients, rather than going with deeply detail analysis of a very well known and studied transient. See references OECD PWR MSLB Benchmark [16–19], OECD NEA PKL-2 [50, 51] project and CRISSUE-S [20–22].

TABLE 6.1: Thermal-hydraulic parameters list

	TH parameter	Unit	Mean	PDF's	Standard Deviation	Max.	Min.
			BRAKES				
1	Initial mixture temperature	K	554.245	Normal	0	-	-
2	Initial pressure	Pa	1.00E+05	Normal	1.00E+04	-	-
			FILLS				
3	Initial mixture temperature	K	333.15	Normal	30	-	-
4	Initial solute ratio	-	2200	Normal	500	-	-
			PIPES				
5	Wall roughness	m	4.00E-05	Normal	4.00E-06	-	-
			JUNCTIONS				
6	Wall roughness	m	4.00E-05	Normal	4.00E-06	-	-
			TEE's				
7	Wall roughness	m	4.00E-05	Normal	4.00E-06	-	-
			VALVES				
8	Wall roughness	m	0	Normal	0	-	-
9	Maximum valve rate	1/s	10	Normal	1	-	-
10	Min. position	-	0	Normal	0.05	-	0
11	Max. position	-	1	Normal	0.05	1	-
			HEAT STRUCTURES				
12	Gas GAP HTC	W/m^2K	1.14E+04	Normal	500	-	-

TABLE 6.2: Neutronic parameters list

	Neutronic parameters	**Unit**	**Mean**	**PDF's**	**Standard Deviation**	**Max.**	**Min.**
1	Rod insertion	cm	110.37	Normal	5.52	-	-
2	Rod step	cm	1.579511	Normal	0.0789756	-	-
3	Control rod banks positions	steps	196	Normal	5	-	-
4	Core power to initiate trip	%	100	Normal	10	-	100
5	SCRAM signal delay time	s	0.2	Normal	1	-	0
6	Rod insertion time	s	2.2	Normal	0.5	-	-
7	Time step size	s	0.07	Normal	0.05	0.5	1.00E-03
8	XS change criterion for requiring at least one nodal update	-	0.01	Normal Normal	5.00E-04	-	-
	Transient convergence parameters						
9	Local fission source convergence criterion	-	1.00E-04	Normal	5.00E-06	-	-
10	Fuel temperature convergence criterion	-	1.00E-06	Normal	5.00E-08	1.00E-05	1.00E-07

Every parameter from the tables above (6.1 and 6.2) is treated by DAKOTA [6–9], under the specifications given by the user. Such internal mechanism gives to every parameter a different value for each one of the Best Estimate Plus Uncertainties calculation. The new values depend on the PDF's and on the standard deviation of each initial parameter value. Figure 6.1 illustrates the wide range of selected values for the rod insertion time in this case. Notice that all the values oscillate around one central value of 2.2 seconds in this case. This type of figure, like figure 6.1, is obtained with every perturbable parameter, in order to avoid to many similar figures in the report, only this representative figure is presented here. These figures are used to have an idea of how the values vary over the each mean value within the different inputs in the BEPU analysis. Also the relevance and the impact of each parameter can be derived from the figures like figure 6.1.

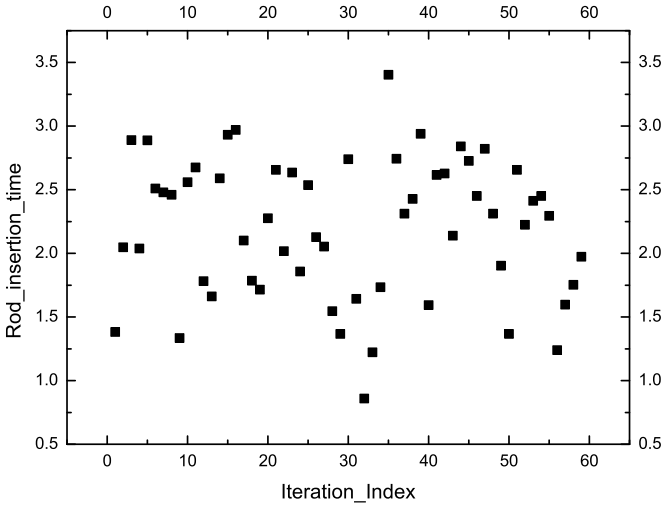

FIGURE 6.1: Rod insertion time BEPU values.

The Uncertainty analysis methodology uses a method for computing sample sizes based on the Wilks method [52–57], described in the paper [52]. The method is used to determine a number of random samplings that must be made to assure a certain degree of confidence that a given probable range of inputs have been covered. The computation has been modified slightly to account for the order of the order statistic method. After identifying the parameters, the DAKOTA input deck is prepared. The authors had considered to achieve the 95% of probability and 95% of confidence for the present calculations. Such range should be enough to illustrate the 3D NK-TH coupled BEPU

calculations methodology. Increasing the number of parameters and the number of calculations will result in better ranges of probability, confidence and safety margins. Figures 6.2 and 6.3 show the total reactivity distribution and total core power distribution against time, for the 59 cases used in the BEPU methodology.

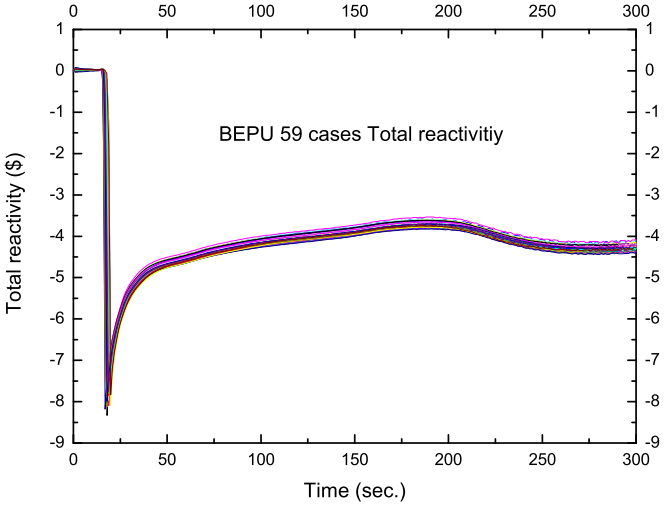

FIGURE 6.2: BEPU calculation total reactivity results.

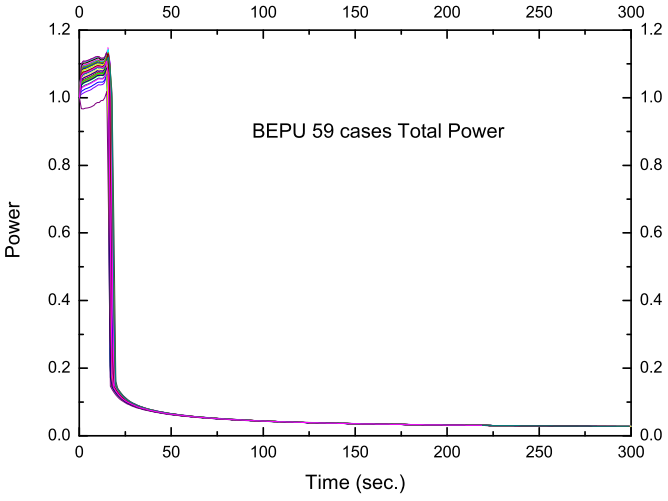

FIGURE 6.3: BEPU calculation total power results.

Once this results are obtained the uncertainty range has been determined. By looking at the figures 6.2 and 6.3, it can be observed that the uncertainty range it is well determined on the total reactivity Figure of Merit, while it is unclear to determine upper and lower limits in the case of the total power (Figure of Merit), specially after the SCRAM event. This noticeable result, made the author to decide to keep the total power in this study but, more information and relevant conclusions will be obtained over the total reactivity Figure of Merit. Once the calculations are done, small fortran program is used to obtain the uncertainty ranges (upper and lower limits) for each quantity (i.e. total reactivity and total power) at each time step. This was particulary difficult due the complexity of the coupled calculations, that makes a different plot points for the different 59 calculations. The program is taking at each computed time step the maximum and the minimum value in order. Once the 59 time trends are passed through the fortran program, the limits are established. Looking at the figure 2.18, by concluding this step the Upper and Lower limits of the Uncertainty range on the right side are set up. From the Best Estimated calculation and also from Best Estimated plus Conservative boundary conditions calculations the other values from figure 2.18 have being also determined. Thus, a comparison between the three methodologies is next. Such comparison is explained in the next chapter of the present report. For future steps and specially looking at the OECD UAM LWR benchmark [23] project, the methodology has being fully established by the previous performed work. Nevertheless some improvements could be introduced specially in the uncertainty propagation and XS library calculation. Within the framework of the OECD UAM LWR benchmark [23] project the uncertainty propagation is being studied from the first calculations and assumptions made in the lattice physics code to the 3D NK-TH system code calculations.

Chapter 7

Comparison results

Finally a comparison between BEPU calculations versus Conservative Case calculation is performed to provide a final overview of the computed cases. Summarizing all the effort, after all the XS library development, different code models construction, source code modification, validation process, conservative assumptions case calculation, Best Estimate case calculation, PIRT's identification and characterization (PDF,s, mean, standard deviation ...) and Best Estimate Plus Uncertainties calculation a figure close to figure 2.18 is expected to be found for the two selected Figures of Merit for the MSLB selected scenario. Essentially if all the methodology is working well, the time trends of the Conservative data should be more critical than the BEPU margins and BE data should fall within BEPU margins for the both Figures of Merit.

As it is expected, BEPU calculations provide a range of values in-between the maximum and the minimum value for each time step of the calculation, such range (see figure 7.1) has been compared with BE plus conservative boundary conditions calculation and it can be seen in figure 7.3. Also Best Estimate Base Case Calculation (BEBCC) is plotted in the same figure, such calculation falls within the BEPU margins, which agrees with figure 2.18. This distribution of the obtained results completely agrees with what was presented in background chapter, where Uncertainty analysis has being widely explained. Specially looking at the figure 2.18 where real BE calculation value it is situated within the uncertainty range and BE plus conservative boundary conditions case is situated above the Upper uncertainty line and closer to the safety limit. This will give some margin of safety improvement for energy production as it is expected with BEPU calculations results. For the simulated transient the return to critically event will be postulated as a safety limit. This limit is not achieved at any case due the assumptions made when modeling the MSLB scenario described in Chapter 2 Section 2.1 *PWR MSLB transient*. Should be noticed here that the closer we get to the 0.0 reactivity

values after the SCRAM event, the worst scenario is being simulated, in this way, the relative situation of the different margins represented in figure 2.18 should be the same as the ones expected for these time trends. The power time evolution, figure 7.4, has been omitted, when extracting conclusions, due to the narrowest BEPU margins in it, specially after SCRAM event. See also the Figure 7.2 where almost after 50.0 seconds, there is no significant difference between upper an lower uncertainty limits values. Thus the relevant Figure of Merit becomes the total reactivity, figure 7.3. It is noticeable to mention the width of the uncertainty range, which seems to be quite narrow compared to other Uncertainty calculations performed with other thermal-hydraulic system codes. This could be attributed to the small list of perturbed parameters. Nevertheless, it becomes enough to illustrate the BEPU methodology with 3D NK-TH coupled system codes. Same comparison can be done in terms of other variables which might became the other Figures of Merit such the local temperature. This comparison will be also interesting if it is done for the region where the control rod remains stuck out. The peak temperatures in this core region will reach higher values and the comparison between BEPU, BE and Conservative methodologies will be significant there as well. Nevertheless the advisors expertise, the author experience and the bibliography [20–22], [16–19], [10–15] and [23] are been used to select the total reactivity comparison (figure 7.3) as a representative Figure of Merit of the MSLB scenario according to all the assumptions made in the Base Case Calculation. Figure 7.3 turns out to be the representative and concluding figure of the present study.

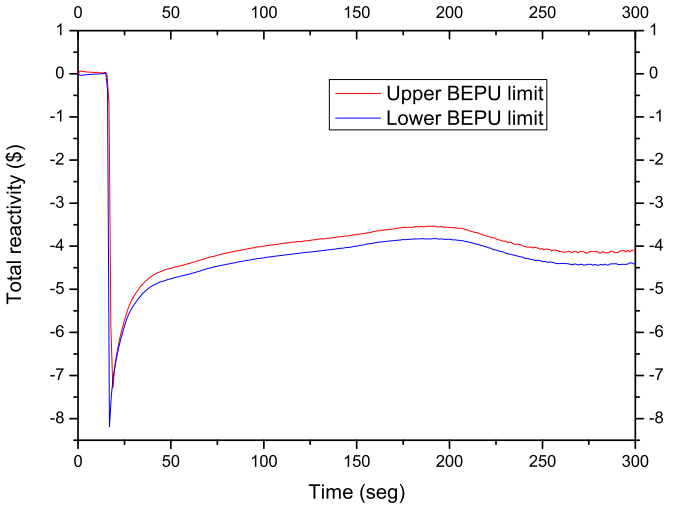

FIGURE 7.1: Reactivity BEPU calculation bands.

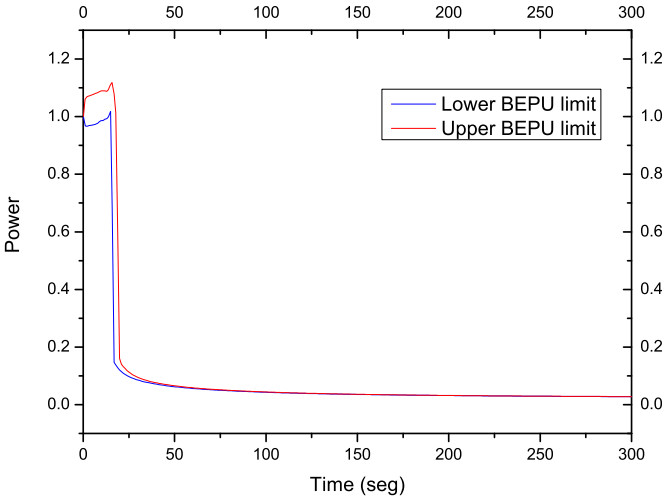

FIGURE 7.2: Power BEPU calculation bands.

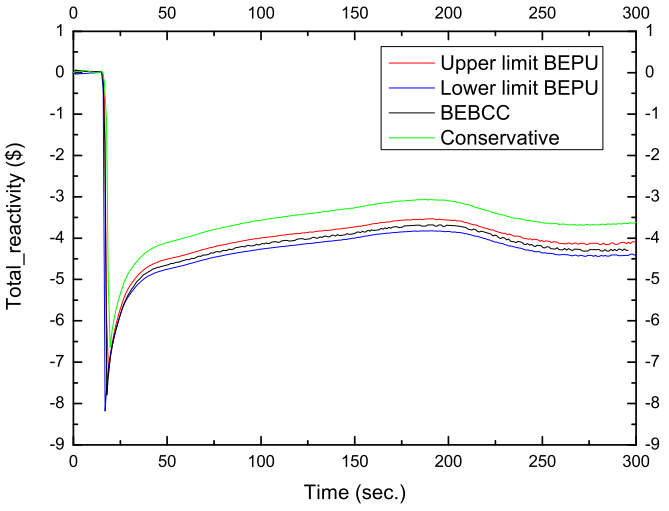

FIGURE 7.3: Reactivity comparison between Conservative and BEPU calculations.

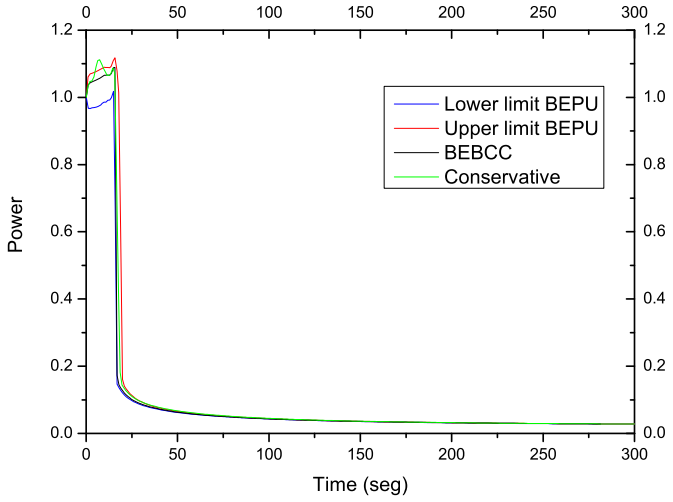

FIGURE 7.4: Power comparison between Conservative and BEPU calculations.

Chapter 8

Conclusions

The conclusions of the work developed are presented in this chapter. Conclusions can be divided into two groups: those concerning the work done are presented in section 8.1; those related to future work are presented in section 8.2.

8.1 Main conclusions

Several conclusions can be drawn from the activities carried out in the development of this doctoral thesis. The author has built, in the framework of this research, two models for coupled 3D neutron kinetics and thermal hydraulics system codes. The system codes used are RELAP5-3D [31–35] and TRACE [1–3], which are coupled, respectively, to NESTLE [31–35] and PARCS [4, 5] neutronic packages.

The models developed have been validated against plant data. Some system code improvements were required in order to obtain a reliable validation of the coupled 3D neutron kinetics and thermal-hydraulics models. In this regard, TRACE/PARCS [1–3], [4, 5] improvement is one of the significant outcomes of the thesis.

Such improvement will let the coupled code have a complete feedback response for the control rod position.

In the modified version of the code, the movement of the control rods can be simulated dynamically; the control rod bank position is calculated by the thermal-hydraulic system code as a function of the thermal hydraulic variables and logic control system considerations. The neutronic code is able to read the time-dependent position of each control rod bank and use this information in the 3D neutron kinetics calculations. In the previous versions of the code, this capability was not available.

The need for this capability was identified during the development of the present work; it was addressed and the solution was implemented in order to obtain more realistic results. This improvement turns out to be necessary in future versions of the TRACE/PARCS [1–3], [4, 5] coupled code.

Establishing guidelines of the Best Estimate Plus Uncertainties methodology for a coupled 3D neutron kinetics and thermal-hydraulics calculations is a second rellevant result set up within the framework of this report.

The multiple comparisons among the three available strategies:

- Conservative,
- Best Estimate with conservative boundary conditions, and
- Best Estimate Plus Uncertainty evaluation

Have shown, in the framework of this thesis, their consistency, the expected relationship of their outcomes and the suitability of each method depending of the final use of their results.

8.2 Future work

Several lines are open for future research, after the development of the present doctoral thesis.

The present thermal-hydraulics models can be improved, especially in the control system block. Also, a finer mesh vessels nodalization can be implemented, in order to match one-to-one fuel assembly to thermal-hydraulic node in the radial direction .This will mean ending up with 157 radial nodes in the thermal-hydraulic model. The same one-to-one (one neutron kinetic node to one thermal-hydraulic node) equivalence can be also applied in axial direction. Some preliminary calculations were already made in this regard, but there was not a significant impact on the results, whereas there was a big increase in the computational time. The one-to-one correspondence in both directions (radial and axial) will provide more detailed information about every core zone, and the prediction of reactivity feedback effects will be more accurate, since there will not be averaged zones concerning the thermal-hydraulic quantities.

Some deficiencies in the uncertainty field were detected in the cross section library performance. The knowledge gained here in the cross section library construction could

be applied in the phases I and II of the OECD Uncertainty Analysis in Best-Estimate Modelling project [23]. Among the cross section library deficiencies, it has been proved that the results present much better agreement to the plant data if the cross section absorption coefficients are increased by 10%. This discrepancy could be attributed to the variety of fuel assemblies which compose the modeled core. Within this variety, there are some fuel assemblies coming from older cycles of the reactor. It is worth to notice here that the reactor power was uprated in previous cycles; thus, part of these old assemblies were burnt in lower nominal power at the beginning and then in a high nominal power at the end; this phenomenon was not taken into account when performing the cross section library calculations and it would also explain some of the discrepancies observed in the presented results. The burnup time steps gap could also be refined in order to hold more information between the different burnup steps. With these modifications, a new cross section library could be built, more accurate than the one used in the present work.

When validating the model in TRACE/PARCS [1–3] and [4, 5], a small deviation was encountered on the control rod positioning, which was corrected by using a modified absorption coefficient cross section set. This point is also another issue for future research. Either the cross section set has some small deficiencies (see the suggested explanation above), or the information exchange between TRACE and PARCS [1–3], [4, 5] is not working properly. Both possibilities need to be investigated in more detail. Even when the present results are within the acceptance criteria (particularly if compared with the previous validated models), they can be improved; the actions to do would be: re-checking of all the control block system existing in the TRACE [1–3] model; re-checking the TRACE/PARCS [1–3], [4, 5] information exchange subroutines; and, finally, re-computing the cross section set. The last option will be performed indeed in the framework of the OECD Uncertainty Analysis in Best-Estimate Modelling project [23] by using the lattice physics code SCALE 6.1. First and second options can be done with a lesser effort, since they only require an exhaustive check of the control logic and of the information exchange subroutines between TRACE and PARCS [1–3], [4, 5], particularly regarding the control rod position (both codes interpret the control rod position in a different manner and this could be some source of error).

Best Estimate Plus Uncertainty methodology with coupled 3D neutron kinetics and thermal-hydraulic calculations has been shown and tested successfully in the framework of this thesis. Several parameters of impact over the figures of merit selected were identified, these parameters have been studied and are listed in the *Best Estimate Plus Uncertainty model* Chapter of this report. Results show the expected behavior of the time trends: Best Estimate calculations are within the envelope of the Best Estimate Plus Uncertainties calculations whereas the Conservative calculation leads to a worst scenario on the return to criticality. Future works should add extra disturbed parameters

in both codes when performing the Best Estimate Plus Uncertainties calculations to obtain more detailed results. Also, other scenarios with significant coupled 3D neutron kinetics and thermal-hydraulic effects should be studied, in order to test the models and to explore the limits of the Best Estimate Plus Uncertainties methodology.

Appendix A

RELAP5-3D Cross section master library creation methodology

A.1 introduction

The present appendix is an explanation of the methodology used at Pennsylvania State University to create a Cross Section Master Library. This methodology was developed by the author during one the research periods spent in RDFMG at Pennsylvania State University. This methodology requires data from the nuclear power plant to be modeled. The final goal of the methodology is to obtain a master cross section library, which is able to predict results either in steady state or transient calculations during all the cycle life of the modeled core. The library will be ready at the end to be read for coupled codes such RELAP5-3D [31–35] where kinetics code is NESTLE [31–35] or RELAP5-3.3 [41–49] where the kinetics coupled code is PARCS [4, 5]. The library will be based in tables instead of polynomial approximations with partial derivatives. The tables based as cross section library have more precise values than the partial derivative approximations. Some tools developed in the Pennsylvania State University, Reactor Dynamics and Fuel Management research Group, are used for that porpoise. These tools are mentioned in this appendix.

This appendix was added in the present study to exemplify the methodology illustrated in the subsection of the Chapter 3 called: *Cross-section library generation*. There the steps for performing a Master Cross-section library are explained, as a result a XS based in HELIOS [27–29] calculations and ready to be entered in GenPMAXS [30] code is obtained. In this appendix the same methodology of creating a XS master library is used, also same lattice physics code is used as well. As a result in here a XS master library generated by HELIOS [27–29] calculations is created, the difference with the one

of the subsection of the Chapter 3 *Cross-section library generation* is that, by following the specifications of the present appendix, the user will obtain a XS master library which will fit RELAP5-3D [31–35]. To obtain that goal source code from RELAP5-3D [31–35] and NEMTAB [16–19] routine needs to be used. In that sense, same initial steps are used on the cross section library creation, but different steps (which are exemplified here) need to be done since the 3D NK-TH coupled system that is going to use the cross section library is different in this case. Due the differences between this final steps on both cases, the author consider important to add this information as appendix chapter in the present report. As a conclusion with the methodology explained in this appendix the multiple use (in terms of different 3d NK-Th environments) of the created cross section library is showed.

A.2 Nuclear Power Plant data

Obtaining the nuclear power plant data for the Ascó NPP as it has been described the previous section is the first step. For Ascó NPP, we used the IDN_ASCO_ciclo13, _ciclo12 and _ciclo11 [24–26] document, where all geometries; compositions; fuel types; burnup ... are carefully described. The main features that the user needs to know for building the cross section library are listed below:

- Fuel types (normal fuel assembly, gadolinium fuel assembly, rodded fuel assembly and reflector fuel assembly).
- Geometries for the different fuel assemblies (pitch, lattice pitch, inner clad radius, outer clad radius, gap, inner guide tube radius, outer guide tube radius, control rod radius).
- Compositions (% uranium 235, % uranium 238, % gadolinium, power density ...).
- Burn up of each fuel assembly for the different axial nodes.
- Reference values for (moderator temperatures, fuel temperatures, moderator density and boron concentration).

A.3 HELLIOS input decks

The first step for generating the cross section master library is to simulate the neutron flux for the different fuel assembly types. This job must be done with any flux simulator code like HELIOS [27–29], CASMO, SCALE ... In our case those calculations were done

using HELIOS-1.9 [27–29]. It is important to accurately set the ranges for moderator density and temperature, boron concentration, fuel temperature and burn up steps. Once the HELIOS-1.9 [27–29] procedure has been completed, the user obtains several results. To obtain the moderator temperature, for each type of fuel assembly, three calculations are run *L*, *N*, and *H*. Any type of fuel assembly can be fitted in one of below listed categories:

- *NA_FA, for normal fuel assembly*
- *Gd_FA, for gadolinium fuel assembly*
- *Reflector, for reflector fuel assembly*
- *Rodded, for rodded fuel assembly*

As an example, if the user has one of each of the above listed fuel assembly types, there will be 12 HELIOS-1.9 [27–29] output files, normally named *NFAL.out, NFAN.out, NFAH.out, GdFAL.out, GdFAN.out, GdFAH.out, ReflectorL.out, ReflectorN.out, ReflectorH.out, RoddedL.out, RoddedN.out, and RoddedH.out.* This will be the minimum number of output files. These files are ready to be processed in TLG-2.0 program. this program is going to transform the created files into some new files able to be read by RELAP5-3D [31–35] and NESTLE [31–35], this step will be similar than the one performed by GenPMAXS [30] when adapting the HELIOS-1.9 [27–29] calculations to TRACE/PARCS [1–3] and [4, 5] environment.

A.4 Power Plant and Input decks description

Just before starting the TLG program it will be very useful to create a document which contains the features of the Nuclear Power Plant and also some features from the input decks used in coupled codes. An example of those documents can be found under the names:

- Angra_II_Neutronic_Model_Revised.doc
- ASCO II NPP core and neutronic data modeling.doc

These documents are not attached in the present study for property data reasons. Basically these documents contain some information from the nuclear power plant which includes ranges of operation; values at normal operation; fuel assembly core distribution;

fuel assembly burn up by nodes and detailed features from the fuel assembly models. Concerning the nuclear power plant code models, a relation from the core mapping used is also provided.

A.5 TLG-2.0

Once the lattice physics calculations have been completed, the next step is to run the TLG-2.0 program. The user needs to change the names of the output files obtained from the HELIOS-1.9 [27–29] calculations. *NFAL.out* will change to *XSSet_1.out*; *NFAN.out* will change to *XSSet_2.out* this format will be continued to the end of the output files. It is important to follow the sequential numbers with the L, $N$and H cases. This will make users tasks easier. Also the files have to be placed in the same folder with the *fc1, xstab.inp, xstabD.A2, xstabD.A2.f, xstab.A2.o, xstabD.A2_a2.f files.* Once all the files have been renamed, the next step is to execute the TLG-2.0 routine. Before the user has to change the format of the files fc1 and xstab.inp according to the XSSet_num.out files and the ranges specifications, chosen during the construction of the HELIOS [27–29] input decks. Before executing the TLG-2.0 routine the user has to change the format of the *fcl* and *xstab.inp* files to the *XSSet.num.out* files and the range specifications chosen during the construction of the HELIOS [27–29] input decks. Finally the TLG-2.0 routine is executed, this will be done by typing the following in the command prompt line:

- *./xstabD.A2 fc1*

As a consequence of the TLG-2.0 routine the user obtains the following files. *XSSet_1, XSSet_2, XSSet_3, XSSet_4, XSSet_5, XSSet_6*... These files without extension are input files for the NEMTAB [16–19] routine.

A.6 NEMTAB

Before using NEMTAB [16–19] routine, it is convenient to place the all *XSSet_num.out* files in a new folder called *OUTS*, as no additional jobs going to will be executed using the "*.out*" files. The *XSSet_num* files will be placed now in a folder called *Nemtab* or *Nemtabr*. The *Nemtab* folder will contain the cross section master library for the unrodded fuel assemblies. *Nemtabr* will be contain the cross section library for the rodded fuel assemblies. After the files have been placed in the folders, the next step is to place the "*ooo*" file in the *Nemtab* or *Nemtabr* folder and execute it, this step is accomplished by typing the following in the command prompt line:

- **./ooo**

As a consequence of the latest action, a file called *nemtab.ML* or *nemtabr.ML* will appear in the folder. The next step is to copy the files, *tlg-2-angra.exe* and *tgl-2-angra.f90* into the folder. Also copied into the folder is the previously prepared file *utlg.inp. Utlsg.inp* file is where the user has set the ranges for burn up, moderator temperature, moderator density, fuel temperature and boron concentration. In addition the user has sets in this file the different burn ups for each node for the used fuel assemblies. A correlation between the nodes and their position in the reactor is also set in this file. Finally the user has to execute the *tlg* execute file, by typing:

- *./tlg-2-angra.exe utlg.inp*

As a consequence of the above command the user should obtain a file called *status.out* which specifies the status of the last calculation. Also a file called *nemtab* or *nemtabr* depending on unrodded or rodded fuel assemblies. Those files are the libraries ready to be used by the user in RELAP5 [41–49] and [31–35].

A.7 RELAP5 user routine

The PSU RELAP5-3D [31–35] user routine is now ready to be used by RELAP5-3D [31–35] coupled with the NESTLE [31–35] kinetic code or with RELAP5-3.3 [41–49] coupled with the PARCS [4, 5] kinetic code. The user needs to compile the source code with the user routine prepared by PSU and place the *nemtab* and *nemtabr* files in the same folder as the RELAP5 [41–49] executables. The code will start extracting the values from the cross section library according the thermal hydraulics parameters calculated by RELAP5 [41–49].

Bibliography

[1] U. S. Nuclear Regulatory Commission Washington DC 20555-0001 Division of System Analysis, Office of Nuclear Regulatory Research. "US NRC. TRACE V5.0 THEORY MANUAL Field Equations, Solution Methods, and Physical Models". Vol. 1, October 2008.

[2] U. S. Nuclear Regulatory Commission Washington DC 20555-0001 Division of System Analysis, Office of Nuclear Regulatory Research. "US NRC. TRACE V5.0 USER's MANUAL Volume 1: Input Specification". October 2008.

[3] U. S. Nuclear Regulatory Commission Washington DC 20555-0001 Division of System Analysis, Office of Nuclear Regulatory Research. "US NRC. TRACE V5.0 USER's MANUAL Volume 2: Modeling Guidelines". October 2008.

[4] T. Downar, Y. Xu, V. Seker, Department of Nuclear Engineering and Radiological Sciences University of Michigan Ann Arbor. "PARCS v3.0, U.S. NRC Core Neutronics Simulator: THEORY MANUAL". December 2010.

[5] T. Downar, Y. Xu, V. Seker, Department of Nuclear Engineering and Radiological Sciences University of Michigan Ann Arbor. "PARCS v3.0, U.S. NRC Core Neutronics Simulator: USER MANUAL". December 2009.

[6] Brian M. Adams[1], Keith R. Dalbey[1], Michael S. Eldred[1], Laura P. Swiler[1], William J. Bohnhoff[2], John P. Eddy[3], Kenneth T. Hu[4], Dena M. Vigil[5], [1]Optimization, Uncertainty Quantification Department, [2]Radiation Transport Department, [3]System Readiness, Sustainment Technologies Department, [4]Validation, and Uncertainty Quantification Department, [5]Multiphysics Simulation Technologies Department, Sandia National Laboratories. "DAKOTA, A Multilevel Parallel Object-Oriented Framework for Design Optimization, Parameter Estimation, Uncertainty Quantification, and Sensitivity Analysis Version 5.2 User's Manual". SAND2010-2183, December 2009.

[7] Brian M. Adams[1], Keith R. Dalbey[1], Michael S. Eldred[1], Laura P. Swiler[1], William J. Bohnhoff[2], John P. Eddy[3], Kenneth T. Hu[4], Dena M. Vigil[5], [1]Optimization, Uncertainty Quantification Department, [2]Radiation Transport Department, [3]System Readiness, Sustainment Technologies Department, [4]Validation, and Uncertainty Quantification Department, [5]Multiphysics Simulation Technologies Department, Sandia National Laboratories. "DAKOTA, A Multilevel Parallel Object-Oriented Framework for Design Optimization, Parameter Estimation, Uncertainty Quantification, and Sensitivity Analysis Version 5.2 Theory Manual". SAND2011-9106, December 2011.

[8] Brian M. Adams[1], Keith R. Dalbey[1], Michael S. Eldred[1], Laura P. Swiler[1], William J. Bohnhoff[2], John P. Eddy[3], Kenneth T. Hu[4], Dena M. Vigil[5], [1]Optimization, Uncertainty Quantification Department, [2]Radiation Transport Department, [3]System Readiness, Sustainment Technologies Department, [4]Validation, and Uncertainty Quantification Department, [5]Multiphysics Simulation Technologies Department, Sandia National Laboratories. "DAKOTA, A Multilevel Parallel Object-Oriented Framework for Design Optimization, Parameter Estimation, Uncertainty Quantification, and Sensitivity Analysis Version 5.2 Reference Manual". SAND2010-2184, December 2009.

[9] Brian M. Adams[1], Keith R. Dalbey[1], Michael S. Eldred[1], Laura P. Swiler[1], William J. Bohnhoff[2], John P. Eddy[3], Kenneth T. Hu[4], Dena M. Vigil[5], [1]Optimization, Uncertainty Quantification Department, [2]Radiation Transport Department, [3]System Readiness, Sustainment Technologies Department, [4]Validation, and Uncertainty Quantification Department, [5]Multiphysics Simulation Technologies Department, Sandia National Laboratories. "DAKOTA, A Multilevel Parallel Object-Oriented Framework for Design Optimization, Parameter Estimation, Uncertainty Quantification, and Sensitivity Analysis Version 5.2 Developers Manual.". SAND2010-2185, December 2009.

[10] Office of Nuclear Regulatory Research, U. S. Nuclear Regulatory Commission. "Next Generation Nuclear Plant Phenomena Identification and Ranking Tables Vol 1: Main Report". NUREG/CR-6944, Vol. 1, March 2008.

[11] Office of Nuclear Regulatory Research, U. S. Nuclear Regulatory Commission. "Next Generation Nuclear Plant Phenomena Identification and Ranking Tables Vol 2: Accident and Thermal Fluid Analysis PIRT's". NUREG/CR-6944, Vol. 2, March 2008.

[12] Office of Nuclear Regulatory Research, U. S. Nuclear Regulatory Commission. "Next Generation Nuclear Plant Phenomena Identification and Ranking Tables

Vol 3: Fission product Transport and Dose PIRT's". NUREG/CR-6944, Vol. 3, March 2008.

[13] Office of Nuclear Regulatory Research, U. S. Nuclear Regulatory Commission. "Next Generation Nuclear Plant Phenomena Identification and Ranking Tables Vol 4: High Temperature Materials PIRT's". NUREG/CR-6944, Vol. 4, March 2008.

[14] David J. Diamond. "Experience Using Phenomena Identification and Ranking Technique (PIRT) for Nuclear Analysis". *Brookhaven National Laboratory*, BNL-76750-2006-CP, September 2006.

[15] Holbrook M. "Phenomena Identification and Ranking Technique (PIRT) for Nuclear Analysis". *Idaho National Laboratory, Next Generation Nuclear Plant Project*, Vol.1, July 2007.

[16] Kostadin N. Ivanov, Tara M. Beam, Anthony J. Baratta, Reactor Dynamics, and Fuel Management research Group, The Pennsylvania State University. "Pressurised Water Reactor Main Steam Line Break (MSLB) Benchmark, Volume I: Final specifications". *U. S. Nuclear Regulatory Commission, OECD Nuclear Energy Agency*, NEA/NSC/DOC(99)8, April 1999.

[17] Kostadin N. Ivanov, Tara M. Beam, Anthony J. Baratta, Reactor Dynamics, and Fuel Management research Group, The Pennsylvania State University. "Pressurised Water Reactor Main Steam Line Break (MSLB) Benchmark, Volume II: Summary results of Phase I (Point kinetics)". *U. S. Nuclear Regulatory Commission, OECD Nuclear Energy Agency*, NEA/NSC/DOC(2000)21, December 2000.

[18] N. Todorova, B. Taylor, K. Ivanov, Reactor Dynamics, and Fuel Management research Group, The Pennsylvania State University. "Pressurised Water Reactor Main Steam Line Break (MSLB) Benchmark, Volume III: Results of Phase II on 3D core boundary conditions model". *U. S. Nuclear Regulatory Commission, OECD Nuclear Energy Agency*, NEA/NSC/DOC(2002)12, December 2002.

[19] N. Todorova, B. Taylor, K. Ivanov, Reactor Dynamics, and Fuel Management research Group, The Pennsylvania State University. "Pressurised Water Reactor Main Steam Line Break (MSLB) Benchmark, Volume IV: Results of Phase III on Coupled core-plant Transient modelling". *U. S. Nuclear Regulatory Commission, OECD Nuclear Energy Agency*, ISBN 92-64-02152-3, December 2003.

[20] OECD Nuclear Energy Agency. "Neutronics/Thermal-hydraulics Coupling in LWR Technology, Vol. 1 CRISSUE-S WP1: Data Requirements and Databases Needed for Transient Simulations and Qualification". ISBN 92-64-02083-7, 1998-2004.

[21] OECD Nuclear Energy Agency. "Neutronics/Thermal-hydraulics Coupling in LWR Technology, Vol. 2 CRISSUE-S WP2: State-of-the-art Report (REAC-SOAR)". ISBN 92-64-02084-5, 1998-2004.

[22] OECD Nuclear Energy Agency. "Neutronics/Thermal-hydraulics Coupling in LWR Technology, Vol. 3 CRISSUE-S WP3: Achivements and Recomendations Report". ISBN 92-64-02085-3, 1998-2004.

[23] OECD Nuclear Energy Agency. "OECD Benchmark for Uncertainty Analysis in Best-Estimate Modelling (UAM) for Design, Operation and Safety Analysis of LWRs (OECD LWR UAM Benchmark)". *Expert Group on Uncertainty Analysis*, NEA/NSC/DOC(2009)11, 2009.

[24] Empresa Nacional del Uranio S.A. ENUSA. "Informe de Diseño Nuclear del Ciclo 11 de la C. N. Ascó II". ITEC-534, July 1996.

[25] Empresa Nacional del Uranio S.A. ENUSA. "Informe de Diseño Nuclear del Ciclo 12 de la C. N. Ascó II". ITEC-668, March 1998.

[26] Empresa Nacional del Uranio S.A. ENUSA. "Informe de Diseño Nuclear del Ciclo 13 de la C. N. Ascó II". ITEC-779, December 1999.

[27] Studsvik Scandpower. "HELIOS user manual: Methods (version 1.9)". December 2005.

[28] Studsvik Scandpower. "AURORA user manual (version 1.9)". December 2005.

[29] Studsvik Scandpower. "ZENITH user manual (version 1.9)". December 2005.

[30] T. Downar, Y. Xu, University of Michigan. "GenPMAXS-V5, Code for Generating the PARCS, Cross Section Interface File PMAXS". Decmber 2009.

[31] The RELAP5-3D Code Development Team; Idaho National Engineering and Environmental Laboratory Idaho Falls; Idaho. "RELAP5-3D Code Manual Volume I: Code Structure, System Models and Solution Methods, Rev. 2.0". *Division of Systems Research, Office of Nuclear Regulatory Research, U. S. Nuclear Regulatory Commission*, INEEL-EXT-98-00834, July 2002.

[32] The RELAP5-3D Code Development Team; Idaho National Engineering and Environmental Laboratory Idaho Falls; Idaho. "Appendix A RELAP5-3D Input Data Requirements, Rev. 2.0". *Division of Systems Research, Office of Nuclear Regulatory Research, U. S. Nuclear Regulatory Commission*, INEEL-EXT-98-00834-V2, July 2002.

[33] The RELAP5-3D Code Development Team; Idaho National Engineering and Environmental Laboratory Idaho Falls; Idaho. "RELAP5-3D Code Manual Volume II: User Guide and Input Requirements, Rev. 2.0". *Division of Systems Research, Office of Nuclear Regulatory Research, U. S. Nuclear Regulatory Commission*, INEEL-EXT-98-00834, July 2002.

[34] The RELAP5-3D Code Development Team; Idaho National Engineering and Environmental Laboratory Idaho Falls; Idaho. "RELAP5-3D Code Manual Volume IV: Models and Correlations, Rev. 2.0". *Division of Systems Research, Office of Nuclear Regulatory Research, U. S. Nuclear Regulatory Commission*, INEEL-EXT-98-00834, July 2002.

[35] R. R. Schultz, Idaho National Engineering and Environmental Laboratory Idaho Falls, Idaho. "RELAP5-3D Code Manual Volume V: User Guidelines, Rev. 2.0". *Division of Systems Research, Office of Nuclear Regulatory Research, U. S. Nuclear Regulatory Commission*, INEEL-EXT-98-00834, July 2002.

[36] F. Reventós, C. Llopis, L. Batet, C. Pretel, I. Sol, Technical University of Catalonia, Department of Physics and Nuclear Engineering. "Analysis of an actual reactor trip operating event due to a high variation of neutron flux occurring in the Vandellós-II nuclear power plant". *Nuclear Engineering and Design, Volume 240, Issue 10 Pages 2999-3008*, ISSN 0029-5493, October 2010.

[37] F. Reventós, C. Llopis, L. Batet, C. Pretel, I. Sol, Technical University of Catalonia, Department of Physics and Nuclear Engineeringl. "Thermal-Hydraulic Analysis Tasks for ANAV NPPs in Support of Plant Operation and Control". *Science and Technology of Nuclear Installations, vol. 2008, Issue 10 Pages 2999-3008*, Article ID 153858, doi:10.1155/2008/153858, 2008.

[38] F. Reventós, L. Batet, C. Llopis, C. Pretel, M. Salvat, I. Sol, Technical University of Catalonia, Department of Physics and Nuclear Engineeringl. "Advanced qualification process of ANAV NPP integral dynamic models for supporting plant operation and control". *Nuclear Engineering and Design,Volume 237, Issue 1, Pages 54-63*, ISSN 0029-5493, Januay 2007.

[39] F. Reventós, L. Batet, C. Pretel; M. Ríos, I. Sol, Technical University of Catalonia, Department of Physics and Nuclear Engineering. "Analysis of the Feed and Bleed procedure for the Ascó NPP: First approach study for operation support". *Nuclear Engineering and Design,Volume 237, Issue 18, Pages 2006-2013*, ISSN 0029-5493, Januay 2007.

[40] R. Pericas; F. Reventós; L. Batet, Technical University of Catalonia, Department of Physics and Nuclear Engineering. "Sensitivity Analyses of a hypothetical 6 inch

break, LOCA in Ascó NPP using RELAP/MOD3.2.". *NUREG/IA-0240*, September 2010.

[41] Information Systems Laboratories; Inc. Rockville Maryland; Idaho Falls; Idaho. "RELAP5/MOD3.3 CODE MANUAL VOLUME I: CODE STRUCTURE, SYSTEM MODELS, AND SOLUTION METHODS". *Division of Systems Research, Office of Nuclear Regulatory Research, U. S. Nuclear Regulatory Commission*, NUREG/CR-5535/Rev P4-Vol I, October 2010.

[42] Information Systems Laboratories; Inc. Rockville Maryland; Idaho Falls; Idaho. "RELAP5/MOD3.3 CODE MANUAL VOLUME II: USER'S GUIDE AND INPUT REQUIREMENTS". *Division of Systems Research, Office of Nuclear Regulatory Research, U. S. Nuclear Regulatory Commission*, NUREG/CR-5535/Rev P4-Vol II, October 2010.

[43] Information Systems Laboratories; Inc. Rockville Maryland; Idaho Falls; Idaho. "RELAP5/MOD3.3 CODE MANUAL VOLUME II: APPENDIX A INPUT REQUIREMENTS". *Division of Systems Research, Office of Nuclear Regulatory Research, U. S. Nuclear Regulatory Commission*, NUREG/CR-5535/Rev P4-Vol II, App A, October 2010.

[44] Information Systems Laboratories; Inc. Rockville Maryland; Idaho Falls; Idaho. "RELAP5/MOD3.3 CODE MANUAL VOLUME III: DEVELOPMENTAL ASSESSMENT PROBLEMS". *Division of Systems Research, Office of Nuclear Regulatory Research, U. S. Nuclear Regulatory Commission*, NUREG/CR-5535/Rev P4-Vol III, October 2010.

[45] Information Systems Laboratories; Inc. Rockville Maryland; Idaho Falls; Idaho. "RELAP3.3 MOD3.3 CODE MANUAL VOLUME IV: MODELS AND CORRELATIONS". *Division of Systems Research, Office of Nuclear Regulatory Research, U. S. Nuclear Regulatory Commission*, NUREG/CR-5535/Rev P4-Vol IV, October 2010.

[46] Information Systems Laboratories; Inc. Rockville Maryland; Idaho Falls; Idaho. "RELAP5/MOD3.3 CODE MANUAL VOLUME V: USERS GUIDELINES". *Division of Systems Research, Office of Nuclear Regulatory Research, U. S. Nuclear Regulatory Commission*, NUREG/CR-5535/Rev P4-Vol V, October 2010.

[47] A. S. Shieh; V. H. Ransom; R. Krishnamurthy; Information Systems Laboratories; Inc. Rockville Maryland; Idaho Falls Idaho. "RELAP5/MOD3 CODE MANUAL VOLUME VI: VALIDATION OF NUMERICAL TECHNIQUES IN RELAP5/MOD3.0". *Division of Systems Research, Office of Nuclear Regulatory Research, U. S. Nuclear Regulatory Commission*, NUREG/CR-5535/Rev P3-Vol VI, October 2010.

[48] Information Systems Laboratories; Inc. Rockville Maryland; Idaho Falls; Idaho. "RELAP5/MOD3.3 CODE MANUAL VOLUME VII: SUMMARIES AND REVIEWS OF INDEPENDENT CODE ASSESSMENT REPORTS". *Division of Systems Research, Office of Nuclear Regulatory Research, U. S. Nuclear Regulatory Commission*, NUREG/CR-5535/Rev P4-Vol VII, October 2010.

[49] Information Systems Laboratories; Inc. Rockville Maryland; Idaho Falls; Idaho. "RELAP5/MOD3.3 CODE MANUAL VOLUME VIII: PROGRAMMERS MANUAL". *Division of Systems Research, Office of Nuclear Regulatory Research, U. S. Nuclear Regulatory Commission*, NUREG/CR-5535/Rev P4-Vol VIII, October 2010.

[50] A. Del Nevo, E. Coscarelli, A. Kovtonyuk, F. DAuria, S. Schollenberger, K. Umminger, H. Austregesilo, S. W. Lee, J. Freixa, A. Manera, R. Pericas, V. Martnez, F. Reventos, S. Carlos, J.F. Villanueva, S. Martorell, B. Serradell. "Analytical Exercise On OECD/NEA/CSNI PKL-2 Project Test G3.1: Main Steam Line Break Transient in PKL-III Facility Phase 2: Post-Test Calculations". *OECD/NEA/CSNI PKL-2 Project*, TH/PKL-2/02(10) Rev. 1, March 2011.

[51] R. Pericas, V. Martnez, F. Reventos, Technical University of Catalonia, Department of Physics and Nuclear Engineering. "Post-test Calculation of PKL III Test G3.1 Main Steam Line Break using RELAP5 / mod3.3". *OECD/NEA/CSNI PKL-2 Project, Pisa, Italia*, TH/PKL-2/02(10) Rev. 1, April 2010.

[52] S. S. Wilks. "Determination of sample sizes for setting tolerance limits". *Annals of Mathematical Statistics*, vol. 12; no. 1; pp. 91-96, March 1941.

[53] S. S. Wilks. "Statistical prediction with special reference to the problem of tolerance limits". *Annals of Mathematical Statistics*, vol. 13; no. 4; pp. 400-409, March 1942.

[54] Code of Federal Regulations. "Acceptance criteria for emergency core cooling systems for light water nuclear power reactors". Appendix K; 10 CFR 50.46, March 1996.

[55] Argonne National Laboratory; Nuclear Engineering Division. "Uncertainty Quantification Approaches for Advanced Reactor Analyses". ANL-GenIV-110, September 2008.

[56] M. Pourgol-Mohammad; A. Mosleh; M. Modarres. "Integrated Methodology for Thermal-Hydraulics Code Uncertainty Analysis". *United States Nuclear Regulatory Commission Office of Research*, CRR Report 2007-M3, March 2007.

[57] International Atomic Energy Agency. "Best Estimate Safety Analysis for Nuclear Power Plants : Uncertainty Evaluation". SAFETY REPORTS SERIES No. 52; IAEAL 08-00517; ISBN 978-92-0-108907-6, March 2008.

[58] A. Cuadra, J.L. Gago, F. Reventós, Technical University of Catalonia, Department of Physics and Nuclear Engineering. "Analysis of a Main Steam Line Break in Ascó Nuclear Power Plant". *Nuclear Technology*, Vol. 146; Pages 41–48, April 2004.

[59] V. H. Ransom and J. A. Trapp. "The RELAP5 Choked Flow Model and Application to a Large Scale Flow Test". *ANS/ASME/NRC International Topical Meeting on Nuclear Reactor Thermal-Hydraulics*, Saratoga Springs, New York, pp. 799-819, 1980.

[60] K. Kones, J. Rothe, W. Dunsford. "Symbolic Nuclear Analysis Package (SNAP) Tutorial". *Division of Systems Research, Office of Nuclear Regulatory Research, U. S. Nuclear Regulatory Commission*, INEEL-EXT-98-00834, March 2005.

[61] Yao, S. C., L. E. Hochreiter, and W. J. Leech. "Heat-Transfer Augmentation in Rod Bundles Near Grid Spacers". *Journal of Heat Transfer*, Vol. 104 pp. 76–81, 1982.

[62] H. A. Van Der Vorst. "BI-CGSTAB: A fast and smoothly converging variant of BI-CG for the solution of nonsymmetric linear systems". *SIAM J. Sci. Stat. Comput*, Vol. 13, pp. 631–644, 1992.

[63] M. R. Hestenes and E. Stiefel. "Methods of Conjugate Gradients for Solving Linear Systems". *J. Res. Nat. Bur. Standardst*, Vol. 49, pp. 409-.436, 1952.

[64] A. Lo Nigro. "Application of coupled 3D neutron kinetic / therma hydraulic tools and methods to the safety analysis of PWR's". *Università degli Studi di Pisa*, Ph.D Thesis, 2005.

[65] V. Martinez-Quiroga, F. Reventos, Technical University of Catalonia, Institute of Energy Technologies. "The Use of System Codes in Scaling Studies: Relevant Techniques for Qualifying NPP Nodalizations for Particular Scenarios". *Science*

and Technology of Nuclear Installations, Vol. 2014, Article ID 138745, December 2013.

[66] V. Martinez-Quiroga, F. Reventos and J. Freixa, Technical University of Catalonia, Institute of Energy Technologies. "Applying UPC Scaling-Up Methodology to the LSTF–PKL Counterpart Test". *Science and Technology of Nuclear Installations*, Vol. 2014, Article ID 292916, December 2013.

[67] R. Miró[1], P. Ana[1], T. Barrachina[1], J. C. Martnez-Murillo[2], C. Pereira[3], G. Verdú[1], [1]Universitat Politècnica de València, [2]Almaraz-Trillo AIE, [3]Universidade Federal de Minas Gerais. "Implementation of the Control Rod Movement Option by means of Control Variables in RELAP5/PARCS v2.7 Coupled Code". *Division of Systems Analysis, Office of Nuclear Regulatory Research, U.S. Nuclear Regulatory Commission*, NUREG/IA–0402, July 2014.

[68] K. Ivanov, M. Avramova, S. Kamerow. "OECD Benchmark for Uncertainty Analysis in Best-Estimate Modelling (UAM) for Design, Operation and Safety Analysis of LWRs (OECD LWR UAM Benchmark). Volume I: Specification and Support Data for Neutronics Cases (Phase I)". *OECD Nuclear Energy Agency, Expert Group on Uncertainty Analysis*, NEA/NSC/DOC(2013)7, May 2013.

[69] International Atomic Energy Agency. "Deterministic Safety Analysis for Nuclear Power Plants". SPECIFIC SAFETY GUIDE No. SSG-2; IAEAL 09-00614; ISBN 978-92-0-113309-0, 2009.

[70] I. Gajev. "Sensitivity and Uncertainty analysis of Boiling water reactor stability simulations". *Stockholm Sweden*, Ph.D Thesis, 2012.